AWARD NUMBER: W81XWH-14-2-0193

TITLE: Prevention of Bone Loss after Acute SCI by Zoledronic Acid: Durability, Effect on Bone Strength, and Use of Biomarkers to Guide Therapy

PRINCIPAL INVESTIGATOR: Thomas J. Schnitzer, MD, PhD

CONTRACTING ORGANIZATION: Northwestern University, Chicago, Illinois

REPORT DATE: June 2021

TYPE OF REPORT: Final Report

PREPARED FOR: U.S. Army Medical Research and Development Command
Fort Detrick, Maryland 21702-5012

REPORT DOCUMENTATION PAGE

Form Approved
OMB No. 0704-0188

1. REPORT DATE	2. REPORT TYPE	3. DATES COVERED
June 2021	Final Report	29 Sep 2014 – 28 Mar 2021

4. TITLE AND SUBTITLE

Prevention of Bone Loss after Acute SCI by Zoledronic Acid:

Durability, Effect on Bone Strength, and Use of Biomarkers to Guide Therapy

5a. CONTRACT NUMBER
W81XWH-14-2-0193

5b. GRANT NUMBER
n/a

5c. PROGRAM ELEMENT NUMBER

6. AUTHOR(S)

Thomas J. Schnitzer, MD, PhD

E-Mail: tjs@northwestern.edu

5d. PROJECT NUMBER

5e. TASK NUMBER

5f. WORK UNIT NUMBER

7. PERFORMING ORGANIZATION NAME(S) AND ADDRESS(ES)

Northwestern University
633 Clark St.
Evanston, IL 60208-0001

8. PERFORMING ORGANIZATION REPORT NUMBER

9. SPONSORING / MONITORING AGENCY NAME(S) AND ADDRESS(ES)

U.S. Army Medical Research and Development Command
Fort Detrick, Maryland 21702-5012

10. SPONSOR/MONITOR'S ACRONYM(S)

11. SPONSOR/MONITOR'S REPORT NUMBER(S)

12. DISTRIBUTION / AVAILABILITY STATEMENT

Approved for Public Release; Distribution Unlimited

13. SUPPLEMENTARY NOTES

14. ABSTRACT

Rapid bone loss is a universal accompaniment of acute spinal cord injury (SCI) and leads to severe loss of bone mass and bone strength with a marked increased risk of fracture. This 24 month double-blind, randomized, placebo-controlled study evaluated in 60 participants the efficacy (bone mass and bone strength) and safety of zoledronic acid (ZOL) administered early after acute SCI to prevent bone loss, the duration of its effects and the value of using biomarkers to guide therapy. Data collection (bone imaging and biomarkers) occurred at baseline and after 3, 6 and 12 months during the first year; participants were re-randomized after 12 months with subsequent data collection at 18 and 24 months. Forty-nine out of the 60 participants who were randomized and treated at baseline completed both years of the study. Data demonstrated that a single infusion of ZOL after acute SCI attenuates bone loss at the hip (proximal femur) and knee (distal femur and proximal tibia) for at least 6 months. Two annual infusions did not provide significant attenuation of bone loss beyond a single baseline infusion, and a single infusion 12 months after baseline did not provide significant attenuation of bone loss beyond two years of placebo. No unanticipated adverse events associated with drug treatment were observed. In summary, ZOL 5 mg infusion after acute SCI was well-tolerated and may provide an effective therapeutic approach to prevent bone loss in the first few years after SCI.

15. SUBJECT TERMS

Spinal cord injury, bone mass, bone strength, osteoporosis, zoledronic acid

16. SECURITY CLASSIFICATION OF:			17. LIMITATION OF ABSTRACT	18. NUMBER OF PAGES	19a. NAME OF RESPONSIBLE PERSON
a. REPORT	b. ABSTRACT	c. THIS PAGE			USAMRMC
Unclassified	Unclassified	Unclassified	Unclassified	56	19b. TELEPHONE NUMBER *(include area code)*

TABLE OF CONTENTS

Page

INTRODUCTION:

Bone loss following spinal cord injury (SCI) is a well-described secondary complication that occurs below the level of the neurological lesion.(1,2) Mechanical disuse associated with diminished motor function is a primary contributor to SCI-related bone loss, but neurogenic and hormonal changes following SCI are likely to play an important role.(3,4) During the first few weeks after SCI, biomarkers of bone resorption rise considerably beyond the upper limits of normal and remain elevated past 6 months of injury; biomarkers of bone formation remain relatively unchanged.(5) Bone loss during this acute period is rapid, on the order of 2-3%/month,(6,7) which is nearly double that observed during spaceflight.(8) Within the first 2-3 years of injury, bone loss begins to plateau, after which time some 25% of the bone mineral at the proximal femur and 50% of the bone mineral at the proximal tibia has been resorbed.(1,9)

The clinical consequence of SCI-related bone loss is an increased risk of fracture that is two-fold greater than the general population.(10) These fractures are a source of considerable morbidity, loss of independence, and increased medical costs;(11,12) in male veterans with SCI, bone fracture is an independent contributor to mortality.(13) Unlike primary osteoporosis, the large majority of fractures after SCI occur around skeletal regions of the knee, but it is also important to note that 10% to 20% of fractures after SCI occur at the hip.(11,14,15) Hip fractures may be of greater concern in those individuals with motor incomplete SCI who retain some level of locomotor function,(16) whereas fractures at the knee may be more common in individuals with motor complete SCI.(11,15) Fractures after SCI are often associated with events characterized by minimal to no trauma, including falls from standing height or lower, wheelchair transfers, and twisting or catching a lower extremity.(11,16,17) Fractures associated with active therapies such as robot-assisted locomotion and functional electric stimulation have been reported.(18,19)

Bisphosphonate therapies to attenuate bone loss in acute SCI have been extensively studied. Early generation bisphosphonates have illustrated some efficacy, particularly at the hip (total hip and femoral neck regions) and during the first 6 months of treatment.(20-22) More recent studies have examined the efficacy of the nitrogen containing, third generation bisphosphonate, zoledronic acid.(23-28) Zoledronic acid (ZOL) is more potent than earlier bisphosphonates, and is delivered in a once-yearly infusion, which ensures long-term compliance and avoids the strict administration requirements of oral bisphosphonates. Treatment with ZOL in acute SCI attenuated bone loss at the hip for up to 12 months after the infusion.(23-28) Attenuation of bone loss around the knee (distal femur and proximal tibia) has also been demonstrated, at least in the first 4-6 months, but in these instances bone loss was larger at the knee than the hip and differences relative to placebo were less.(26,27) In the context of SCI, no trials have examined the efficacy of ZOL to attenuate bone loss beyond 12 months of infusion. Consequently, the durability of the response to a single ZOL infusion remains undefined, the need for repeat treatment has not been explored, and the consequences of delayed intervention with ZOL are not known.

The objectives of this study were to explore the timing and frequency of administration of a ZOL 5 mg infusion to inform the optimal therapeutic approach to prevent bone loss after SCI. Thus, we conducted a 2-year, randomized, controlled clinical trial, in which different treatment regimens of ZOL were compared to each other and to placebo. Specifically, 60 patients with acute SCI (<120 days of injury) were randomized to receive either ZOL or placebo in year 1. These groups were further randomized to receive either ZOL or placebo in year 2 (see diagram below). Dual energy x-ray absorptiometry (DXA) imaging of the hip and spine, computed tomography (CT) imaging of the hip and knee, and serum markers of bone turnover were obtained during the 2-year study. Safety was monitored during both years of the study.

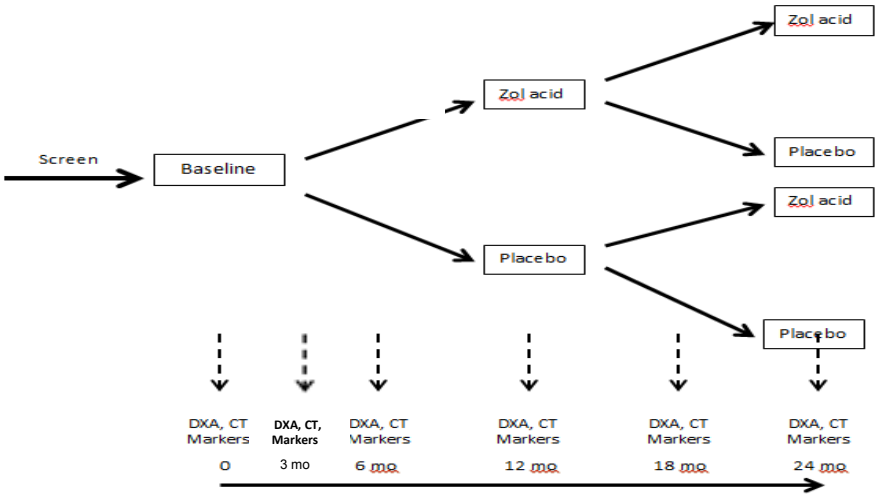

KEYWORDS:
Spinal cord injury, bone mass, bone strength, osteoporosis, zoledronic acid

ACCOMPLISHMENTS:

What were the major goals of the project?

Specific Aim 1: Determine Timing and Frequency of Administration of Zoledronic Acid for Maximum Effect

Major Task 1: Regulatory Approval
Milestone Achieved:
HRPO Approval (Goal - Month 2) – 100% complete

Major Task 2: Prepare Study Documents and Materials
Milestone Achieved:
Study materials completed, ready for use (Goal - Month 2) – 100% complete

Major Task 3: Enroll and Treat Participants
Milestone Achieved:
All participants enrolled (Goal - Month 20) – 100% complete
Milestone Achieved:
Last participant visit (Original goal - Month 44; Modified Goal – Month 66) – 100% of participants have had their last (M24) visit including those who discontinued or withdrew.

Major Task 4: Data Completion and Analysis
Milestone Achieved:
Complete data analysis (Original goal - Month 48; Modified Goal – Month 72) - 100% complete

Specific Aim 2: Evaluate Use of Serum Bone Biomarkers to Guide Therapeutic Decisions

Major Task 1: Obtain results of serum levels of bone biomarkers
Milestone Achieved:
Results of all bone biomarkers available (Original goal - Month 45; Modified Goal – Month 67) - 100% complete.

Major Task 2: Analyze data with regard to BMD changes
Milestone Achieved:
Data analysis completed (Original goal - Month 48; Modified Goal – Month 72) **-** 100% complete

Specific Aim 3: Quantify changes in torsional and compressive strength at the distal femur and proximal tibia
Major Task 1: Application of refined FE model
Milestone Achieved:
Data obtained and entered (Original goal – Month 45-48; Modified Goal – Month 66) - 50% complete

What was accomplished under these goals?

1) Major Activities

All regulatory approvals were obtained and maintained during the duration of the study. Subject enrollment began in February 2015 and was completed in February 2018 with all 60 participants (100% of original goal) enrolled and treated. The last study visit occurred in March 2020. Forty-nine out of 60 participants completed the Month 24 study visit and 11 were lost to follow up or withdrawn, resulting in 82% retention at the end of the 2 year study. Safety was monitored through the last study visit and the medical monitor continued to review all AEs and study procedures at the data safety monitoring committee meetings, with the final meeting taking place in August 2020. Participants' data were entered into the REDCap database and the database was locked. Biospecimens were sent for analysis to Maine Medical Laboratory. The blind was broken and analysis of the primary and key secondary endpoints, as outlined in the statistical analysis plan, were analyzed. A manuscript has been written and submitted for review for publication in the Journal of Bone and Mineral Research.

2) Specific Objectives

Our earlier pilot work, as well as research by others, had indicated that treatment with bisphosphonate after SCI could be effective at preventing bone loss, particularly at the hip. No studies had evaluated effects over longer periods of time nor had any evaluated the effects of such agents at the skeletal sites most prone to fracture after SCI, the distal femur and proximal tibia. This study was designed to specifically address the question of whether the timing and duration of once-yearly dosing with a potent, intravenously administered bisphosphonate, zoledronic acid, would affect outcomes after both one and two years of treatment compared to delayed treatment or no treatment. We also wanted to evaluate if serum markers of bone turnover might provide useful information regarding the value of continued treatment. And finally, taking advantage of having CT imaging, we wanted to evaluate not only changes in bone content but importantly changes in bone strength at the skeletal sites around the knee where most fractures occur in people with SCI. In summary, our study therefore had three specific aims:

Specific Aim 1: Determine Timing and Frequency of Administration of Zoledronic Acid for Maximum Effect

Specific Aim 2: Evaluate Use of Serum Bone Biomarkers to Guide Therapeutic Decisions

Specific Aim 3: Quantify changes in torsional and compressive strength at the distal femur and proximal tibia

3) Significant results or key outcomes

Study Design:
A single-center, randomized, double-blind, placebo-controlled clinical trial (RCT) was conducted at the lead site, Northwestern University. Patients with acute SCI were recruited from Shirley Ryan AbilityLab, consented, and screened for eligibility per study protocol.

Sixty qualified participants were randomized to receive either an intravenous infusion of ZOL (5 mg) or matching placebo (saline) at Baseline, creating two groups in year 1: ZOL (n=30) and Placebo (n=30). At year 2, participants were randomized for a second time, resulting in 4 different treatment groups: 1) ZOL both years (Z-Z), 2) ZOL at year 1, placebo at year 2 (Z-P), 3) placebo at year 1, ZOL at year 2 (P-Z), and 4) placebo both years (P-P). To reduce the incidence of an acute phase response, which is a well-known reaction after an infusion with an intravenous bisphosphonate like ZOL, participants were pre-medicated with acetaminophen prior to each infusion, and as needed, for up to 3 days thereafter. All participants took a daily regimen of calcium and vitamin D during both years of the study.

Ambulation ability was measured with the Walking Index for Spinal Cord Injury II (WISCI) and was collected along with DXA, CT, and serum samples at baseline and follow up visits at months 3 (optional), 6, 12, 18, and 24. DXA images include the lumbar spine and bilateral hips (total hip and femoral neck). Unless precluded by presence of an artifact, the non-dominant side was chosen as the index extremity. CT images captured approximately 15 cm each of the distal femur, proximal tibia, and the hip area of the non-dominant leg. Three biomarkers of bone metabolism were measured: one marker of bone resorption, (I) collagen type 1 cross-linked C-telopeptide (CTX), and two markers of bone formation, (II) procollagen amino-terminal propeptide (P1NP), and (III) bone-specific alkaline phosphatase (BSAP). Safety data were collected every 3 months, either in-person or via telephone.

Primary endpoints were the percent-change in aBMD, evaluated by DXA after month 12, in the (1) total hip and (2) femoral neck skeletal sites. Key secondary endpoints included three CT measurements: (1) integral and (2) trabecular BMC at the femoral epiphysis, and (3) integral BMC at the femoral metaphysis. One-year data analysis of primary, secondary, and exploratory endpoints were carried out using linear mixed-effects models of the percent-changes from baseline to months 6 and 12. Covariate adjustments for baseline value of the corresponding outcome and ambulatory status (measured by WISCI) were performed by fitting these variables as fixed factors. The repeated measures were addressed using participant identification as random intercepts in the model. The aBMD by group interaction was considered statistically significant at $p < 0.05$.

Spine aBMD, all remaining CT measurements, and biomarkers of bone metabolism were considered exploratory endpoints, as well as all variables at Month 24. Data from year 2, were analyzed using non-parametric Wilcoxon-rank tests. Here, the percent-changes were calculated from baseline to month 24 for the four groups. Serum biomarkers were studied as absolute values. Nominal p-values were evaluated and considered statistically significant at $p < 0.05$. It should be noted that there is elevated potential for type I error due to multiple comparisons, thus the findings for the 24-month analyses should be interpreted as exploratory.

Results:
There were no statistically significant differences, with respect to demographic and clinical descriptors, between the two groups at baseline (see Table 1 in Appendix B). Both ZOL and placebo groups were predominantly male (80%) with a mean age of 37.8 (15.4) years. Twenty-three percent of the participants identified as Black/African American, 68% as White, 5% as Asian, and 3% as multiracial. Most SCIs occurred about 66 days prior to baseline, were motor complete (60%), and affected the cervical spine (57%).

The analysis of the primary and key secondary study endpoints are included in Appendix B in table format. A summary description of these outcomes follows, with specific quantitative data available in the Appendix.

Specific Aim 1: Determine Timing and Frequency of Administration of Zoledronic Acid for Maximum Effect

Year 1 Results:
A significant effect of treatment on DXA-derived aBMD measures was observed over the first year ($p \leq 0.001$; Table 2 in Appendix B). After 12 months of treatment, participants receiving placebo lost 12.8 ± 16.2% and 11.3 ± 11.0% aBMD at the total hip and femoral neck, respectively, whereas those receiving ZOL lost 2.2 ± 6.7% and 1.7 ± 5.3%, respectively (Figure 1).

All 3 of the key secondary outcome measures (evaluating skeletal bone changes by CT at the knee) also showed significant differences in favor of the ZOL group compared to placebo. Treatment with ZOL was able to almost completely prevent bone loss at the hip; however, bone loss was still evident at the knee in this group.

Specifically, ZOL attenuated losses in femoral epiphyseal integral BMC (p=0.003), trabecular BMC (p=0.033), and metaphyseal integral BMC (p=0.042). For these measures, participants who received ZOL experienced median losses between 4.7% and 18.6%, while those who received placebo lost between 8.9% and 39.5% (i.e., differences of 4% to 20% between groups, depending on measure). Similar results were observed at the proximal tibia, with differences of 15% to 19% between groups.

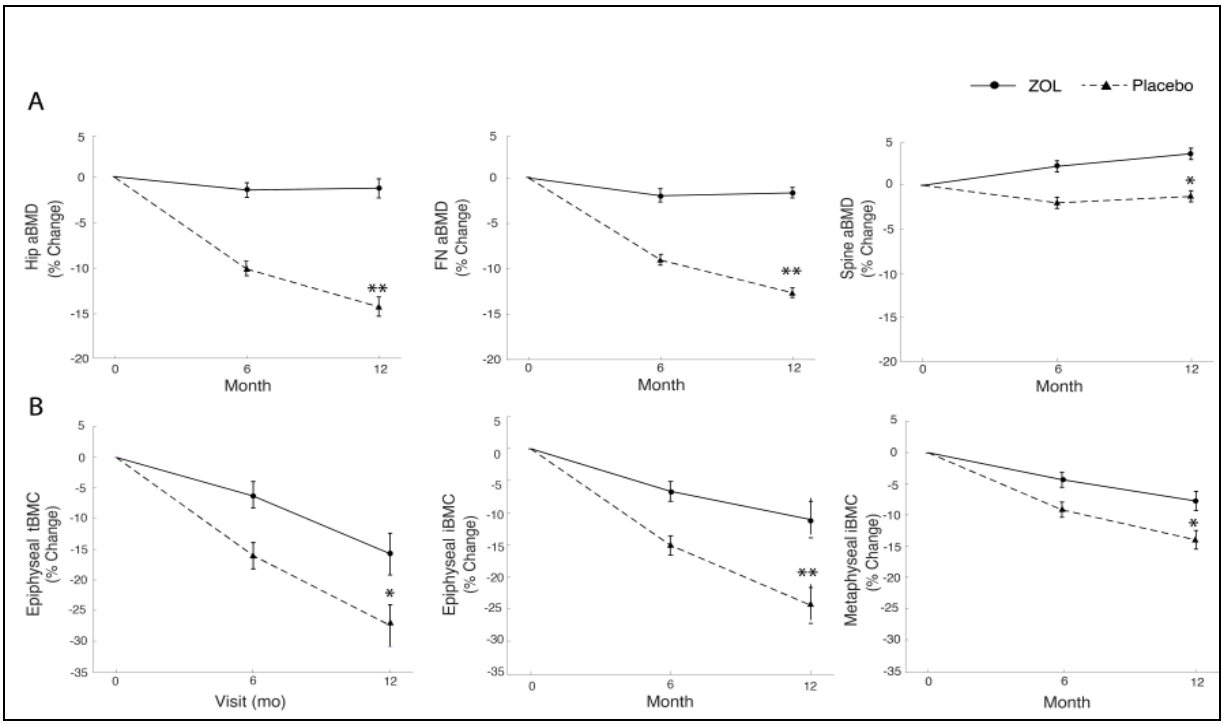

Figure 1. Mean percent change in (A) areal bone mineral density (aBMD) at the hip and femoral neck (FN) and (B) bone mineral content (BMC) at the knee: trabecular (tBMC) and integral (iBMC) epiphyseal and integral metaphyseal content at 6 and 12 months in the zoledronic acid and placebo treated groups.
ZOL (zoledronic acid); mo (months). * $p < 0.05$

Year 2 Results:
Participants who received only placebo (P-P group) demonstrated losses at month 24 in total hip and femoral neck aBMD of 21.8 ± 16.2% and 16.8% ± 14.9 at 24 months, respectively (Table 3, Figure 2). These losses were attenuated in groups that were randomized to zoledronic acid in year 1. Improvements to spine aBMD at 24 months were observed for a single drug infusion at baseline (+5.4 ± 7.1%) as well as two annual infusions (+5.7 ± 4.1%), and these changes were significant relative to the placebo only group (Z-P vs P-P and Z-Z vs P-P; $p \leq 0.036$), which demonstrated a median loss in spine aBMD (-2.0 ± 10.2%). No differences in CT measures at the femur were observed between any groups at 24 months. At the tibia, greater losses in epiphyseal cortical BMC (p=0.028) and cortical BV (p=0.028) at 24 months were observed for the placebo only group (P-P) when compared to the two annual infusions group (Z-Z).

Retreatment with ZOL at the end of year 1 resulted in less bone loss at the hip than only a single initial treatment, meaning that there is a benefit to continued treatment at the hip. However, at the knee, it appeared that a second treatment with ZOL had minimal subsequent effect. It also was evident that delaying treatment with ZOL until 12 months post-SCI resulted in more bone loss than treating people immediately post-SCI, though delayed treatment was still beneficial at the hip compared to no treatment at all. While these effects were evident at the hip, they were less striking or non-existent at the knee skeletal sites.

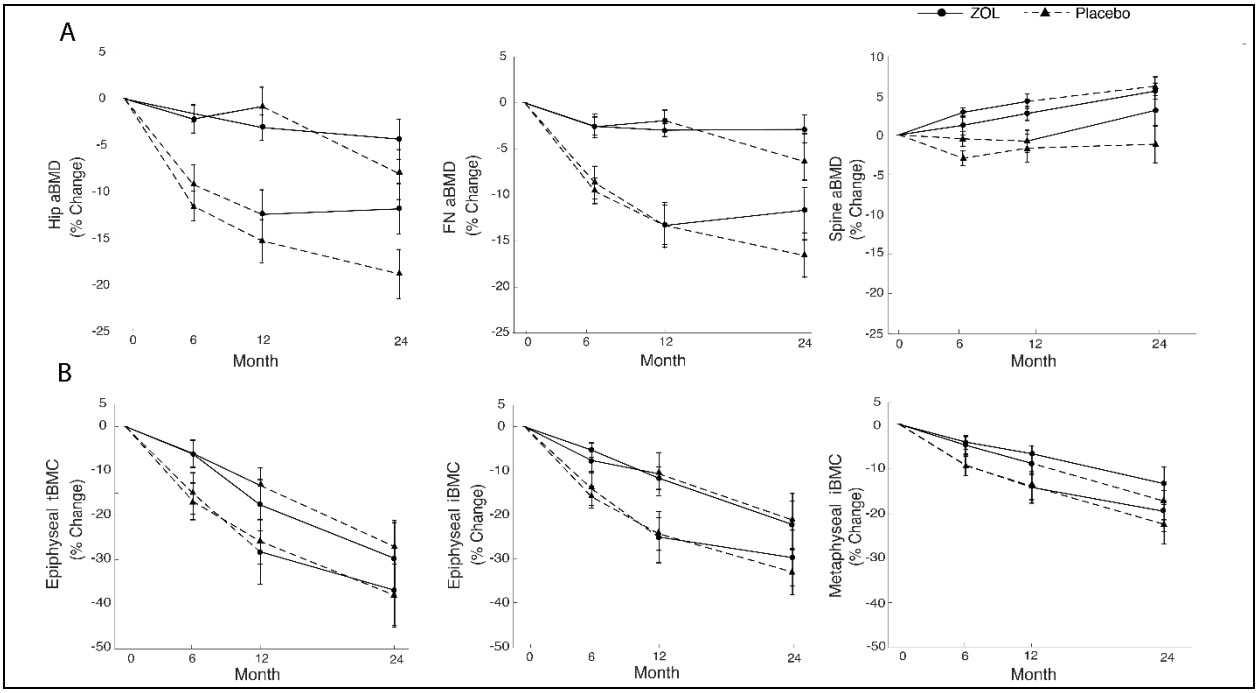

Figure 2. Mean percent change in (A) areal bone mineral density (aBMD) at the hip and femoral neck and (B) bone mineral content (BMC) at the knee: trabecular (tBMC) and integral (iBMC) epiphyseal and integral metaphyseal content. Change was calculated from baseline at month 6, 12, and 24 in the 4 groups: placebo + placebo, placebo + zoledronic acid, zoledronic acid + placebo and zoledronic acid + zoledronic acid. ZOL (zoledronic acid); mo (months).

Safety:
No unanticipated problems involving risks to participants or others occurred in this study. Across both years of the study, 411 adverse events (AEs) were reported, including 53 serious events. The most common AEs (listed in Table 5 in Appendix B), which included urinary tract infections and upper respiratory infections, were those expected for a population with SCI. There were no meaningful differences between treatment groups in the frequency or types of AE occurrence in year 1 and year 2, with the exception of the acute phase response. Although the presence of this response was expected, the incidence (>70% of patients treated) was substantially higher than has been previously reported for post-menopausal women and men treated with ZOL.

Conclusion:
This is the first RCT to examine the effects of timing and frequency of administration of zoledronic acid 5 mg infusion in acute SCI. A single infusion of zoledronic acid attenuated bone loss at the hip and knee for 12 months and at the hip for 24 months. Providing a second infusion of zoledronic acid at 12 months did not show a statistically significant effect in attenuating bone loss at 24 months when compared to a single infusion at baseline. In addition, a single infusion provided 12 months after baseline did not significantly attenuate bone loss by 24 months when compared to placebo only. However, absolute differences between these groups in all cases favored the zoledronic acid-treated groups and in some instances were large. The failure to show statistical significance after 24 months may have been a consequence of the small sample sizes at year 2, due primarily to the presence of 4 groups at 24 months in comparison with 2 larger groups at 12 months. The magnitude of the differences between the placebo only group and the groups who were treated with zoledronic acid may have clinical significance and further investigation is warranted.

In summary, zoledronic acid 5 mg infusion was well tolerated and may provide an effective therapeutic approach to prevent bone loss and fracture in people with acute SCI. The findings of this study have important implications for timing and frequency of administration of this drug in the setting of acute SCI.

Specific Aim 2: Evaluate Use of Serum Bone Biomarkers to Guide Therapeutic Decisions

At year 1, parametric modeling did not detect significant differences in CTX-1 (p=0.081), P1NP (p=0.253) and BSAP (p=0.891) between participants who received ZOL versus participants who received placebo only. (See

Table 4 in the Appendix for bone marker values.) Significant differences in biomarkers of bone turnover between groups were not observed until 24 months, and even then, these differences were primarily observed between participants who received two annual infusions of zoledronic acid and those who received two years of placebo. Given the inherent variability in systemic markers of bone turnover, this was not entirely unexpected, but the observed increases in spine aBMD provides confidence that drug was delivered appropriately and attempted to perform its intended action.

Based on these data, it would not appear that serum bone biomarkers would provide useful information at a group level for making decisions. Analysis is on-going at the individual participant level but it is unlikely that these results will show utility. While group-specific differences in serum bone biomarkers have been shown to differentiate treated from untreated individuals with osteoporosis, they have not been shown to be of value in reflecting BMD responses at the individual participant level in clinical studies.

Specific Aim 3: Quantify changes in torsional and compressive strength at the distal femur and proximal tibia

This task is in progress and is currently 50% complete. A semi-automatic workflow for model generation was developed for this work. Preliminary models were generated from patient imaging data, and closely reviewed to confirm that models were error free. Currently all manual image analysis steps, necessary for model generation, are done for the entirety of the two-year dataset. Automated model generation, and physics-based simulation is currently in progress. This step, and subsequent data analysis will be completed within the next 3 months and a manuscript will be prepared to be submitted late in the year.

Although we have yet to quantify the impact of ZOL on torsional and compressive strength at the knee, we did publish a study utilizing the baseline data from this cohort of patients. This cross-sectional study demonstrated that individuals with SCI experienced rapid and profound reductions in bone stiffness and bone mineral at the knee. Finite element models predicted similar reductions to axial and torsional stiffness, suggesting that both failure modes may be clinically relevant. Importantly, CT-derived measures of bone mineral alone underpredicted the impacts of SCI on bone fragility, when compared to finite element predictions of stiffness.

4) Other Achievements

- Achieving target enrollment goal of 60 patients with acute SCI.
- Retention rate of 82%: 49 out of 60 randomized patients completed the final study visit at 24 months

What opportunities for training and professional development has the project provided?
There have been 5 post-doctoral fellows who have participated in this project and for whom this project has provided valuable training and professional development.

Northwestern University:

- Dr. Elaine Gregory spent her post-doctoral year managed recruitment for this study, performing study visit, and evaluating labs and adverse events.
- Dr. Aman Saini spent his post-doctoral year assisting with patient recruitment and performing study visits. He is currently in a residency program in Physical Medicine and Rehabilitation at Marianjoy Rehabilitation Hospital (class of 2022)
- Dr. Frances Leung spent her postdoctoral year scheduling and performing study visits. She was accepted and is currently attending a medical residency program.
- Dr. Joana Barroso has helped with clinical evaluations for the study as well writing the statistical analysis plan, carrying out analysis, and drafting the final manuscript.

University of Calgary:

- Dr. Ifaz Haider has been involved throughout the course of the study. He has been integral in analyzing all CT data and drafting and editing the final manuscript.

Additionally, this project has provided the PI the opportunity to attend professional meetings (American Society of Bone and Mineral Research) to discuss data with others in the field. The post-doctoral fellow at the University of Calgary has written two journal articles and made multiple presentations using data collected from this study at relevant scientific conferences.

How were the results disseminated to communities of interest?

Portions of the data collected have been utilized for abstracts and presented at the American Society of Bone and Mineral Research meetings in 2018 and 2020, and published in Osteoporosis International and in the Annals of Biomedical Engineering. The final manuscript is currently under review for publication in the Journal of Bone Mineral Research.

Results of the study have been added to the study record in ClinicalTrials.gov and are now available for public viewing. Additionally, information regarding bone health in patients with spinal cord injury has been presented to patient groups at Shirley Ryan AbilityLab every 3-6 months in a lecture, though these lectures have temporarily ceased since the Covid pandemic begun.

What do you plan to do during the next reporting period to accomplish the goals?
Nothing to Report.

4. IMPACT:

What was the impact on the development of the principal discipline(s) of the project?
The results of this study are not publicly available as of yet. The baseline demographics (Table 1), the primary and secondary endpoint data (Tables 2 and 3) along with graphs depicting these endpoints (Figures 1 and 2) are included in this report.

As noted above, some of the baseline data have been incorporated into abstracts presented at this discipline's primary professional meeting, the American Society of Bone and Mineral Research meeting (2018 and 2020) and published in relevant journals.

It is anticipated that these results will lead some physiatrists to consider use of zoledronic acid as treatment after acute SCI. Additionally, these results will serve as an impetus for further study of potent anti-resorptive agents and even anabolic agents that may have a more profound effect on bone metabolism after SCI, particularly at the skeletal sites around the knee.

What was the impact on other disciplines?
The results of this study are not yet publicly available as we are awaiting acceptance for publication in the Journal of Bone and Mineral Research.

What was the impact on technology transfer?
Nothing to report.

What was the impact on society beyond science and technology?
Nothing to report.

5. CHANGES/PROBLEMS:

Changes in approach and reasons for change
Nothing to report.

Actual or anticipated problems or delays and actions or plans to resolve them

There was a delay at the beginning of the grant in obtaining HRPO approval, which was attained at the end of January 2015. With this delay, all milestones were pushed forward by 4 months. Recruitment, which was planned to begin in November 2014, began in February 2015. Recruitment was largely on track until Mach 2017, when the hospital at which we worked moved one block away to a new building. This move significantly disrupted our recruitment and study processes for almost 4 months. However, we were able to resume recruitment and finish enrollment of all 60 patients in 25 months.

In March 2020, the final study visit was completed, immediately before our research site was directed to close by our institution due to the Covid-19 pandemic. The City of Chicago announced a stay-at-home order effective March 21, 2020, and research staff was limited to work at home until the end of June, 2020, when the university allowed a partial re-opening of the clinical research space and operations. During the study at home orders, we were able to continue work on and finalize the statistical analysis plan for the study. However delays still occurred in completing DXA and CT scan analyses, final data entry into the REDCap database, shipment of frozen samples to an outside laboratory for testing, and the final DSMC meeting, as safety data from participants' research charts could not be accessed from home.

Changes that had a significant impact on expenditures
There were 2 significant delays impacting expenditures in the project that have been previously documented. The first was due to time taken to get regulatory approvals in place. The second was due to the fact that the hospital where we recruit subjects moved into a new building and suspended all research activities for several months. Based on these delays, we reduced the effort of various research staff throughout these periods. The subcontract with this hospital was renegotiated. Additionally, as recruitment was somewhat slower than had been forecast, we were able to manage data collection and participants' involvement with fewer resources, allowing us to have funds remaining to allow full data collection of all 60 participants, which was the prespecified enrollment target. We have already been granted two 12 month no cost extensions for the previous two years.

Additionally, as detailed above, the Covid pandemic created additional delays as we were not able to be present in the office to complete procedures scheduled to be done after the last study visit. This latter delay has resulted in our having to utilize departmental funding to provide partial support to personnel during this time to allow their continued employment which was essential for the completion of the study. We requested and were granted an additional 6 month extension to the award duration, though without additional funding.

Significant changes in use or care of human subjects, vertebrate animals, biohazards, and/or select agents
Nothing to report.

Significant changes in use or care of human subjects
Nothing to report.

Significant changes in use or care of vertebrate animals.
Not applicable.

Significant changes in use of biohazards and/or select agents
Not applicable.

6. PRODUCTS:

Publications, conference papers, and presentations

Barroso J, Simonian N, Haider I, Edwards WB, Schnitzer. Zoledronic acid and ambulation ability on hip bone mineral density in acute spinal cord injury: A randomized controlled trial. Poster Presentation at the Association of Academic Physiatrists Meeting, Virtual Event, February 2021.

Haider I, Simonian N, Barroso J, Edwards WB, Schnitzer, TJ. Effects of Zoledronic Acid and Ambulation on Hip Bone Mineral Density after Acute Spinal Cord Injury: Year 1 of a Randomized Controlled Trial. Poster Presentation at the American Society for Bone and Mineral Research Annual Meeting, Virtual Event, September 11-15, 2020.

Haider IT, Lobos SM, Simonian N, Schnitzer TJ, Edwards WB. Finite Element Predicted Fracture Strength at Distal Femur and Proximal Tibia Under Biaxial Loading. Podium Presentation at the Congress of the International Society of Biomechanics (ISB) Meeting, Calgary, July 31-August 4, 2019.

Haider I, Lobos S, Simonian N, Schnitzer TJ, Edwards WB. Bone Fragility after Spinal Cord Injury: Reductions in Stiffness and Bone Mineral at the Distal Femur and Proximal Tibia as a Function of Time. Poster Presentation at the American Society for Bone and Mineral Research Annual Meeting, Montreal, Canada, September 28-October 1, 2018.

Journal publications
Haider IT, Simonian N, Schnitzer TJ, Edwards WB (2020). Stiffness and Strength Predictions from Finite Element Models of the Knee are Associated with Lower-Limb Fractures after Spinal Cord Injury. *Annals of Biomedical Engineering*. PMID 32929557 DOI: 10.1007/s10439-020-02606-w

Haider I, Lobos S, Simonian N, Schnitzer TJ, Edwards WB (2018). Bone Fragility after Spinal Cord Injury: Reductions in Stiffness and Bone Mineral at the Distal Femur and Proximal Tibia as a Function of Time. *Osteoporosis International*, 29(12):2703-2715. doi:10.1007/s00198-018-4733-0.

Books or other non-periodical, one-time publications. Other publications, conference papers, and presentations.
Nothing to report.

Website(s) or other Internet site(s)
Nothing to report.

Technologies or techniques
Nothing to report.

Inventions, patent applications, and/or licenses
Nothing to report.

Other Products
Nothing to report.

7. PARTICIPANTS & OTHER COLLABORATING ORGANIZATIONS

What individuals have worked on the project?

Name:	***Thomas J. Schnitzer, MD, PhD***
Project Role:	*Principal Investigator*
Researcher Identifier (e.g. ORCID ID):	*N/A*
Nearest person month worked:	*2*
Contribution to Project:	*Dr. Schnitzer provided oversight of regulatory and recruitment activities for this project.*
Funding Support:	*Additional funding as outlined in the section below*
Name:	***Narina Simonian, BS, CCRC***
Project Role:	*Lead Study Coordinator*
Researcher Identifier (e.g. ORCID ID):	*n/a*
Nearest person month worked:	*7*
Contribution to Project:	*Mrs. Simonian obtained and maintained regulatory approvals, performed study visits, analyzed DXA scans, and entered data*

	into database.
Funding Support:	*No change*
Name:	***W. Brent Edwards, PhD***
Project Role:	*Principal Investigator (University of Calgary)*
Researcher Identifier (e.g. ORCID ID):	*n/a*
Nearest person month worked:	*3*
Contribution to Project:	*Dr. Edwards was responsible for CT data analysis.*
Funding Support:	*No change*
Name:	***Joana Barroso, MD***
Project Role:	*Post-Doctoral Fellow*
Researcher Identifier (e.g. ORCID ID):	*n/a*
Nearest person month worked:	*2*
Contribution to Project:	*Dr. Barroso helped with physical exams and data analysis.*
Funding Support:	*No change*
Name:	***Ifaz Haider, PhD***
Project Role:	*Post-Doctoral Fellow (University of Calgary)*
Researcher Identifier (e.g. ORCID ID):	*n/a*
Nearest person month worked:	*3*
Contribution to Project:	*Dr. Haider assisted with CT data analysis.*
Funding Support:	*No change*
Name:	***Ryan Pelo***
Project Role:	*Recruitment Coordinator*
Researcher Identifier (e.g. ORCID ID):	*n/a*
Nearest person month worked:	*1*
Contribution to Project:	*Mr. Pelo helped with identifying potential subjects*
Funding Support:	*No change*
Name:	***Matthew Ryan Giffhorn***
Project Role:	*Recruitment Coordinator*
Researcher Identifier (e.g. ORCID ID):	*n/a*
Nearest person month worked:	*1*
Contribution to Project:	*Mr. Pelo helped with identifying potential subjects*
Funding Support:	*No change*

Name:	***Amy Marie Lange***
Project Role:	*Back-up Coordinator*
Researcher Identifier (e.g. ORCID ID):	*n/a*
Nearest person month worked:	*1*
Contribution to Project:	*Ms Lange managed recruitment and performed study visits.*
Funding Support:	*No change*
Name:	***Renita Yeasted***
Project Role:	*Back-up Coordinator*
Researcher Identifier (e.g. ORCID ID):	*n/a*
Nearest person month worked:	*2*
Contribution to Project:	*Mrs. Yeasted managed regulatory approvals, recruitment and performed study visits.*
Funding Support:	*No change*
Name:	***Kendra Harmon***
Project Role:	*Research Assistant*
Researcher Identifier (e.g. ORCID ID):	*n/a*
Nearest person month worked:	*1*
Contribution to Project:	*Ms. Harmon assisted with recruitment and the consent process.*
Funding Support:	*No change*
Name:	***Elaine Gregory, MD***
Project Role:	*Post-Doctoral fellow*
Researcher Identifier (e.g. ORCID ID):	*n/a*
Nearest person month worked:	*5*
Contribution to Project:	*Dr. Gregory managed recruitment, performed study visits, and evaluated labs and adverse events.*
Funding Support:	*No change*
Name:	***Amanpreet Saini, MD***
Project Role:	*Research Intern*
Researcher Identifier (e.g. ORCID ID):	*n/a*
Nearest person month worked:	*5*
Contribution to Project:	*Dr. Saini assisted with recruitment and study visits.*
Funding Support:	*No change*

Name:	***Frances Leung, MD***
Project Role:	*Post-doctoral fellow*
Researcher Identifier (e.g. ORCID ID):	*n/a*
Nearest person month worked:	*3*
Contribution to Project:	*Dr. Leung helped with scheduling visit, data management, and data entry*
Funding Support:	*No change*

Has there been a change in the active other support of the PD/PI(s) or senior/key personnel since the last reporting period?
No change from th previous reporting period.

What other organizations were involved as partners?

Organization Name: University of Calgary
Location of Organization: Calgary, Alberta, Canada
Partner's contribution to the project: The entirety of Aim 3 was accomplished at the University of Calgary. They have provided space and partial personnel support.
In-kind support: Partial personnel support.
Collaboration: Partner's staff work with project staff on the project

Organization Name: Shirley Ryan AbilityLab (previously known as Rehabilitation Institute of Chicago (RIC))
Location of Organization: Chicago, IL, USA
Partner's contribution to the project: Access to patients
Facilities: Project staff use the partner's facilities for project activities; participants were recruited from this facility
Collaboration: Partner's staff work with project staff on the project

8. SPECIAL REPORTING REQUIREMENTS

COLLABORATIVE AWARDS:
Not applicable.

QUAD CHARTS:
Attached

APPENDICES:

Appendix A. Reference List

Appendix B. Tables

Appendix C. Copies of Publications, Abstracts, and Presentations

Appendix D. Quad Chart

Appendix A. Reference List

1. Biering-Sorensen F, Bohr HH, Schaadt OP. Longitudinal study of bone mineral content in the lumbar spine, the forearm and the lower extremities after spinal cord injury. European journal of clinical investigation. 1990;20(3):330-5.
2. Eser P, Frotzler A, Zehnder Y, Wick L, Knecht H, Denoth J, et al. Relationship between the duration of paralysis and bone structure: a pQCT study of spinal cord injured individuals. Bone. 2004;34(5):869-80.
3. Alexandre C, Vico L. Pathophysiology of bone loss in disuse osteoporosis. Joint, bone, spine : revue du rhumatisme. 2011;78(6):572-6.
4. Jiang SD, Dai LY, Jiang LS. Osteoporosis after spinal cord injury. Osteoporosis international : a journal established as result of cooperation between the European Foundation for Osteoporosis and the National Osteoporosis Foundation of the USA. 2006;17(2):180-92.
5. Roberts D, Lee W, Cuneo RC, Wittmann J, Ward G, Flatman R, et al. Longitudinal study of bone turnover after acute spinal cord injury. The Journal of clinical endocrinology and metabolism. 1998;83(2):415-22.
6. Edwards WB, Schnitzer TJ, Troy KL. Bone mineral loss at the proximal femur in acute spinal cord injury. Osteoporosis international : a journal established as result of cooperation between the European Foundation for Osteoporosis and the National Osteoporosis Foundation of the USA. 2013;24(9):2461-9.
7. Edwards WB, Schnitzer TJ, Troy KL. Bone mineral and stiffness loss at the distal femur and proximal tibia in acute spinal cord injury. Osteoporosis international : a journal established as result of cooperation between the European Foundation for Osteoporosis and the National Osteoporosis Foundation of the USA. 2014;25(3):1005-15.
8. Lang T, LeBlanc A, Evans H, Lu Y, Genant H, Yu A. Cortical and trabecular bone mineral loss from the spine and hip in long-duration spaceflight. Journal of bone and mineral research : the official journal of the American Society for Bone and Mineral Research. 2004;19(6):1006-12.
9. Edwards WB, Simonian N, Troy KL, Schnitzer TJ. Reduction in Torsional Stiffness and Strength at the Proximal Tibia as a Function of Time Since Spinal Cord Injury. J Bone Miner Res. Aug 2015;30(8):1422-30. Epub 2015/05/21.
10. Vestergaard P, Krogh K, Rejnmark L, Mosekilde L. Fracture rates and risk factors for fractures in patients with spinal cord injury. Spinal cord : the official journal of the International Medical Society of Paraplegia. 1998;36(11):790-6.
11. Morse LR, Battaglino RA, Stolzmann KL, Hallett LD, Waddimba A, Gagnon D, et al. Osteoporotic fractures and hospitalization risk in chronic spinal cord injury. Osteoporosis international : a journal established as result of cooperation between the European Foundation for Osteoporosis and the National Osteoporosis Foundation of the USA. 2009;20(3):385-92.
12. Gifre L, Vidal J, Carrasco J, Portell E, Puig J, Monegal A, et al. Incidence of skeletal fractures after traumatic spinal cord injury: a 10-year follow-up study. Clinical rehabilitation. 2014;28(4):361-9.
13. Carbone LD, Chin AS, Burns SP, Svircev JN, Hoenig H, Heggeness M, et al. Mortality after lower extremity fractures in men with spinal cord injury. Journal of bone and mineral research : the official journal of the American Society for Bone and Mineral Research. 2014;29(2):432-9.
14. Garland DE, Adkins RH. Bone loss at the knee in spinal cord injury. Topics in Spinal Cord Injury Rehabilitation. 2001;6(3):37-46.
15. Logan WC, Jr., Sloane R, Lyles KW, Goldstein B, Hoenig HM. Incidence of fractures in a cohort of veterans with chronic multiple sclerosis or traumatic spinal cord injury. Archives of Physical Medicine and Rehabilitation. 2008;89(2):237-43.
16. Brotherton SS, Krause JS, Nietert PJ. Falls in individuals with incomplete spinal cord injury. Spinal cord. 2007;45(1):37-40.
17. Comarr AE, Hutchinson RH, Bors E. Extremity fractures of patients with spinal cord injuries. American Journal of Surgery. 1962;103:732-9.
18. Fournier A, Golerberg M, Green B, Brucker B, Petrofsky J, Eismont F, et al. Medical evaluation of the effects of computer assisted muscle stimulation in paraplegic patients. Orthopedics. 1984;7:1129-33.
19. Hartkopp A, Murphy RJ, Mohr T, Kjaer M, Biering-Sorensen F. Bone fracture during electrical stimulation of the quadriceps in a spinal cord injured subject. Archives of Physical Medicine and Rehabilitation. 1998;79(9):1133-6.
20. Gilchrist NL, Frampton CM, Acland RH, Nicholls MG, March RL, Maguire P, et al. Alendronate prevents bone loss in patients with acute spinal cord injury: a randomized, double-blind, placebo-controlled study. The Journal of clinical endocrinology and metabolism. 2007;92(4):1385-90.

21. Bauman WA, Wecht JM, Kirshblum S, Spungen AM, Morrison N, Cirnigliaro C, et al. Effect of pamidronate administration on bone in patients with acute spinal cord injury. Journal of rehabilitation research and development. 2005;42(3):305-13.
22. Nance PW, Schryvers O, Leslie W, Ludwig S, Krahn J, Uebelhart D. Intravenous pamidronate attenuates bone density loss after acute spinal cord injury. Archives of Physical Medicine and Rehabilitation. 1999;80(3):243-51.
23. Shapiro J, Smith B, Beck T, Ballard P, Dapthary M, BrintzenhofeSzoc K, et al. Treatment with zoledronic acid ameliorates negative geometric changes in the proximal femur following acute spinal cord injury. Calcified tissue international. 2007;80(5):316-22.
24. Bubbear JS, Gall A, Middleton FR, Ferguson-Pell M, Swaminathan R, Keen RW. Early treatment with zoledronic acid prevents bone loss at the hip following acute spinal cord injury. Osteoporos Int. Jan 2011;22(1):271-9. Epub 2010/04/01.
25. Bauman WA, Cirnigliaro CM, La Fountaine MF, Martinez L, Kirshblum SC, Spungen AM. Zoledronic acid administration failed to prevent bone loss at the knee in persons with acute spinal cord injury: an observational cohort study. J Bone Miner Metab. Jul 2015;33(4):410-21. Epub 2014/08/27.
26. Schnitzer TJ, Kim K, Marks J, Yeasted R, Simonian N, Chen D. Zoledronic Acid Treatment After Acute Spinal Cord Injury: Results of a Randomized, Placebo-Controlled Pilot Trial. PM R. 09 2016;8(9):833-43. Epub 2016/01/30.
27. Oleson CV, Marino RJ, Formal CS, Modlesky CM, Leiby BE. The effect of zoledronic acid on attenuation of bone loss at the hip and knee following acute traumatic spinal cord injury: a randomized-controlled study. Spinal Cord. Aug 2020;58(8):921-9. Epub 2020/02/13.
28. Goenka S, Sethi S, Pandey N, Joshi M, Jindal R. Effect of early treatment with zoledronic acid on prevention of bone loss in patients with acute spinal cord injury: a randomized controlled trial. Spinal Cord. 12 2018;56(12):1207-11. Epub 2018/09/26.

Appendix B. Tables

Table 1. Baseline demographic data. ZOL group received an infusion of zoledronic acid at baseline and placebo group received saline. Sex was the only significantly different characteristic between the two groups, with p = 0.045. T-tests were performed for continuous data. Chi-square and ANOVA tests were performed for categorical differences.

	ZOL (n=30)	Placebo (n=30)	All Participants (n=60)
Age (years), mean, SD	37.3 ± 15.9	38.2 ± 15.2	37.8 ± 15.4
Sex (male), n, %	21; 70%	27; 90.0%	48; 80.0%
BMI (kg/m^2), mean, SD	25.9 ± 6.0	25.0 ± 5.2	25.5 ± 5.6
Ethnicity (Hispanic/Latino), n, %	4; 13.3%	7; 23.3%	11; 18.3%
Race, n, %			
American Indian/Alaska Native	0; 0%	0; 0%	0; 0%
Asian	2; 6.7%	1; 3.3%	3; 5.0%
Black/African American	8; 26.7%	6; 20.0%	14; 23.3%
Native Hawaiian/Other Pacific Islander	0; 0%	0; 0%	0; 0%
White	20; 66.7%	21; 70.0%	41; 68.3%
More than one race	0; 0%	2; 6.7%	2; 3.3%s
Unknown or Not Reported	0; 0%	0; 0%	0; 0%
WISCI Level, mean, SD	1.2 ± 2.8	1.9 ± 3.6	1.6 ± 3.2
Time Since SCI (days), mean, SD	68.7 ± 28.5	62.7 ± 23.2	65.7 ± 25.9
ASIA Impairment Scale, n, %			
A	12; 40.0%	12; 40.0%	24; 40.0%
B	6; 20.0%	7; 23.3%	13; 21.7%
C	10; 33.3%	8; 26.7%	18; 30.0%
D	2; 6.7%	3; 10.0%	5; 8.3%
Injury Severity, n, %			
Motor Complete	18; 60.0%	19; 63.3%	37; 60.0%
Level, n, %			
Cervical	17; 56.7%	17; 56.7%	34; 56.7%
Thoracic	10; 33.3%	11; 36.7%	21; 35.0%
Lumbar	3; 10.0%	2; 6.7%	5; 8.3%

BMI = body mass index; WISCI = Walking Index of Spinal Cord Injury II; ASIA = American Spinal Injury Association (ASIA)

Table 2. Percent change from baseline over time in BMD in ZOL and Placebo groups at 6 and 12 Months. Statistical significance values derived from mixed model analysis, where subjects were modeled as random effects and treatment group as a fixed effect. Baseline outcome values and WISCI scores were added as covariables in the model (fixed effects). **<0.01; *<0.05

% change from baseline (m±sd)	Spine aBMD	Hip aBMD	Femoral Neck (FN) aBMD	Epiphyseal tBMC	Epiphyseal iBMC	Metaphyseal iBMC
ZOL						
6 Mo	2.16 ± 3.55	-1.9± 4.91	-2.55 ± 4.44	-6.11 ± 11.71	-6.65 ± 8.29	-4.33 ± 6.77
12 Mo	3.6 ± 3.43	-1.78 ± 6.68	-2.35 ± 3.54	-15.24 ± 18.54	-11.04 ± 15.37	-7.74 ± 8.36
PLA						
6 Mo	-1.98 ± 3.67	-10 ± 6.97	-9.21 ± 5.97	-16.05 ± 16.72	-15.05± 11.80	-9.15 ± 8.47
12 Mo	-1.25 ± 6.02	-14.25 ± 8.97	-13.52± 8.38	-27.5 ± 22.16	-24.4 ± 17.25	-13.98 ± 13.31
p-values	0.048*	<0.001**	<0.001**	0.023*	0.004**	0.04*

Table 3. Percent change from baseline over time in BMD in the 4 groups (based on treatment assignment at 0 and 12 mo visits): ZOL+ZOL, ZOL+Placebo, Placebo+ZOL and Placebo+Placebo at 6, 12 and 24 Months.

% change from baseline (m±sd)	Spine aBMD	Hip aBMD	Femoral Neck (FN) aBMD	Epiphyseal tBMC	Epiphyseal iBMC	Metaphyseal iBMC
ZOL + ZOL						
6 Mo	1.21 ± 4.85	-1.57 ± 3.51	-2.54 ± 3.89	-6.18 ± 12.04	-5.37 ± 6.37	-3.94 ± 5.91
12 Mo	2.69 ± 3.27	-3.07 ± 5.29	-2.96 ± 2.62	-17.65 ± 22.20	-11.62 ± 9.85	-6.55 ± 6.79
24 Mo	5.5 ± 4.00	-4.31 ± 8.24	-2.88 ± 5.85	-29.73 ± 31.29	-22.15 ± 20.52	-13.27 ± 14.61
ZOL + PLA						
6 Mo	2.83 ± 2.28	-2.16 ± 5.9	-2.56 ± 4.97	-6.05 ± 11.96	-7.63 ± 9.53	-4.65 ± 7.65
12 Mo	4.21 ± 3.54	-0.82 ± 7.93	-1.89 ± 4.15	-13.27 ± 15.76	-10.64 ± 18.66	-8.72 ± 9.68
24 Mo	6.13 ± 4.57	-8.1 ± 10.39	-5.9 ± 9.85	-28.98 ± 30.73	-22.36 ± 28.05	-17.15 ± 16.57
PLA + ZOL						
6 Mo	-0.5 ± 3.70	-9.21 ± 8.30	-8.67 ± 6.86	-15.06 ± 18.16	-14.05 ± 14.48	-9.11 ± 9.05
12 Mo	-0.79 ± 5.4	-13.18 ± 9.30	-13.75 ± 7.5	-29.1 ± 25.36	-24.56 ± 20.51	-14.1 ± 13.69
24 Mo	3.08 ± 7.25	-12.36 ± 9.50	-12.14 ± 9.80	-37.72 ± 31.47	-29.95 ± 22.23	-19.46 ± 17.63
PLA + PLA						
6 Mo	-2.94 ± 3.41	-11.5 ± 6.07	-9.59 ± 5.52	-16.86 ± 16.1	-15.86 ± 9.62	-9.2 ± 8.31
12 Mo	-1.67 ± 6.20	-15.22 ± 6.80	-13.31 ± 8.90	-25.88 ± 9.46	-24.24 ± 19.45	-13.86 ± 11.38
24 Mo	-1.19 ± 8.96	-18.77 ± 10.1	-16.57 ± 9.4	-38.06 ± 27.72	-32.94 ± 19.74	-22.35 ± 16.97

Table 4. Serum biomarker levels over study duration. Parametric modelling revealed no significant differences after month 12. After month 24, individuals who received ZOL throughout (Z-Z) had lower biomarker levels compared to those who received placebo throughout (P-P) and ZOL followed by placebo (Z-P).

		Serum Biomarkers					
Group	Time (months)	CTX-1 (ng/mL)		P1NP (ng/mL)		BSAP (µg/mL)	
		Median	IQR	Median	IQR	Median	IQR
Z-Z	0	0.67	0.63	93.4	91.6	10.32	4.58
	6	0.14	0.15	63.11	39.290	8.97	3.45
	12	0.12	0.14	40.47	34.68	11.81	6.72
	24	0.06	0.08	29.26	10.93	11.01	3.12
Z-P	0	0.62	0.8	106.7	115.25	11.07	4.2
	6	0.22	0.13	59.46	32.3	10.67	4.48
	12	0.26	0.2	55.92	29.39	13.31	4.47
	24	**0.21**	**0.25**	**65.11**	**36.83**	**14.99**	**4.38**
P-Z	0	0.62	0.97	117.9	91.77	12.04	8.01
	6	0.25	0.15	83.43	55.91	14	6.14
	12	0.25	0.35	69.29	65.06	12.06	8.03
	24	0.11	0.18	30.81	20.71	11.13	6.07
P-P	0	0.5	0.41	79.53	86.5	10.43	3.81
	6	0.29	0.11	78.01	28.81	12.03	9.6
	12	0.19	0.12	69.24	34.72	14.2	8.04
	24	**0.14**	**0.14**	**59.47**	**33.28**	**14.01**	**5.65**

Bold indicates $p < 0.05$ relative to Z-Z group.
Z-Z = ZOL year 1 and 2; Z-P = ZOL year 1, placebo year 2; P-Z = placebo year 1, ZOL year 2; P-P = Placebo in year 1 and 2.

Table 5. Adverse Event Summary. Frequency of occurrence of the most common adverse events (AEs), reported 4 or more times in a given treatment group, over study duration. AEs are classified based on the study treatment year during which they occurred, either while on zoledronic acid (ZOL) or while on placebo.

Adverse Event Name	ZOL	Pla	Total
Urinary Tract Infection	41	52	93
Acute Phase Response	31	6	37
Upper Respiratory Infection	5	9	14
Pressure Ulcer	5	7	12
Hypertension	6	6	12
Myalgia	4	6	10
Joint pain	3	7	10
Heterotopic Ossification (new or worsened)	5	4	9
Autonomic Dysreflexia	4	4	8
Spasticity (new or worsened)	5	2	7
Neuropathy (new or worsened)	2	5	7
Fever	4	3	7
Allergic Reaction (unrelated to study treatment)	2	5	7
Thrombus	1	5	6
Paresthesia	0	5	5
Chills	4	1	5

Appendix C. Copies of Publications, Abstracts, and Presentations

Publications, conference papers, and presentations

1. Barroso J, Simonian N, Haider I, Edwards WB, Schnitzer. Zoledronic acid and ambulation ability on hip bone mineral density in acute spinal cord injury: A randomized controlled trial. Poster Presentation at the Association of Academic Physiatrists Meeting, Virtual Event, February 2021.

2. Haider I, Simonian N, Barroso J, Edwards WB, Schnitzer, TJ. Effects of Zoledronic Acid and Ambulation on Hip Bone Mineral Density after Acute Spinal Cord Injury: Year 1 of a Randomized Controlled Trial. Poster Presentation at the American Society for Bone and Mineral Research Annual Meeting, Virtual Event, September 11-15, 2020.

3. Haider IT, Lobos SM, Simonian N, Schnitzer TJ, Edwards WB. Finite Element Predicted Fracture Strength at Distal Femur and Proximal Tibia Under Biaxial Loading. Podium Presentation at the Congress of the International Society of Biomechanics (ISB) Meeting, Calgary, July 31-August 4, 2019.

4. Haider I, Lobos S, Simonian N, Schnitzer TJ, Edwards WB. Bone Fragility after Spinal Cord Injury: Reductions in Stiffness and Bone Mineral at the Distal Femur and Proximal Tibia as a Function of Time. Poster Presentation at the American Society for Bone and Mineral Research Annual Meeting, Montreal, Canada, September 28-October 1, 2018.

Journal publications

1. Haider IT, Simonian N, Schnitzer TJ, Edwards WB (2020). Stiffness and Strength Predictions from Finite Element Models of the Knee are Associated with Lower-Limb Fractures after Spinal Cord Injury. *Annals of Biomedical Engineering*. PMID 32929557 DOI: 10.1007/s10439-020-02606-w

2. Haider I, Lobos S, Simonian N, Schnitzer TJ, Edwards WB (2018). Bone Fragility after Spinal Cord Injury: Reductions in Stiffness and Bone Mineral at the Distal Femur and Proximal Tibia as a Function of Time. *Osteoporosis International*, 29(12):2703-2715. doi:10.1007/s00198-018-4733-0.

Abstracts of Scientific Papers and Posters Presented at Physiatry '21

February 9–13, 2021

BEST PAPER PRESENTATIONS

Faculty Category Award Winner
OPIOID USE AND SOCIAL DISADVANTAGE IN PATIENTS WITH CHRONIC MUSCULOSKELETAL PAIN

Brian K. Brady, BA, Ethan Bradley, BA, Heidi Prather, DO, Ryan Calfee, MD, MSC, Lisa M. Klesges, PhD, MS, Graham Colditz, MD, DRPH, and Abby L. Cheng, MD

OBJECTIVES: Historically, non-white patients were prescribed less opioid medication than white patients. However, because of persistent differential access to non-opioid pain treatments, this direction of disparity in opioid prescribing may have reversed. This study compared social disadvantage and self-reported health in patients with chronic pain who are currently managed with versus without chronic opioid treatment.

DESIGN: In this cross-sectional analysis of a retrospective cohort, medical record data between 2000 and 2019 was reviewed from a single tertiary academic medical center. Adult patients followed for chronic musculoskeletal pain were sub-grouped by chronic adherent opioid usage versus no opioid usage. The primary comparison was the prevalence difference of social disadvantage in patients using versus not using opioids, measured by living in a zip code within the worst national quartile of the Area Deprivation Index. Secondary outcomes included differences in self-reported health by opioid use (measured by Patient-Reported Outcomes Measurement Information System (PROMIS)), after controlling for age, sex, race, and social disadvantage.

RESULTS: In 1,173 patients (356 chronic opioid users), compared to non-opioid patients, chronic opioid patients were more likely to live in a zip code within the most socially disadvantaged national quartile (34.9% [95%CI 29.9% to 39.9%] vs 24.9% [21.9% to 28.0%], $p < .001$). Opioid use was independently associated with clinically relevant worse PROMIS Depression (3.8 points [2.4 to 5.1]), Anxiety (3.0 [1.4 to 4.5]), and Pain Interference (2.6 [1.7 to 3.5]) scores.

CONCLUSIONS: Patients on chronic opioids were more likely to live in socially disadvantaged neighborhoods, and chronic opioid use was independently associated with worse behavioral health. Improving access to multidisciplinary, non-opioid treatments for chronic pain may be a key approach to successfully overcoming the opioid crisis.

Resident Category Award Winner
DEVELOPING A NOVEL PRE-CLINICAL MODEL OF CANCER REHABILITATION

Ishan Roy, MD, PhD, Benjamin I. Binder-Markey, DPT, PhD,
Danielle Sychowski, BA, Donna McAllister, Dominic D'Andrea, BS,
Colin K. Franz, MD, PhD, Michael Dwinell, PhD, and Richard L. Lieber, PhD

OBJECTIVES: Current knowledge regarding the physiologic mechanisms of functional decline from cancer is poor due to the lack of longitudinal models of cancer. The primary goal of this study was to develop a rehabilitation relevant model of cancer-associated cachexia by identifying a candidate animal model of cancer for optimization using translationally and functionally relevant and then validating the optimized model using longitudinal and functional measures.

DESIGN: After a PubMed MEDLINE search, existing animal models of cancer-associated cachexia were evaluated for five criteria: expression of human-relevant cancer, low cost, longitudinal skeletal muscle loss, cardiac muscle loss, and longitudinal functional decline. Survival of the "KPC orthotopic" pancreatic cancer mouse model was optimized by modifying cell line, cell dose, and vehicle type. *In vivo* muscle volume was measured by micro-computerized tomography. *Ex vivo* analysis included skeletal muscle mass, cardiac mass, and tumor mass. Function was measured using hind-limb grip strength.

RESULTS: Out of the eight existing models of cachexia, none met more than three out of five criteria for translational relevance. The KPC model expressed human relevant cancer and was low cost, but had a short survival period of only 2-3 weeks. Using a matrix of serial dose titrations of multiple cell clones in distinct injection vehicles, we successfully extended the survival of the KPC model to a median survival of 60 days ($p < 0.0001$). *In* and *ex vivo* tissue analysis showed that the optimized model generated skeletal and cardiac muscle mass loss over a 7-8 week time-course ($p < 0.01$). Under optimized conditions, animals had significant decline in grip strength 3-4 weeks prior to endpoint ($p=0.003$).

CONCLUSIONS: This is the first study to develop a longitudinal model of cancer or cachexia that leads to longitudinal functional decline. Future studies can now investigate physiologic mechanisms leading to functional change in cancer and test novel rehabilitation interventions targeting those mechanisms.

Medical Student Category Award Winner
USING XSENS AND SELF-REPORT DATA TO ANALYZE ACCOMMODATION TIMES FOR PATIENTS WITH TRANS-TIBIAL PROSTHETICS

Laura S. Weiss, MS, MD CANDIDATE, Brad E. Dicianno, MD, MS,
and Goeran Fiedler, PhD

OBJECTIVES: This study examined accommodation to a new prosthetic foot and investigated whether demographic factors (age and gender) influence accommodation times.

DESIGN: A Greissinger Plus foot was temporarily installed instead of the Energy Storage and Return (ESAR) foot participants customarily used. During the first hour spent walking with the new foot, gait analysis data was obtained using wearable equipment (XsensMVN, Enschede, NL). Participants also repeatedly rated their perceived accommodation using a visual analog scale (VAS).

In post-processing, VAS values were normalized to individual baselines. Assuming a typical "learning curve", logarithmic functions were fitted through each participant's time series. From this, the amount of time required to reach 95% accommodation was extracted as a comparison variable. The sample was stratified by gender and age, and in separate two-sample t-tests the different groups (male vs. female, age < 50 vs. 50+ years) were compared to one another ($\alpha=0.05$). The variable "maximum flexion angle of the impacted knee", extracted from the Xsens data, was similarly analyzed in an attempt to confirm the subjective VAS ratings.

RESULTS: Data from 14 participants (mean age: 51 ± 16 years, three females), was analyzed. Accommodation trajectories and average times to accommodation, after removing outliers, were not significantly different between either comparison groups (age: $p=0.13$; gender: $p=0.23$). Based on self-report data, 95% accommodation was achieved, on average, at 34 minutes. By comparison, the accommodation curves derived from gait analysis data only reached a level of 60 to 70% at this mark.

CONCLUSIONS: While the data shows no statistically significant difference for either age or gender, the found difference in accommodation times between male and female participants may be considered clinically significant. The found inconsistency between self-reported and Xsens data may be due to the inter-subject variability in how the maximum flexion angle changes with accommodation.

SCIENTIFIC PAPER PRESENTATIONS

A DEEP-LEARNING BASED POSE ESTIMATION APPROACH CAN OBJECTIVELY MEASURE REPETITIVE MOVEMENTS

Hannah L. Cornman, BS, Jan Stenum, PhD, and Ryan Roemmich, PhD

OBJECTIVES: There is a need for a rapid, low-cost approach to measurement of repetitive movements in persons with Parkinson's Disease (PD) that is accurate, objective, and uses equipment that is accessible in the home or clinic. Here, we evaluated the ability of OpenPose, a deep learning-based pose estimation algorithm, to detect the frequency at which repetitive movement tasks from the MDS-UPDRS (the standard clinical rating scale for motor dysfunction in PD) were performed by healthy volunteers in videos recorded on a smartphone camera.

DESIGN: Ten healthy volunteers recorded videos of themselves performing repetitive movement tasks (finger tapping, hand open/close, hand pronation/supination, toe tapping, and leg agility) at four target frequencies (1-4 Hz). We estimated movement frequencies using OpenPose and measured by manual frame-by-frame detection for all tasks and target frequencies. The resulting estimates of movement frequencies were compared using a 2x4 condition (OpenPose, manual measurement) x frequency (1, 2, 3, 4 Hz) repeated measures ANOVA. We also performed Pearson's correlations to

was also assessed. Sub-groups analyzed included misoprostol dosage (200 vs. 400 mcg/day), and length of use (≤1 vs. >1 year).

RESULTS: Twenty-three patients were enrolled. Mean scores for SSSQ satisfaction subscale and total score were 63.7% and 66.4%, respectively. Average NRS score was 6.5. 75% of participants showed improvements in the SPWT with misoprostol, with 67% of this group experiencing no NIC symptoms. Additionally, there was a decrease in ODI scores in the post-treatment group, indicating improved functional disability. Individuals who received 400 mcg/day or have taken misoprostol for over 1 year reported higher (worse) scores than their comparison groups in SSSQ and ODI, indicating greater symptom severity and decreased satisfaction.

CONCLUSIONS: Misoprostol appears to have some utility in managing NIC symptoms in patients with LSS. Improvements in claudication distance and ODI are comparable to published studies reporting outcomes from NSAIDs and other pharmacotherapy in LSS. Future high-quality, prospective studies are needed to further characterize benefits, long-term effects, and optimum dosages for this medication.

UTILITY OF THE PRECHTL GENERAL MOVEMENTS ASSESSMENT AND THE HAMMERSMITH INFANT NEUROLOGICAL EXAMINATION IN THE DEVELOPMENTAL SURVEILLANCE OF INFANTS WITH NEUROLOGICAL RISK FACTORS: A CASE SERIES

Ana Dorina Gomez Garcia, Resident, Carlos Publio Viñals Labañino, PM&R, Elsa Alvarado Solorio, PM&R, and Carla Garcia Ramos, MSC

OBJECTIVES: Over the last years many authors have stated that The Motor Optimality Score for 3 to 5 Month-Old infants (MOS) obtained by The Prechtl General Movement Assessment (GMA) in combination with the Hammersmith Infant Neurological Examination (HINE) demonstrate high predictive value and reliability to identify infants at risk of developing Cerebral Palsy (CP). The objective was to identify the association between HINE and MOS total scores and its relationship to cerebral palsy diagnosis, established at 12 months of age in all subjects included in the sample.

DESIGN: We aim to present a case series of infants with neurological risk factors who received medical attention in the Neurodevelopment and Early Stimulation department of a tertiary level hospital. Information was obtained through retrospective review of individual patient electronic files. All patients evaluated between January and December 2018, with recorded MOS and HINE scores at 3 months (initial) and 12 months (final) were included. All parents gave informed consent for their children to participate in our study.

RESULTS: A sample size of 20 patients met the inclusion criteria. Final diagnosis were: CP (35%), Mild Developmental Delay (35%) Global Developmental Delay (10%), Sensory disorder and typical development (5%). Infants with absent Fidgety movements presented an average initial HINE of 49.14 (SD 10.46), final HINE of 47.14 (SD 17.59) and an average MOS of 7.57 (SD 2.50); while the group which exhibited Fidgety movements had an average initial HINE of 59.54 (SD 9.97), final HINE of 69.54 (SD 11.01) and MOS of 22.85 (SD 3.10).

CONCLUSIONS: We observed a strong correlation between Fidgety and the given diagnosis. Initial and final HINE scores show a high sensitivity for the presence of disability in our sample. At an early age GMA and HINE are useful instruments that represent two important cornerstones in the diagnosis of neurodevelopmental disorders.

UTILIZATION OF TRANSCRANIAL DIRECT CURRENT STIMULATION IN POST-STROKE APHASIA REHABILITATION: A REVIEW OF THE RECENT LITERATURE

Jake Gooing, OMS-IV, Mitchell Sauder, OMS-III, Marcel Fraix, DO, MBA, and Caroline Schnakers, PhD

OBJECTIVES: Recently, transcranial direct current stimulation (tDCS) has been studied as a potential non-invasive treatment for post-stroke aphasia. Its low cost, safety, and ease of application has drawn interest as a possible adjunct to speech language therapy. The review of the recent literature serves a purpose to update researchers and health care professionals on recent advancements of tDCS in post-stroke aphasia rehabilitation.

DESIGN: A PubMed search was performed using the following keywords: transcranial direct current stimulation AND aphasia AND stroke on April 29, 2020. Our results were limited to studies published in the past 5 years (between 2016-2020). Studies were considered eligible if tDCS was utilized in stroke related aphasia, the research was completed in humans, and the manuscripts were accessible in English.

RESULTS: Our search resulted in 64 articles, with 53 of them considered eligible. Among these 53 articles, 26 constituted original research while the remaining 27 articles were reviews of tDCS or of tDCS literature. Results showed targeting the left primary motor cortex improved speech function and recruited the areas of the motor speech network, the left inferior frontal gyrus showed improved picture, noun, and verb naming, and the right cerebellum improved verb generation and retrieval. With current tDCS parameters, benefits appear to be limited to chronic aphasia. Patients with damage to the left basal ganglia, insula, and superior/inferior longitudinal fasciculi showed lower response to tDCS whereas those with the Val/Val BDNF genotype are more likely to respond.

CONCLUSIONS: Although current evidence for tDCS improving noun naming is limited, with no evidence demonstrating improved functional communication per 2019 Cochrane review, consensus remains that tDCS may be a viable therapy for aphasia given its cost, ease, and safety profile. Additional research, including larger RCTs, are recommended to further optimize application of tDCS and to further understand the therapeutic mechanisms in post-stroke aphasia rehabilitation.

ZOLEDRONIC ACID AND AMBULATION ABILITY ON HIP BONE MINERAL DENSITY IN ACUTE SPINAL CORD INJURY: RANDOMIZED CONTROLLED TRIAL

Joana Barroso, MD, MSC, Narina Simonian, Ifaz Haider, Brent Edwards, and Thomas J. Schnitzer, PROFESSOR

OBJECTIVES: Spinal cord injury (SCI) is associated with significant decline in bone mineral density (BMD) and bone fragility. Losses in BMD occur rapidly, plateauing 2-5 years after injury. Recently, zoledronic acid (ZOL) has been shown to effectively attenuate bone loss in individuals with acute SCI. However, the durability of treatment is unclear, as is the potential interaction of patient's ability to ambulate.

DESIGN: We report results from a prospective double-blind clinical trial (NCT02325414), assessing the durability of ZOL for the prevention of bone loss in acute SCI. 60 patients were randomized to receive placebo (PBO; n=30) or ZOL (n=30). Areal bone mineral density (aBMD) at the total hip (TH) and femoral neck (FN) was measured at baseline, 6 and 12 months after treatment, as was ambulation ability - walking index for spinal cord injury (WISCI). Linear mixed modeling was applied with baseline aBMD, visit and WISCI score as covariates, examining the effects of treatment group on % change in total hip (TH) and femoral neck (FN) aBMD from baseline.

RESULTS: Significant differences were found for % change in TH and FN aBMD between groups at both the 6 mo and 12 mo time points, $p < 0.001$ (ZOL and PBO % change ±SE at 6 and 12 months: -1.3±1.4 vs -10.4±1.4 for TH; -3.0±1.4 vs -14.9±1.4 for FN). WISCI had a significant effect on % change in both aBMD TH and FN, ($p=0.004$ and 0.028). Although both treatment and WISCI had a positive effect on % change in aBMD, the interaction between these variables was not significant.

CONCLUSIONS: These initial data support the notion that one-year treatment with ZOL effectively attenuates bone loss after SCI. Although ambulation has a positive effect on aBMD change, the benefits of treatment are independent of the ambulatory ability. Further analyses of this cohort over 2-years of treatment is ongoing.

Effects of Zoledronic Acid and Ambulation on Hip Bone Mineral Density after Acute Spinal Cord Injury: Year 1 of a Randomized Controlled Trial

Ifaz T. Haider[1], Narina Simonian[2], Joana Barroso[2], W. Brent Edwards[1], Thomas J. Schnitzer[2]

[1]Human Performance Laboratory, Faculty of Kinesiology and McCaig Institute for Bone and Joint Health, University of Calgary

[2]Northwestern University Feinberg School of Medicine

BACKGROUND

Spinal cord injury (SCI) is associated with significant decline in bone mineral density (BMD) at sublesional locations.

Bone loss occurs rapidly after injury, with BMD reaching a plateau 2-5 years after injury[1].

Zoledronic acid (ZOL) has recently been shown to attenuate bone loss in individuals with acute SCI[2]. However, durability of treatment, and the influence of covariates like ambulation, are not well understood.

PURPOSE

To quantify the effects of a single ZOL infusion on hip BMD over one year, in individuals with recent SCI

STUDY POPULATION

60 individuals with acute SCI (<4 months) enrolled into a double-blind clinical trial (NCT02325414)

Individuals were randomly assigned to receive infusion of ZOL (n=30) or placebo (PBO; n=30)

Table 1 – Demographics of ZOL and PBO treatment groups

	ZOL	PBO	*p* value
n	30	30	
Age (years), mean ± SD	40.8 ± 15.5	41.1 ± 15.4	0.52
Sex (male)	22	26	0.33
BMI (kg/m^2), mean ± SD	25.8 ± 5.9	25.1 ± 5.1	0.30
ASIA, n, %			0.93
A	13, 40%	11, 41%	
B	6, 24%	7, 19%	
C	9, 32%	9, 36%	
D	2, 4%	3, 8%	
Injury Level, n, %			0.83
Cervical	18, 60%	16, 56%	
Thoracic	10, 32%	11, 33%	
Lumbar	2, 8%	3, 11%	

Age, sex, BMI, injury severity (ASIA score), and level of injury were balanced (p ≥ 0.30) between treatment groups (Table 1)

STUDY MEASURES AND ANALYSIS

Individuals were assessed at 0, 6 and 12 months

aBMD at the total hip (TH) and femoral neck (FN) was measured via DXA

Ambulatory ability was assessed according to the Walking Index for Spinal Cord Injury II (WISCI) scale

Analyzed using linear mixed modelling analysis

Examined %change in aBMD, with baseline aBMD, time, and WISCI treated as covariates

Examined main effects of treatment, time, WISCI, and interactions of treatment x time and WISCI x treatment

RESULTS – TOTAL HIP

A treatment x time effect (p=0.046) was observed for TH aBMD (Table 2 and Figure 1).

Table 2 – TH aBMD Statistics

Term	*p* value
Treatment	<.001
Time	<.001
WISCI	<.001
Treatment x Time	0.046
WISCI x Treatment	0.235

Figure 1 – %Change in TH aBMD over time

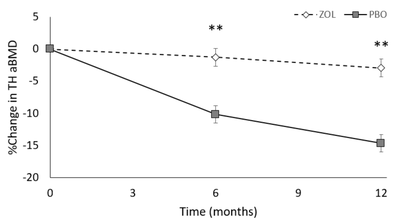

** P < 0.001 for pairwise comparison between groups.

After 12 months, single infusion of ZOL was associated with TH aBMD of -3.0% (SE: 1.4) vs -14.9% (SE: 1.4) with PBO

WISCI had a protective effect independent of treatment; On average, +10 WISIC† score was associated with TH aBMD of +3.4% (95%CI: +0.12% to +5.6%)

RESULTS – FEMORAL NECK

At the FN, the treatment x time effect was n.s. (p=0.076) but a main effect of treatment was detected (p < 0.001; Table 3 and Figure 2)

Table 3 – FN aBMD Statistics

Term	*p* value
Treatment	<.001
Time	0.002
WISCI	0.023
Treatment x Time	0.077
WISCI x Treatment	0.105

Figure 2 – %Change in FN aBMD over time

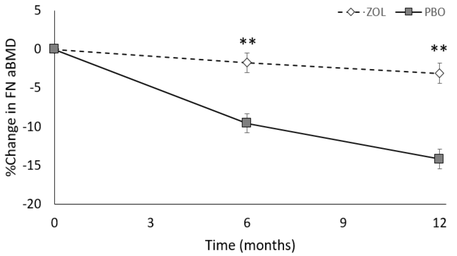

** P < 0.001 for pairwise comparison between groups.

Similar to TH, WISIC had a protective effect; here +10 WISCI† score was associated with +2.5% (95%CI: +1.5% to +3.5%) FN aBMD

† +10 WISCI represents the difference between nonambulatory (WISIC 0) and able to walk over 10m with one cane, braces and physical assistance (WISCI 10)

SUMMARY

Treatment with ZOL attenuated loss of aBMD at the hip following SCI (-3.0% vs –14.9% TH aBMD after 12 months).

Ambulatory ability (WISCI) also had a small protective effect, independent of treatment.

Further analyses are in progress, to confirm the effects of ZOL on bone mineral at the knee – a site prone to fracture after SCI.

ACKNOWLEDGEMENTS

This study was funded by the US Department of Defense, Award # W81XWH-14-2-0193, and supported by CTSA grant # UL1TR001422

REFERENCES

1. Haider et al., *Osteoporosis Int*. 2018. 30(8) 1422-30.
2. Goenka et al., *Spinal Cord*. 2018. 6(12):1207-11.

Haider I, Simonian N, Barroso J, Edwards WB, Schnitzer, TJ. Effects of Zoledronic Acid and Ambulation on Hip Bone Mineral Density after Acute Spinal Cord Injury: Year 1 of a Randomized Controlled Trial. Poster Presentation at the American Society for Bone and Mineral Research Annual Meeting, Virtual Event, September 11-15, 2020.

ABSTRACT:

Spinal cord injury (SCI) is associated with a significant decline in bone mineral density (BMD) and increased risk of fracture at sublesional locations. Losses in BMD occur rapidly after SCI, plateauing 2 to 5 years after injury [1]. Zoledronic acid (ZOL) has been shown to effectively attenuate bone loss in individuals with recent SCI [2]. However, the durability of treatment is unclear, as are the effects of potential covariates such as ambulation. Here, we report results from the first year of a prospective double-blind clinical trial (NCT02325414), assessing the durability of ZOL for the prevention of bone loss in individuals with acute SCI (i.e., < 4 months post-injury). Sixty individuals were randomized to receive an IV infusion of placebo (PBO; n=30) or 5 mg ZOL (n=30). Areal bone mineral density (aBMD) at the total hip (TH) and femoral neck (FN) was measured at baseline and after 6 and 12 months of treatment as was ambulation ability using the Walking Index for Spinal Cord Injury II (WISCI). Linear mixed modeling analysis was applied with baseline aBMD, visit and WISCI score as covariates to examine the effects of treatment group on % change from baseline in total hip (TH) and femoral neck (FN) aBMD. Interaction effects for treatment group*visit and treatment group*WISCI score were also included. There were no significant differences in age, gender, BMI, WISCI, or ASIA scores between treatment groups at baseline. Significant differences were found for % change in TH and FN aBMD between groups at both the 6 mo and 12 mo time points, $p<0.001$ for all. (TH data shown in Fig.1: ZOL and PBO groups LS means % change ±SE in aBMD at 6 months and 12 months; -1.3±1.4 vs -10.4±1.4 and -3.0±1.4 vs -14.9±1.4, respectively, $p<0.001$ for both comparisons). WISCI had a significant effect on % change in both TH and FN aBMD, $p=0.004$ and 0.028, respectively. Although both treatment and WISCI had a positive effect on % change in aBMD, the interaction term between these variables was not significant. Further analyses of this cohort, over 2 years of treatment, is ongoing and will include assessment of treatment durability and computed tomography of bone mineral at the knee. However, these initial data support the notion that one-year treatment with ZOL can effectively attenuate bone loss after SCI, with benefits of treatment observed regardless of ambulatory ability.

[1] Haider, Osteoporosis Int. 2018. [2] Goenka, Spinal Cord. 2018.

Finite Element Predicted Fracture Strength at Distal Femur and Proximal Tibia Under Biaxial Loading

Ifaz T. Haider[1,2], Stacey M. Lobos[1,2], Narina Simonian[3,4],Thomas J. Schnitzer[3], W. Brent Edwards[1,2]
[1]Human Performance Laboratory, Faculty of Kinesiology, and [2]McCaig Institute for Bone and Joint Health, University of Calgary
[3]Department of Physical Medicine and Rehabilitation, and [4]Northwestern University Clinical and Translational Sciences Institute, Northwestern University, Feinberg School of Medicine
Email: ifaz.haider@ucalgary.ca

Summary

CT-based finite element (FE) modelling can be used to assess bone fragility around the knee after spinal cord injury (SCI), but models must be validated using realistic loading scenarios. Activities such as wheelchair transfer are likely associated with biaxial loads (e.g., compression + torsion), however no published FE models have been validated under these conditions. In this work, we adapted a previously developed FE workflow and assessed its accuracy in predicting fracture strength of the proximal tibia and distal femur under biaxial loading.

Introduction

Individuals with SCI experience profound bone loss at the knee resulting in substantially increased fracture risk. To assess disease progression and the efficacy of proposed treatments, it is necessary to have accurate and non-invasive tools to assess bone fragility at the distal femur and proximal tibia. This can be done with CT-based FE modelling, but models must be validated to ensure accuracy under clinically relevant loading conditions. Spiral fractures are commonly reported after SCI, implicating torsion as an important failure mode. Our group recently developed and validated an FE model of the tibia to predict fracture load under simple torsion [1]. However, fractures during activities such as wheelchair transfer likely result from more complex biaxial loading (compression + torsion). Thus, the purpose of this work was to assess the accuracy of our previously developed FE technique to predict stiffness and strength at the proximal tibia and distal femur under biaxial loading

Methods

Seven fresh-frozen cadaveric bones (4 distal femurs, 3 proximal tibia; mean age 82 yrs; 15 cm length) were potted in 2 cm of PMMA and CT scanned prior to mechanical testing. Each bone was loaded in force control to 300N of axial compression. Axial displacement was then held constant while a ramped torsional displacement (internal rotation) was applied until rupture. The highest torque during the test (T_{ult}; N·m) and stiffness (K; N·m/degree) from the linear portion of the torsional ramp to failure was measured.

CT scans were used to develop subject-specific FE models, following previously validated methodology [1]. Bone and PMMA were segmented semi-manually and meshed with 1.5 mm hexahedral elements. Bone was assigned heterogeneous, orthotropic material properties based on CT intensity at each element location, while PMMA was assigned a uniform isotropic stiffness of 2.5 GPa. A bilinear elasto-plastic model, with yield based on Hill's conventional criteria, was used to simulate bone failure. T_{ult} was predicted as the load which caused 10% of surface elements to fail [1], while K was measured from the initial slope of torque vs. rotation angle.

Results and Discussion

Error between FE predicted strength and stiffness was somewhat large, with an average error of 55% and 34% respectively. However, as shown in Figure 1, we observed strong correlations between FE predicted and experimental measurements of K (R^2 = 0.95) and T_{ult} (R^2 = 0.86). At this current stage, the model will still have valuable utility in clinical assessment of relative strength between patients, or within individuals over time.

The FE failure criteria was originally cross validated with only formalin-fixed proximal tibiae under simple torsion. The criterion is likely not robust to different bones (distal femurs) or loading conditions (biaxial loading). We are currently testing additional specimens in order to develop a more robust failure model. Model refinements to better reflect the experimental condition may also yield improved accuracy.

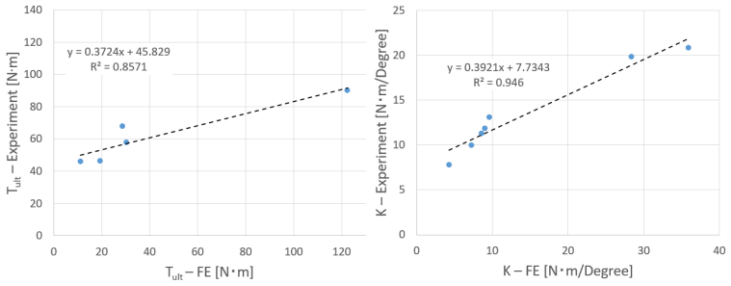

Figure 1: Experimental measurement vs. FE prediction of T_{ult} [LEFT] and K [RIGHT]

Conclusions

FE predictions of torsional stiffness and ultimate load were strongly correlated to experimental measures. Refinements to the model, to better reflect the experimental condition, may further improve accuracy.

Acknowledgments

This research was supported by Department of Defense U.S. Army Medical Research and Materiel Command (Grant Numbers SC090010 and SC130125) and the National Institutes of Health's National Center for Advancing Translational Sciences (Grant Numbers UL1TR001422 and UL1TR000150).

References

[1] Edwards et al. (2013). *J Biomech*, **46(10)**: 1665-1662

ABSTRACT

Introduction

Spinal cord injury (SCI) is associated with bone loss and skeletal fragility at the knee. Understanding the temporal patterns of bone loss after SCI may help develop more effective interventions. The purpose of this investigation was to expand on our previous research [1,2] and more thoroughly quantify temporal changes at the distal femur and proximal tibia in people after SCI. We used patient-specific finite element (FE) modelling to measure stiffness and computed tomography (CT) to measure changes in bone mineral.

Methods

CT scans of the distal femur and proximal tibia were collected from 101 patients (ages 18-72 yrs, 80 males) with SCI between 1 month and 50 years prior to participation. We computed bone mineral density (vBMD), bone volume (BV) and bone mineral content (BMC) at integral, cortical, and trabecular compartments of the epiphyseal, metaphyseal, and diaphyseal regions. We also generated patient-specific FE models of the same three regions to estimate stiffness under axial compression (K_c) and torsion (K_t). Finally, we fit all measures as a function of time since injury using a single decaying exponential (1-DE) and a superposition of two decaying exponential functions (2-DE).

Results

Bone mineral and stiffness decreased exponentially over time ($R^2 \geq 0.47$; Figure 1, TOP), but the more complex 2-DE model did not explain more variation than the 1-DE model ($p \geq 0.67$). All measures reached steady-state by 3.5 years after SCI. After this time, patients had significantly decreased stiffness (40-85%; $p < 0.005$) and bone mineral (12-107%; $p < 0.005$), compared to recently injured patients ($t \leq 47$ days; Figure 1, BOTTOM).

Discussion

Bone loss at the knee after SCI was rapid and profound, with rates of loss greatest immediately after injury. We observed significant reductions to both torsional and axial stiffness, suggesting that both failure modes may be clinically relevant. Changes over time were described by the 1-DE model, which predicts rapid loss within 3.5 year after SCI and negligible change after this time. It is plausible that moderate bone loss occurs after this period, as predicted by the 2-DE model, but the rate of loss is likely small with respect to patient-to-patient variation and could not be detected.

References

[1] Edwards et al. J Bone Miner Res. 30:8, 2015.

[2] Edwards et al. Osteoporos Int. 24:9, 2013.

Haider I, Lobos S, Simonian N, Schnitzer TJ, Edwards WB. Bone Fragility after Spinal Cord Injury: Reductions in Stiffness and Bone Mineral at the Distal Femur and Proximal Tibia as a Function of Time. Poster Presentation at the American Society for Bone and Mineral Research Annual Meeting, Montreal, Canada, September 28-October 1, 2018.

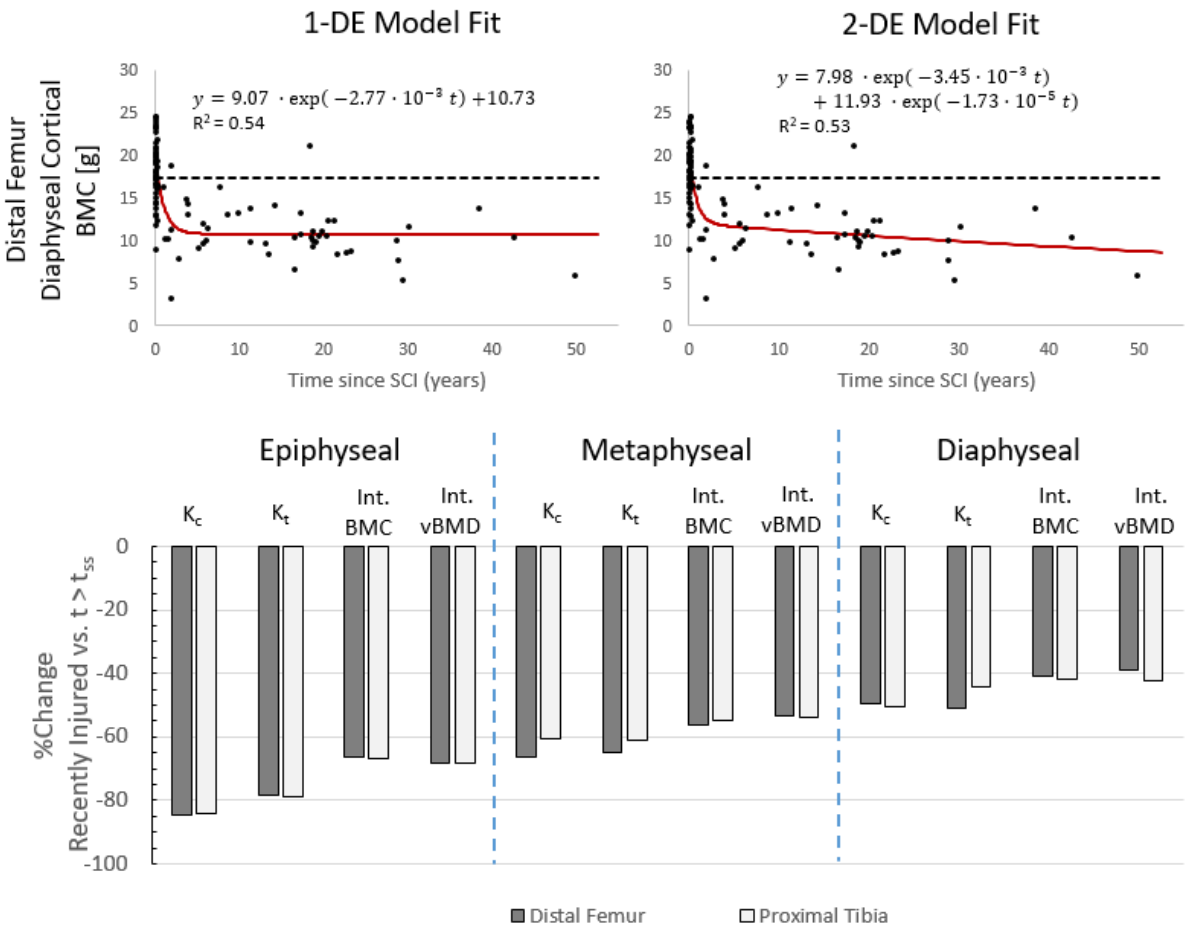

Figure 1: Sample results from model fitting (TOP) and percent change in select stiffness and bone mineral measures (BOTTOM).

Haider I, Lobos S, Simonian N, Schnitzer TJ, Edwards WB. Bone Fragility after Spinal Cord Injury: Reductions in Stiffness and Bone Mineral at the Distal Femur and Proximal Tibia as a Function of Time. Poster Presentation at the American Society for Bone and Mineral Research Annual Meeting, Montreal, Canada, September 28-October 1, 2018.

Bone Fragility after Spinal Cord Injury: Reductions in Stiffness and Bone Mineral at the Distal Femur and Proximal Tibia as a Function of Time

Ifaz T. Haider[a,b], Stacey M. Lobos[a,b], Narina Simonian[c,d], Thomas J. Schnitzer[c,e], W. Brent Edwards[a,b]

[a]Human Performance Laboratory, Faculty of Kinesiology, and [b]McCaig Institute for Bone and Joint Health, University of Calgary
[c]Department of Physical Medicine and Rehabilitation, and [d]Northwestern University Clinical and Translational Sciences Institute, Northwestern University Feinberg School of Medicine
[e]Department of Physical Medicine and Rehabilitation, Rehabilitation Institute of Chicago (d.b.a. Shirley Ryan AbilityLab)

BACKGROUND

- Spinal Cord Injury (SCI) is associated with rapid bone loss and increased fracture risk at the knee [1,2].
- Understanding the temporal patterns of bone loss may help develop timelines for preventative intervention.
- Quantitative tomography (QCT) can be used to measure bone loss *in-vivo*; Subject-specific finite element (FE) models can help explain the mechanical consequences of those losses.

PURPOSE

To examine a cross section of individuals with SCI and thoroughly quantify changes to bone at the distal femur and proximal tibia as a function of time since injury.

METHODS

Participants

- 101 non-ambulatory individuals with SCI (Age = 18-72 years, 80 males, 21 females)
- Individuals experienced SCI 1 month to 50 years prior to participation.

QCT Analysis

- QCT imaging of the knee: 120 kVP, 280 mA; In plane resolution: 0.352 x 0.352 mm; Slice thickness: 1 mm.
- Segmented each bone into integral (int), cortical (cort), and trabecular (trab) compartments using Mimics Innovation Suite.
- Separate analysis of the epiphyseal, metaphyseal and diaphyseal regions of each bone. (Fig. 1).
- Quantified **bone mineral content** (BMC), and **volumetric bone mineral density** (vBMD).

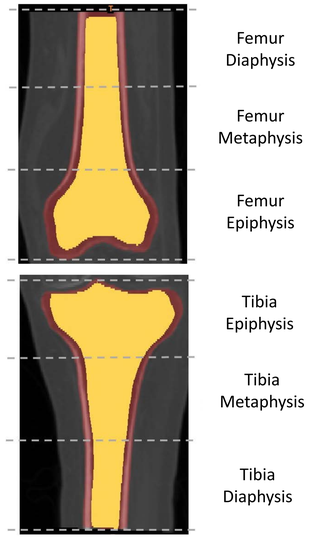

Fig. 1 – Example segmented knee. Bone was separated into cortical (red) and trabecular (yellow) compartments.

METHODS CONT.

FE Modelling

- Generated a voxel mesh of each bone region (Fig. 2). Element size: 1.5mm; Total elements: 40 000 per region.
- Assigned material properties based on CT intensity at each element location and published orthotropic material constants [3,4].
- Fixed one end and applied compressive and torsional load to the other; quantified **compressive stiffness** (K_c) and **torsional stiffness** (K_t).

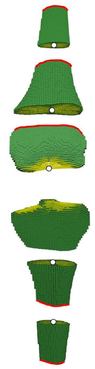

Fig. 2 Example FE Mesh

Data Analysis

- Fit CT and FE measures (y) as a function of time since injury (t), using single (Eq.1) and double (Eq.2) decaying exponential fits:

$$y = A_s \cdot exp(-B_s \cdot t) + C_S \quad \text{Eq.1}$$

$$y = A_d \cdot exp(-B_d \cdot t) + C_d \cdot exp(-D_d \cdot t) \quad \text{Eq.2}$$

- Quantified **time to reach steady-state** (T_{ss}) based on Eq.1 . Compared individuals with $t > T_{ss}$ against recently injured individuals ($t < 47$ days).

RESULTS

- Rapid initial bone loss was followed by a period of little/no change. T_{ss} = 1.2 - 3.5 years (Fig. 3).
- Double exponent fit had no significant improvement in R^2 compared to single exponent fit ($p > 0.67$)

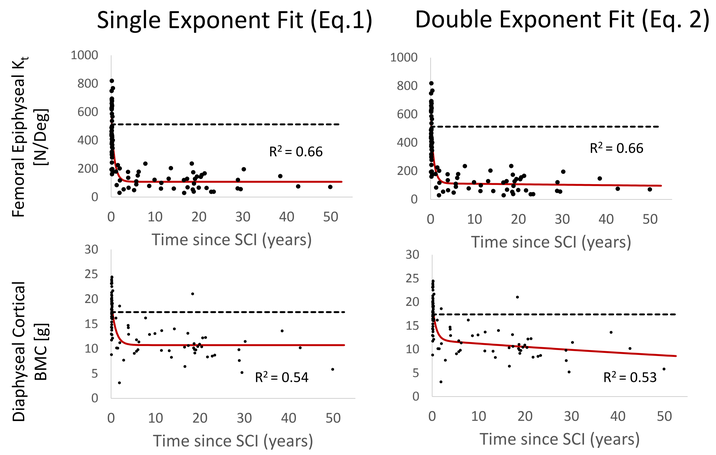

Fig. 3 – Changes in K_t and Diaphyseal Cortical BMC as a function of time since injury. Dotted line shows baseline levels from recently injured individuals.

RESULTS CONT.

- Individuals with $t > T_{ss}$ had lower K_c, K_t, BMC and vBMD ($p < 0.005$) compared to those injured recently ($t < 47$ days).
- Losses were greatest in the epiphysis and progressively decreased moving towards the diaphysis (Fig. 4).
- Losses in K_c and K_t were typically greater than losses in BMC, vBMD, and BMC ($p < 0.005$) ; epiphyseal cortical BMC and metaphyseal trabecular vBMD were exceptions to this trend.

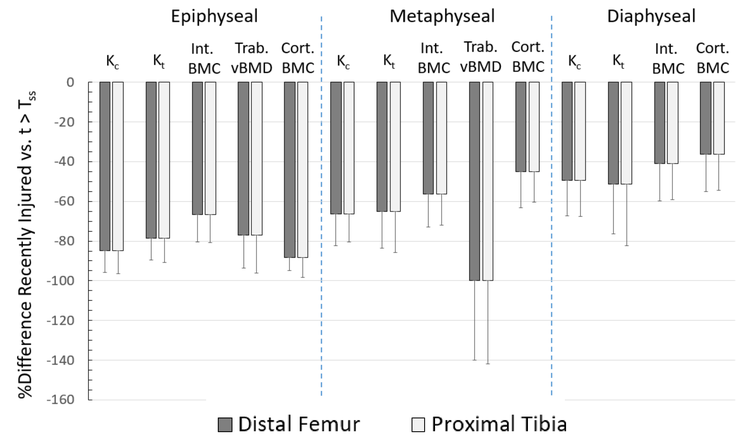

Fig. 4 %Difference in select measures between individuals with $t > T_{ss}$ compared to those who were recently injured ($t < 47$ days).

DISCUSSION

We observed robust decreases to QCT measures of bone mineral. This had important mechanical consequences; FE models predicted stiffness losses of 40%-85% in individuals with $t > T_{ss}$ compared to the recently injured baseline.

The majority of bone loss occurs 1.2-3.5 years after injury. This suggests a very short window for preventative intervention.

Eq. 1 plateaus after $t > T_{ss}$ while Eq. 2 allows moderate bone loss many years after this time. However, Eq. 2 did not better explain our data. It remains plausible that bone loss continues after $t > T_{ss}$, but with a small rate of loss that is difficult to distinguish from variation among individuals.

ACKNOWLEDGEMENTS AND REFERENCES

This research was supported by Department of Defense U.S. Army Medical Research and Materiel Command (Grant Numbers SC090010 and SC130125) and the National Institutes of Health's National Center for Advancing Translational Sciences (Grant Numbers UL1TR001422 and UL1TR000150).

[1] Jiang et al. Osteoporosis Int 2006. 17(2):180-192.
[2] Edwards et al. Curr Osteoporos Rep 2015. 13(5):310-317.
[3] Rho et al. Med Eng Phys 1995. 17(5) 347-355.
[4] Rho. Ultrasonics 1996. 34(8):777-783

Annals of Biomedical Engineering, Vol. 49, No. 2, February 2021 (© 2020) pp. 769–779
https://doi.org/10.1007/s10439-020-02606-w

Original Article

Stiffness and Strength Predictions From Finite Element Models of the Knee are Associated with Lower-Limb Fractures After Spinal Cord Injury

IFAZ T. HAIDER,[1,2] NARINA SIMONIAN,[3,4] THOMAS J. SCHNITZER,[3] and W. BRENT EDWARDS[1,2]

[1]Human Performance Laboratory, Faculty of Kinesiology, University of Calgary, Calgary, Canada; [2]McCaig Institute for Bone and Joint Health, University of Calgary, Calgary, Canada; [3]Department of Physical Medicine and Rehabilitation, Northwestern University Feinberg School of Medicine, Chicago, USA; and [4]Northwestern University Clinical and Translational Sciences Institute, Northwestern University Feinberg School of Medicine, Chicago, USA

(*Received 1 June 2020; accepted 2 September 2020; published online 14 September 2020*)

Associate Editor Eiji Tanaka oversaw the review of this article.

Abstract—Spinal cord injury (SCI) is associated with bone fragility and fractures around the knee. The purpose of this investigation was to validate a computed tomography (CT) based finite element (FE) model of the proximal tibia and distal femur under biaxial loading, and to retrospectively quantify the relationship between model predictions and fracture incidence. Twenty-six cadaveric tibiae and femora (n = 13 each) were loaded to 300 N of compression, then internally rotated until failure. FE predictions of torsional stiffness (K) and strength (T_{ult}) explained 74% (n = 26) and 93% (n = 7) of the variation in experimental measurements, respectively. Univariate analysis and logistic regression were subsequently used to determine if FE predictions and radiographic measurements from CT and dual energy X-ray absorptiometry (DXA) were associated with prevalent lower-limb fracture in 50 individuals with SCI (n = 14 fractures). FE and CT measures, but not DXA, were lower in individuals with fracture. FE predictions of T_{ult} at the tibia demonstrated the highest odds ratio (4.98; p = 0.006) and receiver operating characteristic (0.84; p = 0.008) but did not significantly outperform other metrics. In conclusion, CT-based FE model predictions were associated with prevalent fracture risk after SCI; this technique could be a powerful tool in future clinical research.

Keywords—Biomechanics, Fracture risk, Computed tomography, Disuse osteoporosis.

Address correspondence to Ifaz T. Haider, Human Performance Laboratory, Faculty of Kinesiology, University of Calgary, Calgary, Canada. Electronic mail: ifaz.haider@ucalgary.ca

INTRODUCTION

Sublesional bone loss is a recognized consequence of spinal cord injury (SCI). Losses are most severe around regions of the knee, with reductions in bone mineral up to 50% within the first 5 years after SCI.[3,13,16] Reductions in bone mineral are associated with increased skeletal fragility, resulting in fractures of the proximal tibia and distal femur during routine activities, such as wheelchair transfers and rolling over in bed.[27,44] These fractures are associated with a high rate of complication and concomitant increase in morbidity and mortality,[44] but there is currently no standard of care for bone loss following SCI and treatment for this condition remains an active area of clinical research.[12,23,30,39]

Measurement of areal bone mineral density (aBMD), *via* dual-energy X-ray absorptiometry (DXA), is the current clinical gold standard to assess fracture risk in able-bodied individuals. Several studies also suggest that aBMD is related to fracture risk in individuals with SCI.[1,2,18,29,31,45] However, mechanical fragility of bone depends not only on aBMD, but also on bone size, shape, and mineral distribution, among others. Many of these factors are captured with computed tomography (CT) analysis, and consequently, a number of studies have characterized bone loss after SCI using CT.[9,16,17,22] A few studies have also demonstrated that CT measures of bone are related to fracture risk after SCI.[15,29] Density and geometry information from CT scans are often used to generate

CT-based finite element (FE) models, which are physics-based simulations that predict the mechanical response of bone to an applied load. Previous studies have consistently demonstrated that FE models more accurately predict the strength of bone when compared to DXA and CT analysis alone.[6,7,10] Studies in able-bodied individuals also suggest that FE models are better able to estimate fracture risk,[26,41] though similar studies have not investigated this link within the context of SCI.

Despite the strengths of FE modeling, it should be noted that bone fracture is a complex phenomenon and thorough validation experiments are essential to ensure that predictions reflect reality. Spiral fractures are often reported in individuals with SCI,[27,34] suggesting that torsional loading is an important failure mode. With this in mind, our group previously developed and validated an FE model to predict torsional stiffness (r^2 = 0.95, error = 10%) and failure load (r^2 = 0.91, error = 9%) at the proximal tibia.[10] The FE model was subsequently used to estimate the mechanical consequence of bone loss after SCI[11,13] and in response to drug therapy.[12,23] However, additional testing is needed to ensure that the model provides meaningful predictions at the distal femur, which is also a common site of fracture after SCI.[5,15,29] Additionally, fractures during activities such as wheelchair transfer are likely to result from a combination of loads, e.g., compression and torsion. Tissue-level tests indicate that torsional failure load is dependent on the magnitude of superimposed compressive loading,[4] but our previous validation experiment did not explore this phenomenon. Finally, we have not compared modeling results against clinical fracture data to quantify the link between FE-predictions and fracture risk after SCI.

This work seeks to address the aforementioned limitations. Specifically, the purpose of this investigation was to validate an FE model of the distal femur and proximal tibia under biaxial loading, and to quantify the association between model predictions and prevalent fracture. A CT-based FE model of the distal femur and proximal tibia was validated in combined axial-compression and torsion using *ex vivo* experimentation. Models were then used to quantify the relationship between FE predictions and prevalent lower-limb fracture in a cohort of 50 individuals with SCI, who were identified in a previous clinical trial.[12] For comparison, fracture risk was also assed *via* DXA at the hip, spine and knee, and regional CT analysis of bone mineral at the knee.

MATERIALS AND METHODS

Part 1: Model Development and Validation

Specimen Preparation, Imaging, and Mechanical Testing

Thirteen fresh-frozen cadaveric knee joints from nine donors (mean age = 85 years, range = 68–95 years) were acquired from Science Care Inc. (Phoenix, USA) and the University of Calgary's Body Donation Program (see Table 1 for available demographic data). Cadaveric work was approved by the University of Calgary's Conjoint Health Research Ethics Board (REB16-0812) and the Department of Defense Human Research Protection Office (HRPO). Donors (prior to death), or their next-of-kin, provided consent for these tissues to be used for scientific purposes. The knee joints, which received osteotomy near the mid-thigh and shank, were first cleaned of soft tissue and disarticulated. Proximal tibiae (n = 13) were then cut 15 cm distal to the intercondylar eminence and distal femora (n = 13) were cut 15 cm proximal to the intercondylar fossa. The proximal and distal ends of both bones were potted in 2 cm of polymethyl methacrylate (PMMA), measured from these datums, leaving 11 cm exposed. Potted specimens were imaged using clinical CT, on a GE Revolution GSI (GE, Healthcare, Chicago, USA). Images were acquired at 120 kV and 500 mA, with an in-plane resolution of 0.352 mm and slice thickness of 0.625 mm. A calibration phantom (QRM GmbH; Mohrendorf, Germany) was placed in the field-of-view of each scan to identify a linear relationship between CT intensity in Hounsfield units (HU) and hydroxyapatite equivalent density (ρ_{HA}; g/cm^3).

After imaging, specimens were mounted into custom fixtures and loaded on a biaxial material testing machine (858 Mini Bionix II, MTS Inc., Minneapolis, USA). Each bone was loaded at a rate of 100 N/s up to 300 N of axial-compression, corresponding roughly to one-half of a typical bodyweight. The vertical position of the arm was then held in displacement control while internal rotation was applied at a fixed rate of 9°/s until fracture or 90 Nm, which was the maximum safe limit of the load cell. As shown in Fig. 1, torsional stiffness (K) was measured by fitting a second-order polynomial to the initial loading region (0–20 Nm) of the torque-rotation data, and computing the tangent to this curve at the start of loading (0°). If fracture occurred, ultimate torsional strength (T_{ult}) was reported as the highest torque achieved during the test.

TABLE 1. Donor demographics.

Donor	Age (years)	Weight (lbs)	Sex	Cause of death	Anatomical locations (R = right, L = left)
1	89	115	Female	Aortic stenosis	R-femur, R-tibia
2	74	161	Male	Liver cancer	R-femur, R-tibia, L-femur, L-Tibia
3	68	130	Male	Brain aneurysm/heart attack	R-femur, R-tibia, L-femur, L-tibia
4	84	175	Male	Failure to thrive	L-femur, L-tibia
5	90	150	Male	Natural causes	L-femur, L-tibia
6	90	137	Male	Pulmonary fibrosis	R-femur, R-tibia
7	87	148	Male	Stroke	R-femur, R-tibia
8	95	149	Male	Terminal pneumonia	R-femur, R-tibia, L-femur, L-tibia
9	87	140	Male	Indeterminate	R-femur, R-tibia, L-femur, L-tibia

Donors 1–7 were obtained *via* Science Care Inc (Phoenix, USA) while donors 8 and 9 were obtained *via* the University of Calgary's body donation program.

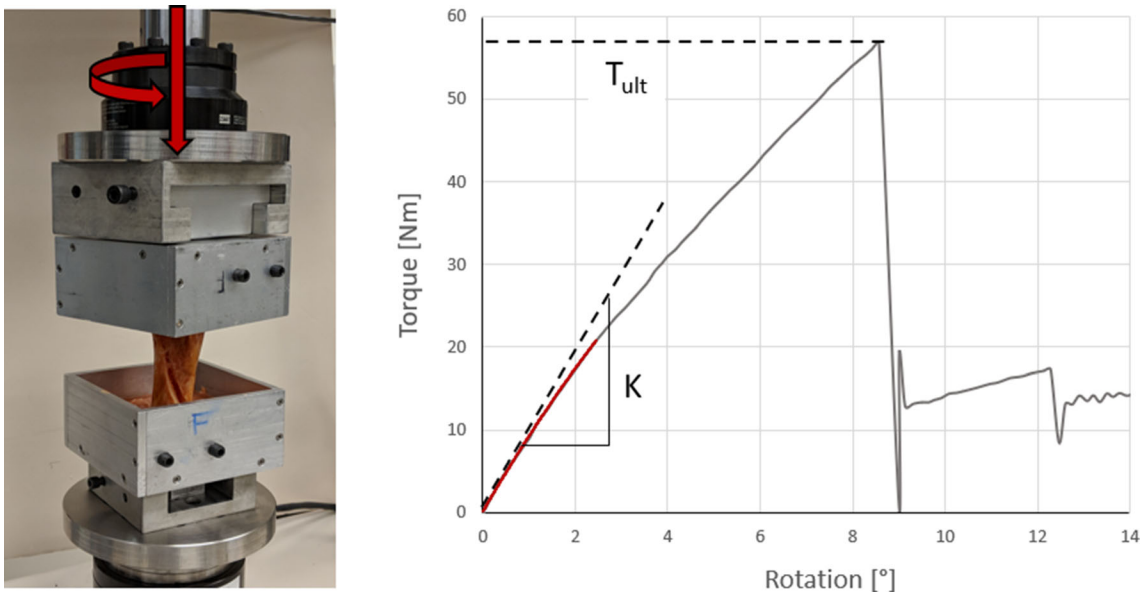

FIGURE 1. (Left) Experimental setup illustrating spiral fracture pattern of a proximal tibia after being loaded in 300 N of compression and internally rotated until failure. (Right) Representative torque-rotation behavior for a specimen that fractured. Stiffness (*K*) was calculated by fitting a second order polynomial to the torque-rotation data (red line) and computing the slope of the tangent at 0°. Torsional strength (T_{ult}) was calculated as the highest torque achieved during the test.

Finite Element Modeling

Subject-specific FE models of each bone were generated from CT images, and solved using ABAQUS software (version 2016, Dassault Systèmes, France). Details of the FE model can be found in our previous validation study,[10] but these are also reviewed for the reader's convenience. Briefly, a trained operator segmented CT images to identify bone and potting from each scan. A threshold of 0.15 g/cm^3 was used to identify the periosteal surface of bone, with some manual "clean-up" to identify surfaces near the epiphyses. Images were then resampled to an isotropic voxel resolution of 1.5 mm, and a linear hexahedral FE mesh of the bone and conforming PMMA was generated by direct voxel conversion. All PMMA voxels were assigned an elastic modulus of 2.5 GPa and Poisson's ratio of 0.3.[33] Bone voxels were assigned heterogeneous orthotropic material properties with elastic moduli based on CT-derived bone density at each voxel location. A bilinear material model was used to simulate failure, with yield determined by Hill's conventional criterion.[25] Details of the material model are provided in the online supplementary materials (Appendix A).

Loads and boundary conditions mimicked conditions of the experimental test (Fig. 2). Surface nodes at the sides and ends of diaphyseal potting were fully

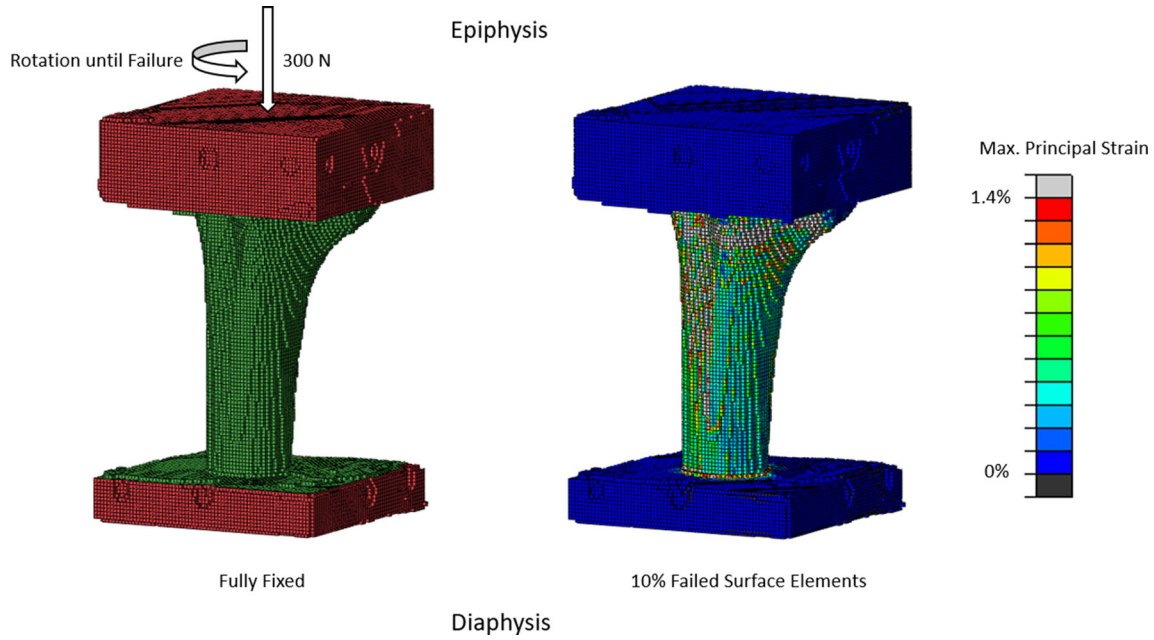

FIGURE 2. Representative FE models of the femur. [Left] Loads and boundary conditions were distributed over the surface of the potting (red); the diaphyseal end was fully fixed while a biaxial load was applied to the epiphyseal end. [Right] Maximal principal strain was predicted by the model; failure was reported as the torque required for 10% of the surface elements to exceed a maximum principal strain of 1.410%.

fixed. For surface nodes at the sides and ends of epiphyseal potting, vertical displacement and rotation about the long axis was permitted and all other degrees of freedom were fixed. Axial-compressive load of 300 N was distributed over the epiphyseal potting in the initial step. Next, the vertical displacement caused by the 300 N of compression was held constant, and a ramping angular rotation was applied about the long axis. Models with 0 N and 3000 N of compression were also developed to assess the sensitivity of model results to the magnitude of axial-compression. FE predicted K was calculated as the ratio between reaction moment and rotation angle over the first time-increment (0°–0.5° of rotation). FE predicted T_{ult} was calculated as the torque required for 10% of surface elements to exceed a maximum principal strain of 1.410%, which was the failure criterion adopted from our previous study.[10]

Part 2: Associations with Prevalent Fracture

Study Population

The second phase of this work sought to determine if FE predictions and radiographic measurements from CT and DXA were associated with prevalent lower-limb fracture after SCI. We examined baseline imaging and fracture history data from a cohort of 50 individuals with SCI who recently participated in a pharmaceutical intervention trial.[12] Research was approved by ethical review boards at Northwestern University (STU00033380), the University of Calgary (REB13-1108) and the Department of Defense HRPO. The study was also registered at ClinicalTrials.gov (NCT01225055). Individuals with SCI were recruited from Northwestern University Feinberg School of Medicine, Schwab Rehabilitation Hospital, Edward Hines, Jr. VA Hospital, and the Shirley Ryan Ability Lab. All participants were 21 years of age or older and non-ambulatory following an SCI that occurred at least 1 year prior to enrollment in the intervention. Further eligibility criteria included: (1) low bone mass at the hip or femoral neck, with DXA Z-score ≤ -1.5, T-score ≤ -2.5, or T-score ≤ -2.0 in individuals with a history of fragility fractures, (2) normal calcium, renal function and thyroid stimulating hormone, and (3) 25-OH vitamin D levels ≥ 20 ng/mL. Individuals were excluded if they had: (1) an allergy to teriparatide (the drug being studied), (2) any history of bone metastasis, radiation therapy or Paget's disease, (3) current use of anticonvulsants at a dose determined by the investigators to interfere with bone metabolism, or (4) were pregnant or lactating.[12] SCI was described according to standards of the American Spinal Injury Association (ASIA)[28]; these results, and demographic details, are summarized in Table 2.

TABLE 2. Summary of participant demographics.

Total individuals	50
Age (years), mean ± SD	40.8 ± 13.7
Time (years) since SCI, mean ± SD	15.4 ± 11.1
Sex, *n* (%)	
Male	39 (78)
Female	11 (22)
Race/ethnicity, *n* (%)	
African-American	25 (50)
White: not Hispanic	10 (20)
White: Hispanic	12 (24)
Asian, Pacific Islander, or other	3 (6)
Classification of injury, *n* (%)	
Motor complete*	40 (80)
Motor incomplete*	10 (20)
ASIA A†	35 (70)
ASIA B†	6 (12)
ASIA C†	9 (18)

*Injures were classified as either motor complete, with no sensory or motor function was below the fourth and fifth sacral vertebrae (S4–S5), or incomplete, where some function below S4–S5 was preserved.

†Injury severity was further classified according to the ASIA impairment scale: ASIA A = no sensory or motor function below S4–S5, ASIA B = sensory but no motor function below S4-S5, ASIA C = motor function preserved below the neurological lesion but more than half of key muscles have compromised innervation, and ASIA D = motor function preserved below the neurological lesion and less than half of key muscles have compromised innervation.

Imaging Protocols

DXA scans of the spine and hip were acquired using standard image acquisition protocols[19] on a Hologic QDR 4500A (Hologic, Waltham, MA); aBMD at the spine, total hip and femoral neck (FN) were reported. The same machine was also used to measure aBMD at the knee using a custom protocol.[35] Two regions of interest were identified at the femur, measured from the distal end of the bone at 0-10% of segment length (''distal'' femur region) and 10–20% of segment length (''proximal'' femur region). The aBMD at the proximal tibia was also reported at 0–10% of segment length measured from the tibial plateau.

CT scans were performed using a Sensation 64 Cardiac Scanner (Siemens Medical Systems, Forchheim, Germany) at 120 kVP and 280 mA. The non-dominant leg was imaged, unless there was visible fixation hardware in the field of view or a history of fracture at that knee. In these cases, the contralateral leg was imaged instead. These images were acquired with a 1 mm slice thickness and an in-plane resolution of 0.352 × 0.352 mm. Distal femora and proximal tibiae were separately segmented, similar to Part 1, and aligned about the long axis of each bone. After alignment, we performed regional analysis of bone mineral. The bone was then separated into three regions based on estimated segment length (SL), with the epiphysis at 0–10% SL, the metaphysis at 10–20% SL and diaphysis at 20–30% SL.[9,10] Volumetric bone mineral density (vBMD) and bone mineral content (vBMC) were reported for the integral compartment of each region, which contained all bone within the periosteal surface. Finally, FE models were developed from CT scans of each bone, based on the workflow used in the validation experiments described in Part 1. For both Parts 1 and 2, images were resampled to a 1.5 mm isotropic voxel before meshing, reducing the differences associated with the fact that images in the two studies were acquired at slightly different resolutions. Here, pure torsion was simulated by applying a rotational displacement to surface nodes of the last 2 cm of epiphyseal bone, while surface nodes of the last 2 cm of diaphyseal bone were held fixed; axial-compression was neglected based on the results from Part 1. FE predicted K and T_{ult} were reported for each bone.

Statistical Analysis

Participants were separated into two groups based on their history of lower-limb fracture following SCI. All study measures, described above, were compared between these groups. Pairwise comparison *via* Student's *t*-tests were used to identify differences between fracture groups and logistic regression was used to quantify the relationship between each measure and the likelihood of prevalent fracture. To facilitate comparison, this relationship was expressed as the increase in odds of fracture associated with a one standard deviation (SD) decrease in the measured parameter. Probability estimates from logistic regression were subsequently used to calculate the receiver operating characteristic (ROC) curve, and the area under the curve (AUC) was reported. Multiple regression was not considered, as these models may be unreliable if the dataset does not include at least 10 events per regression variable.[29,37] All statistical measures were assessed at a significance level of 0.05 and analyses were performed using SPSS software (version 24, IBM, NY, USA).

RESULTS

Part 1: Model Development and Validation

Experimentally measured K for all 26 bones ranged from 5.7 to 44.5 Nm/°. FE model predictions were well-correlated to experimental measurements, explaining 74% of the variance in observed stiffness across both bones (Fig. 3a). Absolute errors in FE predictions were modest, on average 15% of the

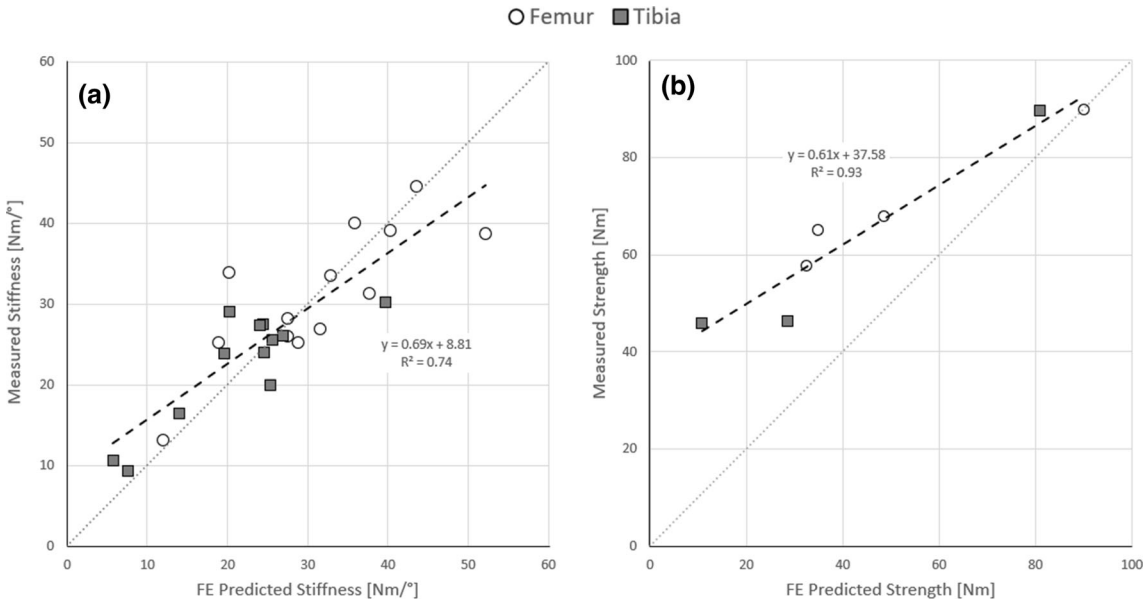

FIGURE 3. Comparison between experimental and FE measures of *K* (Nm/°; a) and T_{ult} (Nm; b). FE prediction explained 93% and 74% of the observed variance in each measure, respectively.

measured value. Similar results were observed when considering each bone separately, with the FE model explaining 72% and 64% of the variance in K observed at the tibia and femur, respectively. Seven specimens fractured (4 femur 3 tibia) prior to the 90 Nm safe limit of the load cell. These fractures illustrated a spiral pattern and occurred between 49.8 and 89.8 Nm of torque. T_{ult} was highly correlated with experimental measurements, accounting for 93% of the observed variance across both bones (Fig. 3b). However, mean absolute error was 34% of the measured value, with the trendline indicating larger errors in specimens with lower T_{ult} (Fig. 3b).

The FE models also provided additional insight into the effect of changing axial-compressive load magnitude. Models under 300 N of compression (i.e., the experimental test condition) failed at nearly identical torque when compared to models in pure torsion (Fig. 4). On average, the difference in predicted T_{ult} between these two test conditions was only 0.05% (range: − 0.3 to 0.87%). Increasing the compressive load to 3000 N demonstrated a somewhat larger effect, with T_{ult} being on average 1.49% (range: + 0.88 to − 3.62%) lower than models in pure torsion.

Part 2: Associations with Prevalent Fracture

Of the 50 participants, 14 (28%) had a prevalent fragility fracture of the lower limb. Seven individuals had a fracture at the femur, while three had a fracture at the tibia. One individual had a fracture of the foot, while another individual had experienced a fracture of the ankle; both were classified in the lower-limb fracture group. Among the remaining individuals, we were unable to identify which bone was broken. Falls were the most common cause of fracture; three individuals reported that fracture occurred after a fall during wheelchair transfer, while another five individuals reported that fracture occurred during low-velocity falls during other activities. One individual experienced a fracture when attempting to use an exercise exoskeleton, while another individual was unable to identify the cause of their fracture. Finally, the remaining four fractured cases were the result of other activities, such as getting their leg or foot caught against an object, or minor accidents in a wheelchair. Demographic characteristics and results from pairwise comparisons are presented in the online supplementary materials (Appendix B). Briefly, individuals with fracture had a longer duration of SCI (23.3 years compared to 12.9 years; $p = 0.003$). No other demographic characteristics were statistically different among the groups. Based on the criteria described in the methods, all individuals with prevalent knee fracture were imaged at the contralateral knee.

Pairwise comparisons between participants with or without prevalent fracture revealed significant differences in T_{ult}, *K*, and CT measures at both the tibia and femur, but no differences were detected in DXA at the spine, hip or knee. Logistic regression further elucidated the relationship between measures and the risk of prevalent fracture (Table 3). T_{ult} at the tibia was the measure most strongly related to fracture risk; here, one SD decrease in T_{ult} was associated with a 4.98

(95% CI 1.57–15.78; $p = 0.006$) increased odds of fracture. K at the tibia was also associated with an increased odds ratio (4.26, 95% CI 1.41–12.86; $p = 0.010$). Relationships were not as strong at the femur, where one standard deviation decrease in T_{ult} was associated with a 2.46 (95% CI 1.17–5.17; $p = 0.018$) increased odds of fracture, and the odds ratio for K was 2.21 (95% CI 1.00–4.88; $p = 0.049$). Similar patterns were observed when considering CT measures of bone mineral. Among these measures, epiphyseal vBMC at the tibia was the best predictor of fracture risk, with an odds ratio of 4.19 (95%CI 1.46–12.01; $p = 0.008$). In general, odds ratios were largest at the epiphysis, and decreased progressively at more distal locations. Similarly, odds ratio was typically somewhat greater for measures at the tibia compared to the equivalent site of the femur. AUC was greatest for T_{ult}, epiphyseal vBMC, and epiphyseal vBMD at the tibia, with values of 0.84 (SE = 0.07; $p = 0.001$), 0.81 (SE = 0.07; $p = 0.004$), and 0.81 (SE = 0.07; $p = 0.004$) respectively. AUC for all other parameters varied between 0.57 and 0.79, with spatial patterns mirroring the logistic regression from which the ROC was computed.

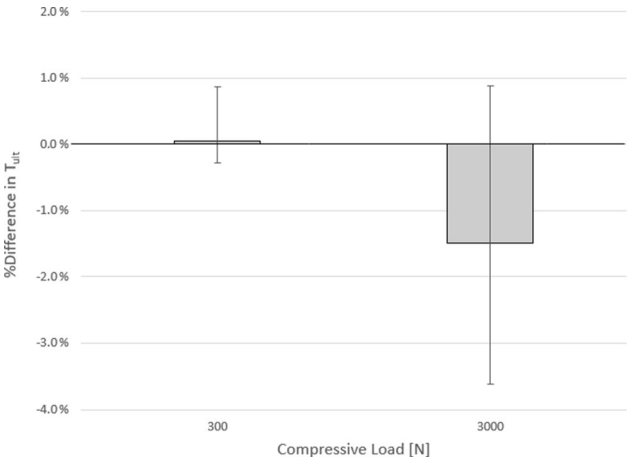

FIGURE 4. Influence of biaxial loading, predicted by the FE model. %Difference in T_{ult} under biaxial load, with 300 and 3000 N of compression, is shown relative to a model under pure torsion (0 N).

DISCUSSION

The purpose of this investigation was to validate an FE model of the distal femur and proximal tibia under biaxial loading, and to quantify the association between model predictions and prevalent lower-limb

TABLE 3. Associations between fracture and radiographic/FE measures of bone.

	Logistic regression		ROC	
	OR change per SD (95% CI)	*p* value	AUC (SE)	*p*-value
DXA				
Spine	0.73 (0.38–1.4)	0.341	0.63 (0.11)	0.235
Hip	1.87 (0.92–3.81)	0.083	0.64 (0.11)	0.190
FN	1.12 (0.59–2.16)	0.729	0.5 (0.13)	1.000
Proximal femur	1.64 (0.77–3.51)	0.202	0.61 (0.09)	0.295
Distal femur	1.48 (0.72–3.04)	0.287	0.59 (0.11)	0.399
Proximal tibia	1.84 (0.86–3.91)	0.114	0.67 (0.09)	0.111
Tibia FE/CT				
T_{ult}	4.98 (1.57–15.78)	**0.006**	0.84 (0.07)	**0.001**
K	4.26 (1.41–12.86)	**0.010**	0.79 (0.08)	**0.007**
Epiphyseal vBMC	4.19 (1.46–12.01)	**0.008**	0.81 (0.07)	**0.004**
Epiphyseal vBMD	4.00 (1.39–11.51)	**0.010**	0.81 (0.07)	**0.004**
Metaphyseal vBMC	2.62 (1.14–6.00)	**0.023**	0.74 (0.1)	**0.023**
Metaphyseal vBMD	2.04 (0.95–4.38)	0.068	0.67 (0.1)	0.111
Diaphyseal vBMC	2.03 (0.95–4.35)	0.068	0.75 (0.09)	**0.021**
Diaphyseal vBMD	1.63 (0.82–3.22)	0.164	0.64 (0.11)	0.179
Femur FE/CT				
T_{ult}	2.46 (1.17–5.17)	**0.018**	0.72 (0.08)	**0.012**
K	2.21 (1.00–4.88)	**0.049**	0.66 (0.09)	0.063
Epiphyseal vBMC	3.30 (1.34–8.13)	**0.009**	0.74 (0.07)	**0.004**
Epiphyseal vBMD	3.62 (1.40–9.40)	**0.008**	0.76 (0.07)	**0.002**
Metaphyseal vBMC	2.26 (1.05–4.86)	**0.037**	0.67 (0.08)	**0.048**
Metaphyseal vBMD	2.10 (0.95–4.66)	0.067	0.66 (0.08)	0.069
Diaphyseal vBMC	2.17 (1.02–4.64)	**0.045**	0.67 (0.09)	0.052
Diaphyseal vBMD	1.45 (0.78–2.68)	0.242	0.57 (0.08)	0.407

Bold values indicate $p \leq 0.05$.

fracture after SCI. FE predictions of K ($r^2 = 0.74$) and T_{ult} ($r^2 = 0.93$) demonstrated strong correlations with experimental measurements. Application to a clinical cohort of individuals with SCI revealed that several FE and CT measurements at the knee were associated with prevalent lower-limb fracture. T_{ult} at the tibia was most strongly related to fracture risk, and demonstrated strong sensitivity and specificity, with AUC of 0.84 (SE = 0.07; $p = 0.001$). This is the first study to quantify the relationship between FE predictions and fracture risk within the context of SCI.

Organ-level FE models of bone are typically validated for a single anatomical location. This is largely because the density-modulus relationship used for material property assignment is site-specific.[38] In this work, however, validation experiments demonstrated that the model explained a similar percentage of experimental variance in K for the tibia and femur. This suggests that it is appropriate to use the same density-modulus relationship, likely because of the close anatomical proximity of these two sites. Overall, the model explained 74% of the variance in K, which is comparable, if somewhat lower, than the values reported in literature (82–95%, in FE models of various bones).[7,10,14,40,43] The model was also able to account for 94% of the variance in T_{ult}, but the difference between measurements and predictions was larger than expected. On average, absolute error was 34% and the model tended to underestimate T_{ult}, with a trendline suggesting larger errors for weaker specimens (Fig. 3b). It is plausible that this error is due to the specific failure criterion used in this study. Failure was predicted as the load at which 10% of surface volume exceeded a maximum principal strain criterion; this was adopted from our previous work, which demonstrated a high level of accuracy for pure torsional loading (average error = 8.84%).[10] However, this previous validation study utilized formalin fixed specimens and a different torsional testing apparatus. The 90 Nm load-cell limit in this study also biased our validation towards fewer and weaker specimens. Stronger, stiffer bone tends to exhibit more brittle behaviour,[8,24,32] which may explain why T_{ult} was underpredicted here. Errors could be reduced by adjusting model parameters, but more fractured samples would be needed to establish independent training and validation datasets. Moreover, our findings regarding fracture risk suggest this is unnecessary. A significant association between T_{ult} and prevalent fracture was observed, suggesting the model is sufficiently accurate to obtain clinically meaningful results. After image segmentation, the model is easily automated, and it takes < 2 h to simulate and analyze each bone. In the short term, this model may be a powerful and practical tool in future studies of bone fragility after SCI.

Clinical reports commonly describe spiral fracture patterns around the knee in patients with SCI,[27,34] suggesting torsion as a critical mode of failure. In this work, we validated models under biaxial load (torsion with superimposed axial-compression) because this may better describe scenarios such as wheelchair transfer, which was a commonly reported cause of fracture in our population and in previous studies.[20,29] Failure under complex loading was modeled using Hill's conventional criterion, as this criterion was shown to accurately describe tissue-level behaviour of bone under biaxial load.[4] The failure model predicts reductions in torsional yield strength as the magnitude of compression is increased. Here, organ-level models demonstrated this expected trend; however, the magnitude of the effect was negligible. Even with a high compressive load of 3000 N, T_{ult} decreased by only 1.5%, compared to a model under pure torsion. This suggests that superimposed compression had little influence on torsional failure loads. Accordingly, it may be acceptable for future studies examining distal femoral and proximal tibial bone strength after SCI to focus solely on pure torsion loading.

Both FE predictions and CT-based mineral measurements at the tibiae demonstrated higher odds of fracture compared to measurements at the femur, despite the fact that more than half of fracture cases occurred at the femur. A previous radiographic investigation by Lala *et al.* suggested a similar trend[29]; after adjusting for motor complete injury, their model demonstrated that proximal tibia aBMD was associated with 6.1 increased odds of fracture, compared to only 4.9 at the femur, though the reason remains unclear. Previous studies reported that the magnitude of bone loss at the tibia and femur are similar,[9,22] and we noted here that T_{ult} at the femur was typically greater than T_{ult} at the tibia. These data suggest that fractures of the femur may not be the result of localized weakness of that bone, but instead the consequence of the specific real-world loading scenario.

Results of this study also suggest that CT mineral analysis of the knee has potential for fracture risk assessment. In general, vBMD and vBMC of the metaphysis and diaphysis demonstrated lower odds of fracture compared to measures at the epiphysis. This finding is consistent with a previous study by Eser *et al.*,[15] who also reported that pQCT derived measures at the epiphysis were the strongest determinants of fracture risk. In this study, epiphyseal vBMC of the tibia was the radiographic measure most strongly related to fracture risk, with an odds ratio of 4.19 (95% CI 1.46–12.01)—only slightly lower than the odds ratio of 4.98 (95% CI 1.54–15.78) associated with T_{ult}. This

measure could be a suitable substitute to FE modeling, in clinical settings where specialized software and personnel to perform FE analyses are not available.

In this study, we did not detect an association between any DXA measures and prevalent fracture risk, though some previous works have reported results that disagree with this finding. A few studies reported differences in aBMD at the hip or femoral neck in individuals with and without subsequent fracture after SCI, but these studies included individuals with less severe injuries[31] than our cohort, or also included individuals with upper limb fracture in the case definition.[1] However, fractures after SCI occur most commonly around the knee, and measurement at this site is more clinically relevant. A number of studies have reported differences in DXA derived measures at the knee in individuals with and without fracture after SCI.[2,18,29,45] In particular, Lala *et al.*[29] recently used a logistic regression model to demonstrate an association between aBMD at the knee and fracture risk; this association remained significant even after accounting for motor complete injuries. These findings are not consistent with the finding of this study, but the reason is unclear. Noting that the sample size and number of fracture cases did not differ substantially between our two studies, we speculate that differences in the DXA protocol and scanned region of interest could contribute to the difference in findings.

There are a several important limitations to this work. Experimental validation of T_{ult} was based on a modest sample size of seven, as only the weakest bones failed under the 90 Nm limit of the loadcell. SCI is also associated with changes at the microscale (trabecular architecture, collagen-cross linking or changes to remodeling spaces),[9,36,42] which cannot be accounted for using our CT-based FE modeling approach. Though not a focus of this study, compressive stiffness measured at the crosshead was two orders of magnitude lower than FE predictions. We suspect this was related to system/fixture compliance, as the anisotropic material definitions used in this study already illustrated excellent agreement with experimentally measured principal strains for a cadaveric tibia loaded in axial-compression ($r^2 = 0.98$; error = 6.0%).[21] Regarding the clinical cohort, we were not able to use multivariable logistic regression to assess whether combinations of different measurements provided improved predictions of prevalent fracture risk. As a rule of thumb, regression results are considered unreliable unless there are at least 10 events per variable in the model[29,37] and the population observed in this study included only 14 prevalent fractures. Future investigations involving longitudinal surveillance of a larger SCI population is, of course, warranted.

Conclusions

CT-based FE models of the proximal tibia and distal femur were validated under biaxial loading. Model predicted K and T_{ult} were well correlated to experimental measures, with r^2 values of 0.74 and 0.93, respectively. Prediction error for K was modest, only 15% of the measured value, but error in T_{ult} was larger (34%). Measurements of aBMD at the spine, hip, and knee were unable to predict prevalent fracture of the lower-extremity in a small cohort of individuals with SCI ($p \geq 0.111$). CT measurements of bone mineral at the knee were associated with prevalent fracture, but the strength of association varied across different measurement sites (odds ratio = 4.19 to 1.45; $p = 0.008$ to 0.242). Overall, T_{ult} at the tibia was the most sensitive predictor of prevalent fracture, where a 1 SD decrease in strength was associated with 4.98 increased odds of fracture ($p = 0.006$), and an AUC of 0.84 ($p = 0.001$). These data demonstrate that FE modeling provides sufficiently accurate, clinically meaningful, information regarding bone fragility and fracture risk at the knee in individuals with SCI, and may be a powerful tool for future studies of bone fragility after SCI.

ELECTRONIC SUPPLEMENTARY MATERIAL

The online version of this article (https://doi.org/10.1007/s10439-020-02606-w) contains supplementary material, which is available to authorized users.

ACKNOWLEDGMENTS

This study was funded by the Department of Defense U.S. Army Medical Research and Materiel Command (Grant #: SC090010 and BA150039). Research infrastructure for this study was funded by a Canadian Foundation for Innovation (CFI) John R. Evans Leaders Fund (JELF; Project #37134).

REFERENCES

[1]Abderhalden, L., F. M. Weaver, M. Bethel, H. Demirtas, S. Burns, J. Svircev, H. Hoenig, K. Lyles, S. Miskevics, and L. D. Carbone. Dual-energy X-ray absorptiometry and fracture prediction in patients with spinal cord injuries and disorders. *Osteoporos. Int.* 28:925–934, 2017.

[2]Biering-Serensen, F., H. Bohr, and O. Schaadt. Bone mineral content of the lumbar spine and lower extremities years after spinal cord lesion. *Paraplegia* 26:293–301, 1988.

[3]Biering-Sorensen, F., H. H. Bohr, and O. P. Schaadt. Longitudinal study of bone mineral content in the lumbar

spine, the forearm and the lower extremities after spinal cord injury. *Eur. J. Clin. Invest.* 20:330–335, 1990.
[4]Cezayirlioglu, H., E. Bahniuk, D. T. Davy, and K. G. Heiple. Anisotropic yield behavior of bone under combined axial force and torque. *J. Biomech.* 18:61–69, 1985.
[5]Cirnigliaro, C. M., M. J. Myslinski, M. F. La Fountaine, S. C. Kirshblum, G. F. Forrest, and W. A. Bauman. Bone loss at the distal femur and proximal tibia in persons with spinal cord injury: imaging approaches, risk of fracture, and potential treatment options. *Osteoporos. Int.* 28:747–765, 2017.
[6]Cody, D. D., G. J. Gross, F. J. Hou, H. J. Spencer, S. A. Goldstein, and D. P. Fyhrie. Femoral strength is better predicted by finite element models than QCT and DXA. *J. Biomech.* 32:1013–1020, 1999.
[7]Crawford, R. P., C. E. Cann, and T. M. Keaveny. Finite element models predict in vitro vertebral body compressive strength better than quantitative computed tomography. *Bone* 33:744–750, 2003.
[8]Currey, J. D. Tensile yield in compact bone is determined by strain, post-yield behaviour by mineral content. *J. Biomech.* 37:549–556, 2004.
[9]Edwards, W. B., T. J. Schnitzer, and K. L. Troy. Bone mineral and stiffness loss at the distal femur and proximal tibia in acute spinal cord injury. *Osteoporos. Int.* 24:2461–2469, 2013.
[10]Edwards, W. B., T. J. Schnitzer, and K. L. Troy. Torsional stiffness and strength of the proximal tibia are better predicted by finite element models than DXA or QCT. *J. Biomech.* 46:1655–1662, 2013.
[11]Edwards, W. B., T. J. Schnitzer, and K. L. Troy. The mechanical consequence of actual bone loss and simulated bone recovery in acute spinal cord injury. *Bone* 60:141–147, 2014.
[12]Edwards, W. B., N. Simonian, I. T. Haider, A. S. Anschel, D. Chen, K. E. Gordon, E. K. Gregory, K. H. Kim, R. Parachuri, K. L. Troy, and T. J. Schnitzer. Effects of teriparatide and vibration on bone mass and bone strength in people with bone loss and spinal cord injury: a randomized controlled trial. *J. Bone Miner. Res.* 33:1729–1740, 2018.
[13]Edwards, W. B., N. Simonian, K. L. Troy, and T. J. Schnitzer. Reduction in torsional stiffness and strength at the proximal tibia as a function of time since spinal cord injury. *J. Bone Miner. Res.* 30:1422–1430, 2015.
[14]Edwards, W. B., and K. L. Troy. Finite element prediction of surface strain and fracture strength at the distal radius. *Med. Eng. Phys.* 34:290–298, 2012.
[15]Eser, P., A. Frotzler, Y. Zehnder, and J. Denoth. Fracture threshold in the femur and tibia of people with spinal cord injury as determined by peripheral quantitative computed tomography. *Arch. Phys. Med. Rehabil.* 2005. https://doi.org/10.1016/j.apmr.2004.09.006.
[16]Eser, P., A. Frotzler, Y. Zehnder, L. Wick, H. Knecht, J. Denoth, and H. Schiessl. Relationship between the duration of paralysis and bone structure: a pQCT study of spinal cord injured individuals. *Bone* 34:869–880, 2004.
[17]Frey-Rindova, P., E. D. De Bruin, E. Stüssi, M. A. Dambacher, and V. Dietz. Bone mineral density in upper and lower extremities during 12 months after spinal cord injury measured by peripheral quantitative computed tomography. *Spinal Cord* 38:26–32, 2000.
[18]Garland, D., R. Adkins, and C. Stewart. Fracture threshold and risk for osteoporosis and pathologic fractures in individuals with spinal cord injury. *Top. Spinal Cord Inj. Rehabil.* 11:61–69, 2005.
[19]Gordon, K. E., M. J. Wald, and T. J. Schnitzer. Effect of parathyroid hormone combined with gait training on bone density and bone architecture in people with chronic spinal cord injury. *PM&R* 5:663–671, 2013.
[20]Grassner, L., B. Klein, D. Maier, V. Bühren, and M. Vogel. Lower extremity fractures in patients with spinal cord injury characteristics, outcome and risk factors for non-unions. *J. Spinal Cord Med.* 41:676–683, 2018.
[21]Gray, H. A., F. Taddei, A. B. Zavatsky, L. Cristofolini, and H. S. Gill. Experimental validation of a finite element model of a human cadaveric tibia. *J. Biomech. Eng.* 130:031016, 2008.
[22]Haider, I. T., S. M. Lobos, N. Simonian, T. J. Schnitzer, and W. B. Edwards. Bone fragility after spinal cord injury: reductions in stiffness and bone mineral at the distal femur and proximal tibia as a function of time. *Osteoporos. Int.* 30:1422–1430, 2018.
[23]Haider, I. T., N. Simonian, A. S. Saini, F. M. Leung, W. B. Edwards, and T. J. Schnitzer. Open-label clinical trial of alendronate after teriparatide therapy in people with spinal cord injury and low bone mineral density. *Spinal Cord* 57:832–842, 2019.
[24]Hayes, W. C., and D. R. Carter. Postyield behavior of subchondral trabecular bone. *J. Biomed. Mater. Res.* 10:537–544, 1976.
[25]Hill, R. A theory of the yielding and plastic flow of anisotropic metals. *Proc. R. Soc. A Math. Phys. Eng. Sci.* 193:281–297, 1948.
[26]Imai, K., I. Ohnishi, T. Matsumoto, S. Yamamoto, and K. Nakamura. Assessment of vertebral fracture risk and therapeutic effects of alendronate in postmenopausal women using a quantitative computed tomography-based nonlinear finite element method. *Osteoporos. Int.* 20:801–810, 2009.
[27]Keating, J. F., M. Kerr, and M. Delargy. Minimal trauma causing fractures in patients with spinal cord injury. *Disabil. Rehabil.* 14:108–109, 1992.
[28]Kirshblum, S. C., W. Waring, F. Biering-Sorensen, S. P. Burns, M. Johansen, M. Schmidt-Read, W. Donovan, D. Graves, A. Jha, L. Jones, M. J. Mulcahey, and A. Krassioukov. International standards for neurological classification of spinal cord injury (Revised 2011). *J. Spinal Cord Med.* 34:547–554, 2011.
[29]Lala, D., B. C. Craven, L. Thabane, A. Papaioannou, J. D. Adachi, M. R. Popovic, and L. M. Giangregorio. Exploring the determinants of fracture risk among individuals with spinal cord injury. *Osteoporos. Int.* 25:177–185, 2014.
[30]Lambach, R. L., N. E. Stafford, J. A. Kolesar, B. J. Kiratli, G. H. Creasey, R. S. Gibbons, B. J. Andrews, and G. S. Beaupre. Bone changes in the lower limbs from participation in an FES rowing exercise program implemented within two years after traumatic spinal cord injury. *J. Spinal Cord Med.* 43:306–314, 2018.
[31]Lazo, M. G., P. Shirazi, M. Sam, A. Giobbie-Hurder, M. J. Blacconiere, and M. Muppidi. Osteoporosis and risk of fracture in men with spinal cord injury. *Spinal Cord* 39:208–214, 2001.
[32]Les, C. M., S. M. Stover, J. H. Keyak, K. T. Taylor, and A. J. Kaneps. Stiff and strong compressive properties are associated with brittle post-yield behavior in equine compact bone material. *J. Orthop. Res.* 20:607–614, 2002.
[33]Lewis, G. Properties of acrylic bone cement: state of the art review. *J. Biomed. Mater. Res.* 38:155–182, 1997.

[34]Martínez, Á. A., J. Cuenca, A. Herrera, and J. Domingo. Late lower extremity fractures in patients with paraplegia. *Injury* 33:583–586, 2002.
[35]McPherson, J. G., W. B. Edwards, A. Prasad, K. L. Troy, J. W. Griffith, and T. J. Schnitzer. Dual energy X-ray absorptiometry of the knee in spinal cord injury: methodology and correlation with quantitative computed tomography. *Spinal Cord* 52:821–825, 2014.
[36]Modlesky, C. M., S. Majumdar, A. Narasimhan, and G. A. Dudley. Trabecular bone microarchitecture is deteriorated in men with spinal cord injury. *J. Bone Miner. Res.* 19:48–55, 2004.
[37]Moons, K. G. M., J. A. H. de Groot, W. Bouwmeester, Y. Vergouwe, S. Mallett, D. G. Altman, J. B. Reitsma, and G. S. Collins. Critical appraisal and data extraction for systematic reviews of prediction modelling studies: the CHARMS checklist. *PLoS Med.* 11:15, 2014. https://doi.org/10.1371/journal.pmed.1001744.
[38]Morgan, E. F., H. H. Bayraktar, and T. M. Keaveny. Trabecular bone modulus–density relationships depend on anatomic site. *J. Biomech.* 36:897–904, 2003.
[39]Morse, L. R., K. L. Troy, Y. Fang, N. Nguyen, R. Battaglino, R. F. Goldstein, R. Gupta, and J. A. Taylor. Combination therapy with zoledronic acid and FES-row training mitigates bone loss in paralyzed legs: results of a randomized comparative clinical trial. *JBMR Plus* 3:e10167, 2019.
[40]Nishiyama, K. K., S. Gilchrist, P. Guy, P. Cripton, and S. K. Boyd. Proximal femur bone strength estimated by a computationally fast finite element analysis in a sideways fall configuration. *J. Biomech.* 46:1231–1236, 2013.
[41]Orwoll, E. S., L. M. Marshall, C. M. Nielson, S. R. Cummings, J. Lapidus, J. A. Cauley, K. Ensrud, N. Lane, P. R. Hoffmann, D. L. Kopperdahl, and T. M. Keaveny. Finite element analysis of the proximal femur and hip fracture risk in older men. *J. Bone Miner. Res.* 24:475, 2009.
[42]Reiter, A. L., A. Volk, J. Vollmar, B. Fromm, and H. J. Gerner. Changes of basic bone turnover parameters in short-term and long-term patients with spinal cord injury. *Eur. Spine J.* 16:771–776, 2007.
[43]Schileo, E., F. Taddei, L. Cristofolini, and M. Viceconti. Subject-specific finite element models implementing a maximum principal strain criterion are able to estimate failure risk and fracture location on human femurs tested in vitro. *J. Biomech.* 41:356–367, 2008.
[44]Vestergaard, P., K. Krogh, L. Rejnmark, and L. Mosekilde. Fracture rates and risk factors for fractures in patients with spinal cord injury. *Spinal Cord* 36:790–796, 1998.
[45]Zehnder, Y., M. Lüthi, D. Michel, H. Knecht, R. Perrelet, I. Neto, M. Kraenzlin, G. Zäch, and K. Lippuner. Long-term changes in bone metabolism, bone mineral density, quantitative ultrasound parameters, and fracture incidence after spinal cord injury: a cross-sectional observational study in 100 paraplegic men. *Osteoporos. Int.* 15:180–189, 2004.

Osteoporosis International (2018) 29:2703–2715
https://doi.org/10.1007/s00198-018-4733-0

ORIGINAL ARTICLE

Bone fragility after spinal cord injury: reductions in stiffness and bone mineral at the distal femur and proximal tibia as a function of time

I.T. Haider[1,2] · S.M. Lobos[1,2] · N. Simonian[3,4] · T.J. Schnitzer[3,5] · W.B. Edwards[1,2]

Received: 4 April 2018 / Accepted: 4 October 2018 / Published online: 17 October 2018

Abstract

Summary Computed tomography and finite element modeling were used to assess bone structure at the knee as a function of time after spinal cord injury. Analyzed regions experienced degradation in stiffness, mineral density, and content. Changes were well described as an exponential decay over time, reaching a steady state 3.5 years after injury.

Introduction Spinal cord injury (SCI) is associated with bone fragility and an increased risk of fracture around the knee. The purpose of this study was to investigate bone stiffness and mineral content at the distal femur and proximal tibia, using finite element (FE) and computed tomography (CT) measures. A cross-sectional design was used to compare differences between non-ambulatory individuals with SCI as a function of time after injury (0–50 years).

Methods CT scans of the knee were obtained from 101 individuals who experienced an SCI 30 days to 50 years prior to participation. Subject-specific FE models were used to estimate stiffness under axial compression and torsional loading, and CT data was analyzed to assess volumetric bone mineral density (vBMD) and bone mineral content (BMC) for integral, cortical, and trabecular compartments of the epiphyseal, metaphyseal, and diaphyseal regions of the distal femur and proximal tibia.

Results Bone degradation was well described as an exponential decay over time ($R^2 = 0.33$–0.83), reaching steady-state levels within 3.6 years of SCI. Individuals at a steady state had 40 to 85% lower FE-derived bone stiffness and robust decreases in CT mineral measures, compared to individuals who were recently injured ($t \leq 47$ days). Temporal and spatial patterns of bone loss were similar between the distal femur and proximal tibia.

Conclusions After SCI, individuals experienced rapid and profound reductions in bone stiffness and bone mineral at the knee. FE models predicted similar reductions to axial and torsional stiffness, suggesting that both failure modes may be clinically relevant. Importantly, CT-derived measures of bone mineral alone underpredicted the impacts of SCI, compared to FE-derived measures of stiffness.

Trial registration ClinicalTrials.gov (NCT01225055, NCT02325414)

Keywords CT imaging · Finite element modeling · Osteoporosis · Spinal cord injury

Electronic supplementary material The online version of this article (https://doi.org/10.1007/s00198-018-4733-0) contains supplementary material, which is available to authorized users.

✉ I.T. Haider
ifaz.haider@ucalgary.ca

[1] Human Performance Laboratory, Faculty of Kinesiology, University of Calgary, Calgary, AB T2N 1N4, USA

[2] McCaig Institute for Bone and Joint Health, Cumming School of Medicine, University of Calgary, Calgary, AB T2N 1N4, USA

[3] Department of Physical Medicine and Rehabilitation, Northwestern University Feinberg School of Medicine, Chicago, IL 60611, USA

[4] Northwestern University Clinical and Translational Sciences Institute, Northwestern University Feinberg School of Medicine, Chicago, IL 60611, USA

[5] Department of Physical Medicine and Rehabilitation, Rehabilitation Institute of Chicago (d.b.a. Shirley Ryan AbilityLab), Chicago, IL 60611, USA

Introduction

Spinal cord injury (SCI) is associated with severe, rapid bone loss at sublesional locations [1–4]. Mechanical disuse, potentially combined with post-injury neurogenic, circulatory, and hormonal changes [1, 5], results in an imbalance of the natural resorption and formation of bone. The losses in bone are most significant around the knee, and previous studies have reported reductions in cortical and trabecular bone mineral content at the distal femur and proximal tibia of up to 50% within the first 5 years after injury [6–8]. These changes have important clinical implications as SCI patients are more than twice as likely to suffer a lower limb fracture in their lifetime compared to able-bodied controls [9]. These fractures often occur from relatively minimal trauma experienced from routine events such as rolling in bed or transferring from a wheelchair [10]. Spiral fracture patterns are commonly reported, implicating torsional loading as the cause of failure [11]. The rate of secondary complications associated with fracture after SCI is high, and these injuries have significant consequences for patient morbidity and mortality [12–14].

Pharmaceutical interventions to reduce fracture risk after SCI may be most effective if administered soon after injury, before bone loss becomes critical. Knowledge of the temporal patterns of bone loss after SCI may help to establish timelines for treatment and assessment. To this end, a number of previous studies have reported changes to bone mineral after SCI as measured by dual-energy x-ray absorptiometry (DXA) or computed tomography (CT) [6, 7, 15, 16]. These studies have reported that magnitude and rate of bone loss vary by region and type of bone measured [7], but it is difficult to interpret how these changes act in concert to reduce the overall mechanical competence of the bone. Subject-specific finite element (FE) modeling is a powerful, non-invasive, tool that can be used to answer this question. Indeed, studies of able-bodied patients have demonstrated FE modeling is a better predictor of bone fragility [17, 18] and osteoporotic fracture risk [19, 20] compared to radiographic measurement alone. This is likely because FE modeling is better able to assess the mechanical consequence of bone loss, which is a complex, multifactorial phenomenon that depends on both the changing properties of bone tissue as well as the geometric distribution of that tissue and the type of loading experienced.

With this in mind, our research group has used a combination of FE and CT measures to study bone loss after SCI [3, 4, 8, 21, 22]. We originally quantified regional changes in the distal femur and proximal tibia in the acute phase of bone loss, i.e., less than 8 months after SCI [3]. A subsequent cross-sectional study quantified whole bone temporal changes in the proximal tibia over a longer duration, 0–50 years after SCI [8]. However, that study did not analyze the distal femur, nor did it explore regional changes to bone stiffness. FE models were used to explore changes to torsional stiffness over time, but axial stiffness was not computed. In this study, we expand on our previous investigations. Our purpose was to examine a cross section of individuals with SCI and thoroughly quantify changes to bone at the distal femur and proximal tibia, as a function of time since injury. We used subject-specific FE models to predict mechanical stiffness (axial and torsional) at three separate regions (epiphysis, metaphysis, and diaphysis) of each bone. We also performed CT mineral analyses of integral, cortical, and trabecular compartments at epiphyseal, metaphyseal, and diaphyseal locations, in order to better understand the source of any FE-predicted changes. It is hoped that a more complete understanding of bone loss following SCI may help inform the future development of effective intervention strategies.

Methods

Participants

One hundred one individuals with SCI (ages 18–72 yrs; 80 males and 21 females) were recruited from the Northwestern University Feinberg School of Medicine, the Rehabilitation Institute of Chicago (now known as the Shirley Ryan AbilityLab), and the Schwab Rehabilitation Hospital (Table 1) for participation in one of two clinical research studies conducted between June 2011 and February 2018. All participants had sustained SCI between 1 month and 50 years prior to participation. All participants were non-ambulatory at the time of participation and experienced a range of neurological impairment, evaluated using the American Spinal Injury Association (ASIA) impairment scale (AIS A through D). Individuals were excluded from this study based on the following major criteria: (1) a history of Paget's disease, bone metastasis, or skeletal malignancies, (2) taking Dilantin and/or phenobarbital, as these drugs are known to affect bone health, (3) current or recent use of any bone-active agents, (4) individuals who are pregnant, lactating, or planning to become pregnant, (5) known endocrinopathies excluding diabetes and treated thyroid conditions, (6) abnormal TSH levels and T4 levels. Both clinical trials were conducted in accordance with Good Clinical Practice Guidelines; study protocols were approved by the institutional review board (IRB) of each participating site and by the Department of Defense Human Research Protection Office. All participants provided informed consent prior to participation. The clinical trials are registered with ClinicalTrials.gov (NCT01225055, NCT02325414).

CT image acquisition

Ninety-one of 101 participants were CT scanned using a Sensation 64 Cardiac Scanner (Siemens Medical Systems,

Table 1 Participant characteristics

Parameter	Mean ± SD
Subjects, *n*	101
Female, *n*	21
Age (years)	38.6 ± 14.6; range 18–72
Height (cm)	175.1 ± 10.4
Weight (kg)	75.2 ± 18.0
Time since injury (years)	7.7 ± 10.8; range 0.2–49.9

Forchheim, Germany). During the study, the Rehabilitation Institute of Chicago (now known as the Shirley Ryan AbilityLab) moved to a new building, and this scanner became unavailable. Thus, the remaining 10 participants were scanned using a SOMATOM Perspective (Siemens Medical Systems, Forchheim, Germany). Regardless of the machine, all CT scans were acquired with settings of 120 kVp and 280 mA. Images were reconstructed with an in-plane resolution of 0.352 mm × 0.352 mm and a slice thickness of 1 mm (voxel size: 0.352 mm × 0.352 mm × 1 mm). A hydroxyapatite calibration phantom (QRM, Moehrendorf, Germany) was placed in the field of view. The phantom had three regions with known mineral densities of 0.0, 0.4, and 0.8 g/cm^3. It served as a tool for inter-scan calibration, allowing us compute a linear regression relationship between CT absorption (HU) and equivalent mineral density (g/cm^3). A single 30-cm-long scan was used to capture approximately 15 cm each of the distal femur and proximal tibia. During the scan, participants lay with the superior-inferior axis of the leg approximately parallel to the axial direction of the CT scanner. As discussed in greater detail below, images were later re-aligned in order to minimize errors due to positioning. Scans were taken of the individuals' non-dominant knee, unless they had implants and/or a history of fracture on this knee. In these cases, the dominant knee was imaged instead. All image analysis was performed using a combination of the Mimics (Materialise, Leuven, Belgium) and Matlab (MathWorks, Natick, MA, USA) software. The workflow was similar to our previously reported protocol [3, 18], but with some changes to the alignment procedure which allowed for better automation.

CT analysis

CT image voxel intensities, or Hounsfield units (HU), were converted to hydroxyapatite equivalent density (ρ_{ha}; g/cm^3) using a linear fit of the mean HU values from the calibration phantom against known densities provided by the phantom manufacturer's certificate. Using the Mimics (Materialise, Leuven, Belgium) software, each bone was segmented from the CT image semi-automatically. A 0.15 g/cm^3 threshold was used to identify the periosteal surface of each bone. This threshold value was used in our previous investigations of bone density of individuals with SCI and was found to discriminate between background and bone for the majority of image slices [3, 4, 8, 23]. However, some manual clean-up was still required to isolate each bone and fill in any gaps which occurred at low density regions, i.e., locations where the cortical shell was very thin (Fig. A1 in the online Appendix). All image analysis tasks were performed by two trained operators with 1–2 years of experience and reviewed by a researcher with 6 years of experience analyzing medical images of bone.

Following segmentation, alignment and registration were performed separately for femora and tibiae creating two image series per scan. For each segmented bone, we used a standard operation available in Mimics to generate a stereolithography (STL) model of the periosteal surface, and images were aligned by comparing this STL to a template. The template was generated from one randomly selected tibia and femur (male; 64 days after SCI; left bone), which had been manually re-aligned along the longitudinal axis of the bone. An iterative closest point algorithm (Open-source Matlab implementation, URL: https://www.mathworks.com/matlabcentral/fileexchange/24301-finite-iterative-closest-point) was used to transform each individual's CT image data to match the template's orientation. This automatic alignment procedure generated final measurements of bone volume and mineral that were, on average, within 3% of measurements made using manual alignment procedures reported previously [3].

After alignment, we performed CT mineral analysis using previously published protocols [3]. Using published proportionality constants [24], segment lengths (SL) were estimated from the individual's stature. As it is challenging to obtain a precise measure of stature in non-ambulatory individuals with SCI, we chose to use self-reported stature as a reasonable best-estimate. Segment lengths were then used to separate each bone into three regions: the epiphysis at 0–10% SL, the metaphysis at 10–20% SL, and the diaphysis at 20–30% SL. Volumetric bone mineral density (vBMD; g/cm^3) and bone mineral content (BMC; g) were computed for integral, trabecular, and cortical compartments. The integral compartment represented all bone within the periosteal surface, as determined by our segmentation method described above. Next, the trabecular compartment was defined by performing a 4.9-mm (14 pixel) in-plane erosion of the integral region, using the erosion function available in Mimics. We selected this value because it ensured that the trabecular region was free of cortical bone, regardless of the individual's size or image slice location. Finally, the cortical compartment was defined by Boolean subtraction of the trabecular region from the integral region, followed by a thresholding of 0.35 g/cm^3 to remove any remaining trabecular bone. We computed vBMD and BMC for all three compartments at the epiphysis and metaphysis, but omitted the trabecular

compartment at the diaphysis. We also computed a cortical thickness index (cTI) for the metaphyseal region [25]:

$$cTI = \frac{1}{2}\cdot\left(\sqrt{\frac{iBV_{met}}{\frac{0.1\cdot SL}{\pi}}}-\sqrt{\frac{iBV_{met}-cBV_{met}}{\frac{0.1\cdot SL}{\pi}}}\right) \quad (1)$$

where iBV_{met} is the volume of the integral region of the metaphysis, cBV_{met} is the volume of the cortical region of the metaphysis, and SL is the bone segment length estimated from the individual's stature, as described above.

FE analysis

FE modeling was performed using our previously reported methodology [3], which has been experimentally validated using cadaveric proximal tibia loaded in torsion [18]. In this study, we used the same technique to make separate models of the epiphyseal, metaphyseal, and diaphyseal regions of each bone (101 tibia, 101 femurs), and computed structural stiffness in torsion (K_t) and axial compression (K_c) for each region. Models were subject specific, i.e., generated from the acquired CT images. Images were first resampled to isotropic voxels (1.5-mm edge length), and an FE mesh was generated by direct conversion of segmented bone voxels into first-order hexahedral elements. Element size was selected based on a convergence analysis, where it was found that decreasing edge length from 1.5 to 1.0 mm changed FE-predicted stiffness by less than 2%. Thus, the final models had up to 40,000 hexahedral elements. Bone was modeled as an inhomogeneous, linear elastic, orthotropic material. Elastic moduli in the axial direction, E_3, were computed from CT-derived ρ_{ha} using Eq. 2 [26]:

$$E_3 = 6570\cdot\rho_{app}^{1.37} \quad (2)$$

where E_3 is the elastic modulus (MPa) in the axial direction and ρ_{app} is the apparent density of bone ($\rho_{app} = \rho_{HU}/0.626$; g/cm^3) [27]. The other elastic constants were computed assuming constant anisotropy throughout: $E_1 = 0.574\cdot E_3$, $E_2 = 0.577\cdot E_3$, $G_{12} = 0.195\cdot E_3$, $G_{23} = 0.265\cdot E_3$, $G_{31} = 0.216\cdot E_3$, $\nu_{12} = 0.427$, $\nu_{23} = 0.234$, and $\nu_{31} = 0.405$ [28], with subscripts 1, 2, and 3 denoting the medial, anterior, and proximal directions, respectively.

Each model was subject to axial loading, in compression, and torsional loading, in internal rotation. A fixed displacement of 1 mm or rotation of 1° was applied, respectively. As shown in Fig. A1, surface nodes were fully fixed at one end of the bone, while a displacement/rotation-type load was applied to the opposite end. This load was applied at a reference node located at the geometric center of the cross section, which was kinematically coupled to the other nodes of the corresponding bony surface. All other degrees of freedom of the reference node were constrained and the reaction force, or torque, was monitored and used to calculate stiffness.

Curve fitting and statistical analysis

Similar to previous work [7, 8], we first fit CT and FE measures as a function of time since injury, using a single decaying exponential function:

$$y = A\cdot exp(-B\cdot t) + C \quad (3)$$

where y is the CT or FE parameter to be estimated, t is the time since injury (years), and A, B, and C are unknown parameters determined by the fitting algorithm. The form of this equation forces the predictor to asymptotically approach a steady-state value of C as time becomes large with respect to the loss rate parameter B. Thus, we computed additional parameters to quantify the behavior at a steady state. First, for each curve fit, the time to achieve 95% of the total change (t_{95}) was first determined using Eq. 4:

$$t_{95} = -\frac{ln(0.05)}{B}. \quad (4)$$

where B is the decay parameter computed using Eq. 3. Means and standard deviations (SD) for each parameter were then quantified for those with an SCI duration greater than t_{95}, i.e., the individuals who had reached the new steady state after SCI. To account for variance among individuals, the actual time to reach the new steady state (t_{ss}) was reported as the mean ± 0.5 SD of the data for those individuals with an SCI duration greater than t_{95}:

$$t_{ss} = -ln\left(\frac{SD}{2A}\right)/B. \quad (5)$$

CT and FE parameters were computed for all individuals with SCI who had an injury duration greater than t_{ss}. A reference group of uninjured controls against which to compare individuals with $t > t_{ss}$ was not available. Instead, they were compared to recently injured individuals, with an SCI injury ≤ 47 days before participation in this study. These recently injured individuals had mean integral vBMD at the tibia that was within 3% of the values previously reported for uninjured controls [8], across all three regions of the bone.

Previous studies have reported that a steady state is reached 1.7–7.6 years after injury, depending on the location and bone measure, when using Eq. 3 to model bone loss [7, 8]. However, there is some evidence that bone loss after SCI may slowly progress for much longer durations, up to 25 years after injury [29]. This behavior may not be adequately described by a single exponential decay, which asymptotes

quickly for all $t > t_{ss}$. With this in mind, we also fit our data to a double exponential decay function:

$$y = A_d \cdot exp(-B_d \cdot t) + C_d \cdot exp(-D_d \cdot t) \quad (6)$$

where y and t are, again, the parameter to be estimated and the time since SCI, respectively. A_d, B_d, C_d, and D_d are four new unknown parameters determined by the curve fit. The form of Eq. 6 allows the data to be described as the superposition of two processes, a fast process causing rapid bone loss soon after injury, and a slower process which allows for slow steady bone loss many years after injury.

Equations 3 and 6 were fit to CT and FE data using the Matlab Curve Fitting Toolbox (MathWorks, Natick, MA, USA). An F-statistic was computed from regression results [30] and used to test the null hypothesis that the more complex double exponential decay model (Eq. 6) provides no additional information compared to the simpler single exponential decay model (Eq. 3); this hypothesis test was evaluated at a criterion alpha level of 0.05. We also performed independent samples t tests, at the same criterion alpha level, comparing FE and CT measures from recently injured individuals ($t \leq$ 47 days) relative to individuals with SCI who reached a steady state ($t > t_{ss}$).

Results

From the 101 individuals with SCI participating in this study, scans of three bones from three different individuals were omitted because they did not pass quality control standards. Two tibia scans were omitted, one due to extreme motion artifact and the second due to metal artifact from a recent fracture fixation surgery. One femur scan was also omitted because the knee was not sufficiently centered in the field of view, and we were unable to image the entire diaphyseal region (20–30% SL). All reported analyses were computed using the remaining 99 scans of the femur and 100 scans of the tibia.

Most CT-derived measures of bone mineral and all FE-derived measures of stiffness were well described as exponential decays as a function of time. As shown in Figs. 1 and 2, the single and double decay functions, Eq. 3 and Eq. 6 respectively, behaved similarly before reaching a steady state (t_{ss}) in the first few years after SCI ($t \leq 3.5$ years). However, the two models often predicted very different behavior many years after the injury ($t > 3.5$ years); Eq. 6 often predicted continuous, slower, bone loss, while Eq. 3 asymptotes quickly to a steady-state value. For most measures, both models explained a nearly identical percentage of the total variation in the dataset with differences in R^2 less than 0.02. In two of the 56 measures, however, Eq. 6 fits the data very poorly compared to Eq. 3, with R^2 values lower by 0.17–0.34 (Tables 2 and 3). In all cases, the more complex Eq. 6 model failed to provide a statistically significant increase in the percentage of variation explained, compared to the simpler Eq. 3 model ($p \geq$ 0.67).

The FE-derived axial and torsional stiffness, in all three regions of both bones, reached new steady-state values within 3 years after injury (Tables 2 and 3). After this duration, bone stiffness was 40 to 85% lower ($p < 0.005$), compared to equivalent bone stiffness measured from individuals with recent SCI ($t \leq 47$ days). The magnitude and pattern of stiffness reduction was similar between both bones, with both axial and torsional stiffness varying based on bone region (Fig. 3). Stiffness losses were greatest at the epiphysis where we observed an 85% reduction in axial stiffness and 79% reduction in torsional stiffness ($p < 0.005$). These losses became somewhat attenuated moving away from the epiphysis. At the metaphysis, we observed 60–66% ($p < 0.005$) and 61–65% ($p < 0.005$) reductions in axial and torsional stiffness, respectively, while the diaphysis illustrated reductions of 49–50% ($p < 0.005$) and 44–51% ($p < 0.005$) for axial and torsional stiffness, respectively.

All CT-derived measures of bone mineral reached a steady state within 3.6 years (Tables 2 and 3). Individuals with an SCI injury duration > t_{ss} illustrated significant reductions in cortical BMC, cortical BV, trabecular BMC, and trabecular vBMD in all regions, with measures that were 23–107% lower than those who recently experienced SCI ($p < 0.005$). Reductions greater than 100% were observed at the trabecular compartment of the metaphysis, where negative mean values were observed at a steady state (Table 3), suggesting a region with little remaining hydroxyapatite. Changes to cortical vBMD were somewhat more modest by comparison, with reductions between 12 and 26% ($p < 0.005$). In contrast to all other measures observed in this study, variation in integral BV was not well modeled as a function of time ($R^2 < 0.02$), and the value of this measure was not significantly different between the baseline individuals with recent SCI ($t \leq 47$ days) compared to the rest of the cohort ($p \geq 0.30$).

Discussion

The purpose of this investigation was to thoroughly quantify regional changes to stiffness and bone mineral at the distal femur and proximal tibia as a function of time since SCI. We compared CT-derived measures of bone mineral and FE-derived measures of axial and torsional stiffness at three locations of each bone (epiphyseal, metaphyseal, and diaphyseal). The study demonstrated that bone degradation after SCI was well described as an exponential decay over time which, consistent with previous findings, reached steady-state levels within 3.6 years after injury [6–8]. The observed and robust

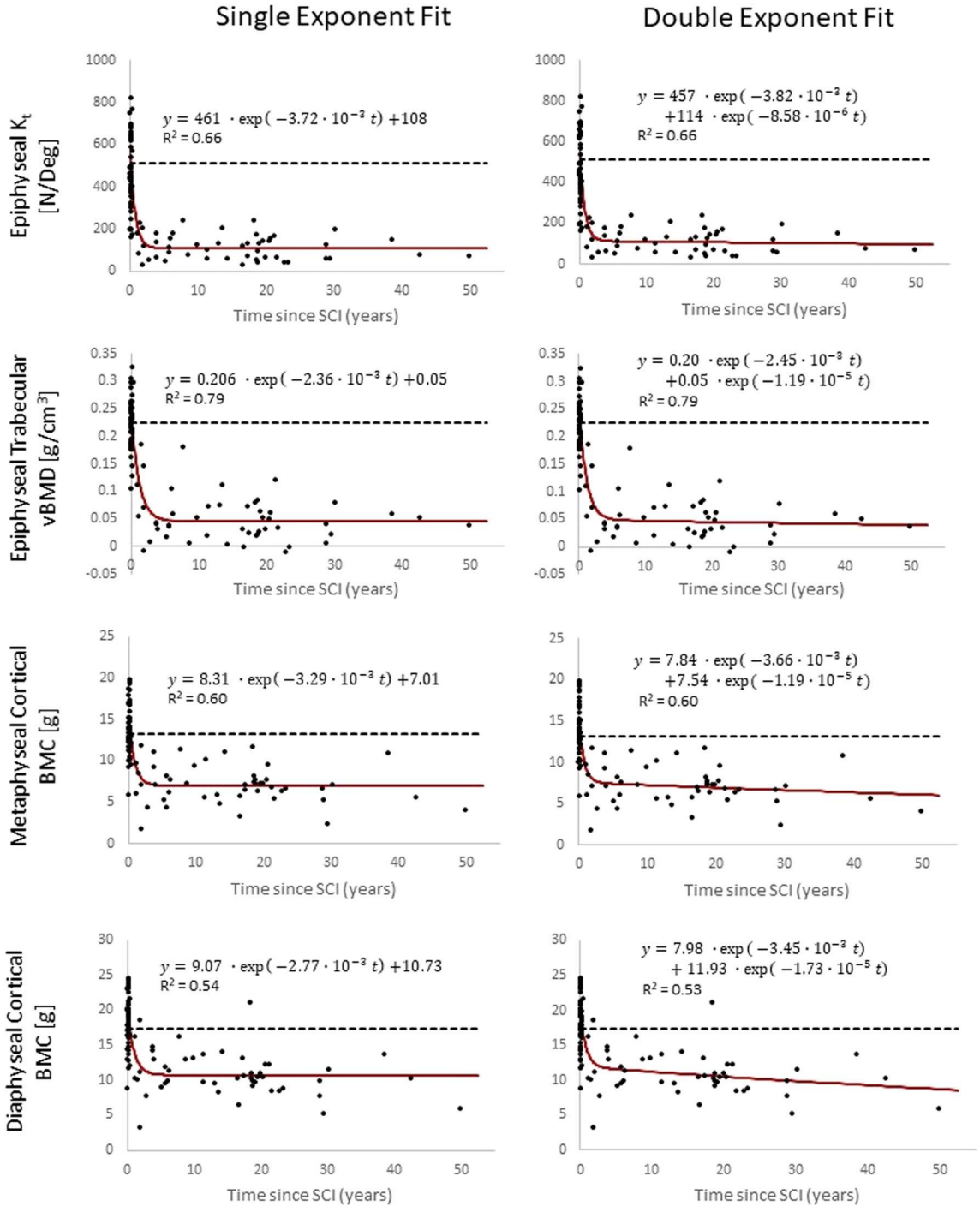

Fig. 1 Model fits at the distal femur for select FE and CT parameters. Both models match the rapid bone loss observed in the acute phase, soon after injury. The single exponent model (Eq. 3; left) quickly reaches a steady-state value, while the double exponent model (Eq. 6; right) predicts progressive bone loss up to 50 years after SCI. Both models explained a similar percentage of the total variation in measured data ($R^2 > 0.51$)

decreases to CT-measured bone mineral had important mechanical consequences, with FE models predicting that steady-state values in axial and torsional stiffness were 40 to 85% lower than those who recently experienced SCI ($t \leq$ 47 days). Moreover, individuals with recent SCI were not statistically different in age compared to those with $t > t_{ss}$, ($p = 0.67$) suggesting that these observations were not significantly confounded by age-related bone loss.

To our knowledge, this is the first study to explore changes to FE-derived measures of bone stiffness at the distal femur as a function of time. We found that the magnitude and rate of stiffness loss was similar between equivalent regions of the

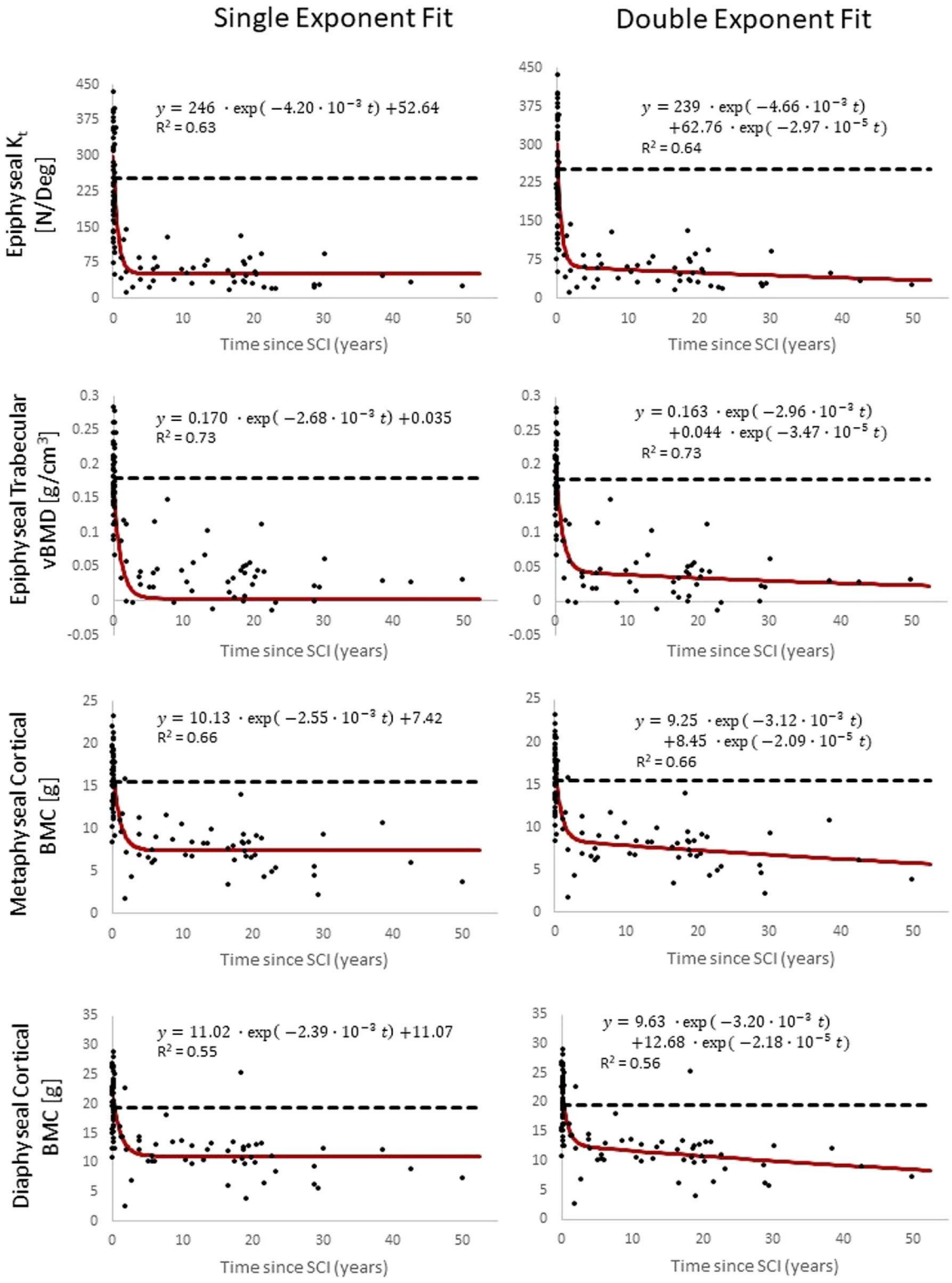

Fig. 2 Model fits at the proximal tibia for select FE and CT parameters. As with the distal femur, shown in Fig. 1, both models match the rapid bone loss observed in the acute phase, soon after injury. The single exponent model (Eq. 3; left) quickly reaches a steady-state value, while the double exponent model (Eq. 6; right) predicts progressive bone loss up to 50 years after SCI. Both models explained a similar percentage of the total variation in measured data ($R^2 > 0.52$)

tibia and femur. We also found that torsional and axial stiffness losses were similar in magnitude, suggesting that both failure modes may be clinically relevant. Indeed, previous studies have reported that both spiral [10, 11] and impacted

Table 2 FE and CT measures at the epiphyseal, metaphyseal, and diaphyseal regions of the distal femur

Region	Parameter	Eq. 2: single exponential fit (R^2)	Eq. 5: double exponential fit (R^2)	Single vs double (p)	Baseline group (mean ± SD)	Chronic SCI group (mean ± SD)	%Change	t test (p)	t_{ss} (years)
Epiphysis	K_c [kN/mm]	0.72	0.72	0.99	180.8 ± 40.36	27.47 ± 19.96	− 84.8	< 0.005	2.6
	K_t [N/Deg]	0.66	0.66	1.00	512.9 ± 152.0	109.9 ± 56.07	− 78.6	< 0.005	2.1
	iBMC [g]	0.72	0.72	0.98	32.40 ± 7.990	10.84 ± 4.480	− 66.5	< 0.005	2.3
	iBMD [g/cm^3]	0.80	0.80	0.98	0.260 ± 0.030	0.080 ± 0.030	− 68.4	< 0.005	2.8
	iBV [cm^3]	0.01	0.01	1.00	124.1 ± 31.10	126.4 ± 21.65	1.80	0.763	0.0
	cBMC [g]	0.74	0.74	1.00	9.380 ± 2.970	1.080 ± 0.620	− 88.4	< 0.005	3.1
	cBMD [g/cm^3]	0.52	0.52	0.67	0.520 ± 0.026	0.460 ± 0.030	− 12.4	< 0.005	1.5
	cBV [cm^3]	0.69	0.68	0.96	9.733 ± 3.183	1.958 ± 1.052	− 79.9	< 0.005	2.5
	tBMC [g]	0.83	0.83	1.00	32.40 ± 7.992	4.350 ± 3.200	− 86.6	< 0.005	2.6
	tBMD [g/cm^3]	0.79	0.79	0.99	0.225 ± 0.028	0.050 ± 0.040	− 77.7	< 0.005	2.8
Metaphysis	K_c [kN/mm]	0.69	0.69	0.95	85.57 ± 18.75	28.68 ± 13.66	− 66.5	< 0.005	2.4
	K_t [N/Deg]	0.58	0.59	0.98	111.3 ± 33.28	38.80 ± 20.43	− 65.2	< 0.005	1.6
	iBMC [g]	0.65	0.65	0.95	21.35 ± 5.825	9.360 ± 3.620	− 56.2	< 0.005	1.9
	iBMD [g/cm^3]	0.68	0.68	0.94	0.290 ± 0.051	0.140 ± 0.050	− 53.3	< 0.005	2.8
	iBV [cm^3]	0.00	0.01	0.94	74.45 ± 20.35	69.16 ± 14.78	− 7.10	0.300	0.0
	cBMC [g]	0.60	0.60	0.95	13.19 ± 3.763	7.200 ± 2.390	− 45.4	< 0.005	1.7
	cBMD [g/cm^3]	0.64	0.64	0.96	0.765 ± 0.060	0.650 ± 0.050	− 15.3	< 0.005	1.9
	cBV [cm^3]	0.49	0.50	0.94	17.06 ± 4.140	11.01 ± 3.079	− 35.5	< 0.005	1.3
	tBMC [g]	0.87	0.53	1.00	21.35 ± 5.825	−0.020 ± 2.000	− 100.	< 0.005	2.7
	tBMD [g/cm^3]	0.61	0.61	1.00	0.130 ± 0.036	−0.000 ± 0.050	− 101.	< 0.005	2.4
	cTI [cm]	0.61	0.61	0.91	0.145 ± 0.021	0.093 ± 0.021	− 35.8	< 0.005	2.1
Diaphysis	K_c [kN/mm]	0.65	0.65	0.93	106.6 ± 20.23	53.93 ± 15.89	− 49.4	< 0.005	2.6
	K_t [N/Deg]	0.47	0.47	0.95	87.90 ± 24.27	42.88 ± 22.52	− 51.2	< 0.005	1.5
	iBMC [g]	0.57	0.58	0.91	19.25 ± 4.824	11.36 ± 3.620	− 41.0	< 0.005	1.9
	iBMD [g/cm^3]	0.63	0.64	0.92	0.461 ± 0.078	0.280 ± 0.070	− 39.1	< 0.005	3.1
	iBV [cm^3]	0.01	0.01	0.98	41.99 ± 9.565	40.82 ± 8.500	− 2.80	0.683	0.0
	cBMC [g]	0.54	0.55	0.91	17.37 ± 4.517	11.06 ± 3.280	− 36.3	< 0.005	1.8
	cBMD [g/cm^3]	0.67	0.50	1.00	0.997 ± 0.043	0.820 ± 0.070	− 17.3	< 0.005	2.2
	cBV [cm^3]	0.32	0.33	0.93	17.33 ± 4.199	13.27 ± 3.370	− 23.4	< 0.005	1.2

[2] fracture patterns are observed in clinical settings, consistent with torsional and compressive failure modes, respectively. FE results also revealed that losses in torsional stiffness were much more rapid than losses in axial stiffness (1.2–2 years vs. 2.3–2.8 years, respectively). This has important implications for future pharmaceutical trials seeking to attenuate SCI-induced bone loss before it becomes critical. These results suggest the window of opportunity to prevent torsional stiffness degradation is very short; to observe potential benefits, treatment and follow-up assessments should occur well before the first 1.2 years after SCI.

Similar to previous findings [7, 8], we observed that integral BV did not change as a function of time after SCI. However, cortical BV decreased by up to 87%, while cortical vBMD decreased by up to 26%, depending on the region. Together, these results suggest that cortical bone loss after SCI is primarily driven by resorption at the endosteal surface, with some additional losses due to intercortical resorption, and no change to periosteal surface geometry.

We also found that reductions in axial stiffness, torsional stiffness, integral BMC, integral vBMD, and cortical BV were greatest at the epiphysis and progressively decreased moving toward the diaphysis. Similar patterns of bone loss have been reported previously at the proximal femur [22] and proximal tibia [8], though the mechanisms for this regional discrepancy are not well understood. It has been speculated that this may be due to differences in timelines associated with distinct osteoclastogenic events at different locations [2]. A murine disuse model has demonstrated immediate bone loss at the epiphysis, mediated by basal osteoclast activity, followed by losses at the diaphysis, as a consequence of osteoclastogenesis within the marrow space [31], which is consistent with this hypothesis.

In a previous investigation examining the entire proximal tibia (15-cm length), our group observed that integral BMC and torsional stiffness illustrated similar magnitudes of reduction over time after SCI [8]. In this study, however, this was not necessarily the case when comparing bone mineral and stiffness loss at different anatomical regions of bone. Indeed, percent changes in integral BMC were similar in magnitude to percent changes in torsional stiffness at the diaphysis only (Fig. 3; Table 3). The stiffer diaphyseal region likely plays a dominate role in the structural behavior of the entire proximal tibia, thereby explaining our previous finding. At the epiphyseal and metaphyseal regions, however, losses in integral BMC were 6–14 percentage points less than losses in torsional stiffness (Fig. 3). Similarly, losses in integral BMC were 5–18 percentage points less than losses in axial stiffness. These findings further demonstrate, as others have suggested [8, 32], that CT-derived measures of bone mineral alone tend to underestimate the mechanical consequences of bone loss.

The time to reach a steady state was computed based on a decaying single exponential model (Eq. 3), which has been examined previously [7, 8]. The model predicts rapid bone loss soon after injury, which asymptotically approaches a steady-state level over time. In other words, this model predicts negligible change in bone parameters after t_{ss}, or within 3.6 years after injury. While a number of studies reported that bone loss does indeed cease to change after approximately 2-year post-injury [6–8], other studies reported that bone degrades steadily for much longer durations [29, 33]. To explore this question further, we also fit data using a double exponential model (Eq. 6), which allowed for an initial period of rapid bone loss, followed by a period of slower bone loss that continues beyond the end of our data record (50 years). The double exponential model was not able to explain any additional variation in bone or stiffness loss when compared to the single exponential model ($p \geq 0.67$; Figs. 1 and 2). Although it remains plausible that bone loss after SCI continues following an initial period of exponential decay, the data presented here suggest that the rate of bone loss after the initial period is small with respect to other sources of variation among individuals, and could not be detected in this cross-sectional study. Presumably, bone loss many years after SCI may be the result of aging. Indeed, after 3.6 years, Eq. 6 predicts losses in cortical vBMD of approximately 0.12%/decade, which is similar to the rate of bone loss reported in able-bodied males over 50 years old [34].

The study has a number of important strengths. We collected CT data from a large cohort of 101 individuals with SCI across a large range of time since injury (1 month to 50 years). The effects of SCI were evaluated using both CT measures of bone mineral, and state-of-the-art subject-specific FE modeling techniques. Moreover, we performed regional FE analyses in order to understand the mechanical implications of bone loss, and how these effects differ, in the epiphysis, metaphysis, and diaphysis of each bone.

Despite these strengths, the study also has some noteworthy limitations. First, we lacked uninjured controls against which to compare individuals with SCI. In lieu of these data, we utilized data from recently injured participants ($t \leq 47$ days) as a baseline for comparison. While it is extremely likely that these recently injured individuals have already begun to experience bone loss after SCI, data from previous investigations suggest that magnitude of bone loss over such a short duration is relatively small (< 4%) [8, 35] and likely indistinguishable from normal variation among individuals.

Another important limitation is that FE models were used to assess stiffness only; ultimate load, i.e., strength, was not evaluated as we do not have a validated nonlinear model to predict failure at the distal femur. In the past, however, we validated [18] and used [8] more complex nonlinear material models in order to study strength of the proximal tibia and found that deceases in strength were somewhat greater in magnitude than decreases in stiffness.

Table 3 FE and CT measures at the epiphyseal, metaphyseal, and diaphyseal regions of the proximal tibia

Region	Parameter	Eq. 2: single exponential fit (R^2)	Eq. 5: double exponential fit (R^2)	Single vs double (p)	Baseline group (mean ± SD)	Chronic SCI group (mean ± SD)	%Change	t test (p)	t_{ss} (years)
Epiphysis	K_c [kN/mm]	0.61	0.61	0.97	99.97 ± 34.08	15.90 ± 11.63	− 84.1	< 0.005	2.3
	K_t [N/Deg]	0.63	0.62	0.96	252.9 ± 107.5	53.51 ± 30.99	− 78.8	< 0.005	1.9
	iBMC [g]	0.68	0.68	0.96	21.67 ± 6.301	7.170 ± 3.100	− 66.9	< 0.005	2.1
	iBMD [g/cm^3]	0.75	0.75	0.94	0.218 ± 0.034	0.070 ± 0.030	− 68.4	< 0.005	2.5
	iBV [cm^3]	0.00	0.02	0.91	100.5 ± 28.31	102.8 ± 18.29	2.20	0.729	0
	cBMC [g]	0.67	0.67	0.97	5.245 ± 1.854	0.910 ± 0.520	− 82.7	< 0.005	2.7
	cBMD [g/cm^3]	0.63	0.64	0.89	0.535 ± 0.028	0.456 ± 0.029	− 14.8	< 0.005	2.5
	cBV [cm^3]	0.69	0.68	0.96	9.733 ± 3.183	1.958 ± 1.052	− 79.9	< 0.005	2.5
	tBMC [g]	0.68	0.68	0.97	11.91 ± 4.026	2.431 ± 2.184	− 79.6	< 0.005	2.1
	tBMD [g/cm^3]	0.73	0.73	0.96	0.179 ± 0.033	0.036 ± 0.034	− 80.1	< 0.005	2.4
Metaphysis	K_c [kN/mm]	0.63	0.63	0.95	83.09 ± 19.02	32.89 ± 11.73	− 60.4	< 0.005	2.9
	K_t [N/Deg]	0.49	0.49	0.96	89.66 ± 37.81	34.95 ± 18.50	− 61.0	< 0.005	1.8
	iBMC [g]	0.62	0.63	0.92	19.99 ± 6.527	8.985 ± 3.160	− 55.1	< 0.005	2.3
	iBMD [g/cm^3]	0.69	0.70	0.90	0.364 ± 0.044	0.168 ± 0.053	− 54.0	< 0.005	3.3
	iBV [cm^3]	0.00	0.00	0.97	54.84 ± 16.63	54.56 ± 11.42	− 0.50	0.944	0.0
	cBMC [g]	0.66	0.66	0.92	15.46 ± 4.423	7.468 ± 2.375	− 51.7	< 0.005	2.3
	cBMD [g/cm^3]	0.79	0.80	0.89	0.886 ± 0.055	0.655 ± 0.054	− 26.0	< 0.005	2.8
	cBV [cm^3]	0.51	0.52	0.91	17.36 ± 4.526	11.23 ± 3.351	− 35.3	< 0.005	1.6
	tBMC [g]	0.51	0.51	0.95	3.346 ± 2.146	−0.260 ± 1.231	− 108.	< 0.005	2.2
	tBMD [g/cm^3]	0.53	0.53	0.97	0.102 ± 0.041	−0.008 ± 0.043	− 108.	< 0.005	2.6
	cTI [cm]	0.65	0.67	0.88	0.176 ± 0.015	0.110 ± 0.025	− 38.0	< 0.005	2.7
Diaphysis	K_c [kN/mm]	0.64	0.64	0.94	107.2 ± 21.58	52.90 ± 19.45	− 50.7	< 0.005	2.7
	K_t [N/Deg]	0.34	0.33	0.97	64.30 ± 24.87	35.94 ± 19.88	− 44.1	< 0.005	1.2
	iBMC [g]	0.53	0.55	0.90	20.08 ± 5.907	11.71 ± 3.655	− 41.7	< 0.005	2.0
	iBMD [g/cm^3]	0.69	0.70	0.88	0.586 ± 0.053	0.340 ± 0.078	− 42.5	< 0.005	3.6
	iBV [cm^3]	0.01	0.00	1.00	34.18 ± 9.438	34.93 ± 7.443	2.20	0.766	0.0
	cBMC [g]	0.55	0.56	0.91	19.46 ± 5.655	11.12 ± 3.553	− 42.8	< 0.005	2.1
	cBMD [g/cm^3]	0.78	0.78	0.89	1.052 ± 0.050	0.810 ± 0.061	− 22.8	< 0.005	3.0
	cBV [cm^3]	0.34	0.35	0.91	18.463 ± 5.261	13.66 ± 3.983	− 26.0	< 0.005	1.2

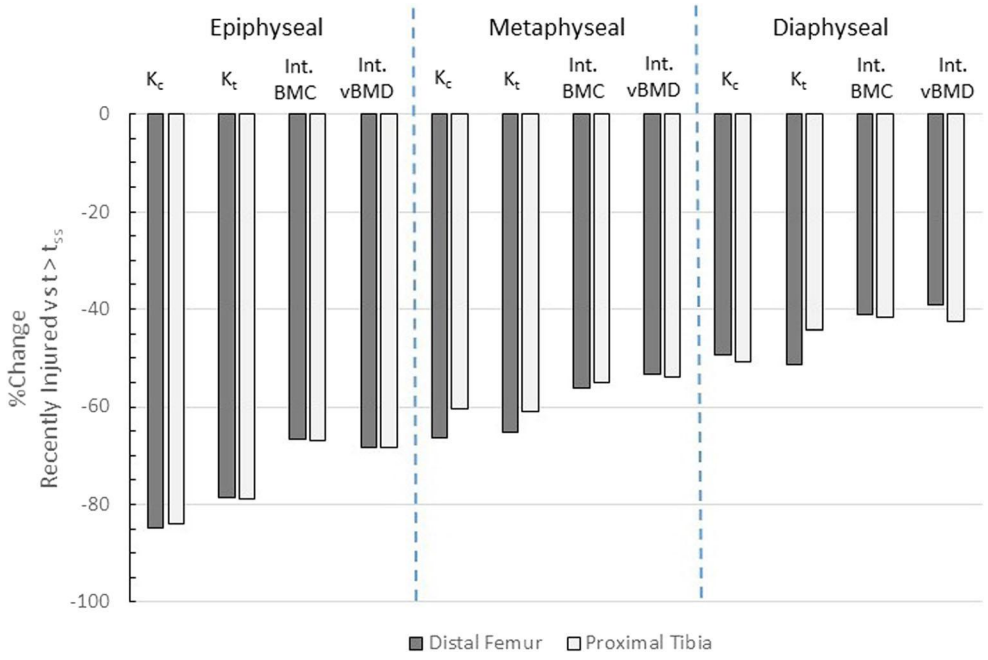

Fig. 3 %Change in FE-derived stiffness and select CT mineral measures, in patients who reached a steady state ($t > t_{ss}$) compared to a recently injured reference group ($t \leq 47$ days). The magnitude and spatial pattern of bone loss was similar between the proximal tibia (white) and distal femur (gray). Losses were greatest at the epiphysis and progressively decreased, moving toward the diaphysis

Also, only 21 of 101 participants were female. As a result, we were unable to determine if the effects of SCI were dependent on sex. Post-hoc analyses revealed that males and females who reached $t > t_{ss}$ experienced reductions in bone stiffness that were not statistically different ($p \geq 0.26$), with percent reductions computed relative to a sex-matched group of recently injured individuals ($t \leq 47$ days). However, only nine female participants reached a steady state, and it is plausible that this result was due to a lack of statistical power.

Another limitation of this study stems from the fact that a clinical CT-based FE modeling technique was used to assess local bone material properties as a function of average vBMD at element locations. Clinical resolution scans are unable to assess changes to bone microarchitecture (e.g., trabecular architecture, collagen-cross linking, changes to remodeling spaces), and there is some evidence that microarchitecture changes in the context of SCI are more significant compared to other forms of osteoporosis [1]. While the mechanical consequences of these microarchitectural changes are not fully understood, we speculate that our models based on CT-derived density alone may underpredict the mechanical consequences of SCI-induced bone deterioration.

We are unable to quantify precision errors of the CT and FE analysis, as we do not have repeated scans of the same individual over a short duration. However, a previous study using comparable hardware reported an inter-scan coefficient of variation of only 1.7% [36]. Furthermore, using a similar CT analysis protocol [3], we previously found that inter-operator precision errors resulted in a coefficient of variation less than 0.6%. These findings suggest that precision errors are likely small compared to the magnitude of SCI-induced bone loss observed in this study.

Finally, there are limitations associated with our cross-sectional study design. We are unable to control for the effects of individual variation in bone mineral and stiffness before injury, nor are we able to quantify variability due to differences in patient-specific responses to SCI [6, 22]. Together, these factors may account for some of the unexplained variation in our regression results (Tables 2 and 3; $R^2 = 0.34$–0.79).

Conclusion

The results of this study demonstrate that torsional and axial stiffness in the distal femur and proximal tibia decay exponentially as a function of time after SCI. Both bones experienced similar magnitudes and rates of bone loss, with reaching steady-state levels 1.2–3.6 years after injury. Stiffness losses were greatest at the epiphysis and progressively decreased moving toward the diaphysis. Similar patterns were observed in integral BMC and vBMD, though these parameters underestimated the mechanical consequences of bone loss after SCI. Changes over time were well modeled with a single decaying exponential function, which predicted rapid bone loss immediately after injury, and little bone loss after 3.6 years. Data were also modeled using a double exponential decay function, which predicted a secondary period of more moderate bone loss that continued for many years after injury. However, this double decay model did not provide a better fit to the observed data ($p \geq 0.67$). It is plausible that patients continue to suffer moderate bone loss for many years after SCI, but it is likely that the rate of loss is small, with respect to variation among individuals.

In summary, the findings presented here support the general notion that bone loss at the knee after SCI is rapid and profound, with rates of bone loss that are greatest immediately after injury. We found that CT-derived measures of density alone may underestimate the consequences of SCI, compared to patient-specific FE models, which provide a mechanistic assessment of the mechanical consequences of bone loss. Finally, we found that SCI-induced bone loss results in significant reductions to both torsional and axial stiffness, suggesting that both failure modes may be clinically relevant.

Acknowledgements We thank our colleagues Dr. Alan S. Anschel, Dr. David Chen, and Dr. Ki H. Kim at the Shirley Ryan AbilityLab (formerly Rehabilitation Institute of Chicago) and Dr. Michelle Gittler and Dr. Ray Lee at Schwab Rehabilitation Hospital for their support in our recruitment efforts. We would also like to thank Matthew Giffhorn, Dr. Elaine Gregory, Kendra Harmon, Amy Lange, Julia Marks, Dr. Amanpreet Saini, Bernard Stephens, and Renita Yeasted for their help with recruitment and data collection.

Funding information This research was supported by Department of Defense U.S. Army Medical Research and Materiel Command (Grant Numbers SC090010 and SC130125). REDCap is supported at FSM by the Northwestern University Clinical and Translational Science (NUCATS) Institute. Research reported in this publication was also supported, in part, by the National Institutes of Health's National Center for Advancing Translational Sciences (Grant Numbers UL1TR001422 and UL1TR000150). The content is solely the responsibility of the authors and does not necessarily represent the official views of the National Institutes of Health.

Compliance with ethical standards

Conflicts of interest None.

References

1. Jiang S-D, Dai L-Y, Jiang L-S (2006) Osteoporosis after spinal cord injury. Osteoporos Int 17:180–192. https://doi.org/10.1007/s00198-005-2028-8
2. Edwards WB, Schnitzer TJ (2015) Bone imaging and fracture risk after spinal cord injury. Curr Osteoporos Rep 13:310–317. https://doi.org/10.1007/s11914-015-0288-6
3. Edwards WB, Schnitzer TJ, Troy KL (2013) Bone mineral and stiffness loss at the distal femur and proximal tibia in acute spinal cord injury. Osteoporos Int 24:2461–2469. https://doi.org/10.1007/s00198-013-2557-5
4. Edwards WB, Schnitzer TJ, Troy KL (2014) Reduction in proximal femoral strength in patients with acute spinal cord injury. J Bone Miner Res 29:2074–2079. https://doi.org/10.1002/jbmr.2227
5. Jiang SD, Jiang LS, Dai LY (2006) Mechanisms of osteoporosis in spinal cord injury. Clin Endocrinol 65:555–565. https://doi.org/10.1111/j.1365-2265.2006.02683.x
6. Biering-Sorensen F, Bohr HH, Schaadt OP (1990) Longitudinal study of bone mineral content in the lumbar spine, the forearm and the lower extremities after spinal cord injury. Eur J Clin Investig 20:330–335
7. Eser P, Frotzler A, Zehnder Y et al (2004) Relationship between the duration of paralysis and bone structure: a pQCT study of spinal cord injured individuals. Bone 34:869–880. https://doi.org/10.1016/j.bone.2004.01.001
8. Edwards WB, Simonian N, Troy KL, Schnitzer TJ (2015) Reduction in torsional stiffness and strength at the proximal tibia as a function of time since spinal cord injury. J Bone Miner Res 30:1422–1430. https://doi.org/10.1002/jbmr.2474
9. Vestergaard P, Krogh K, Rejnmark L, Mosekilde L (1998) Fracture rates and risk factors for fractures in patients with spinal cord injury. Spinal Cord 36:790–796. https://doi.org/10.1038/sj.sc.3100648
10. Keating JF, Kerr M, Delargy M Minimal trauma causing fractures in patients with spinal cord injury. Disabil Rehabil 14:108–109
11. Martínez ÁA, Cuenca J, Herrera A, Domingo J (2002) Late lower extremity fractures in patients with paraplegia. Injury 33:583–586. https://doi.org/10.1016/S0020-1383(02)00163-8
12. Morse LR, Battaglino RA, Stolzmann KL et al (2009) Osteoporotic fractures and hospitalization risk in chronic spinal cord injury. Osteoporos Int 20:385–392. https://doi.org/10.1007/s00198-008-0671-6
13. Gifre L, Vidal J, Carrasco J et al (2014) Incidence of skeletal fractures after traumatic spinal cord injury: a 10-year follow-up study. Clin Rehabil 28:361–369. https://doi.org/10.1177/0269215513501905
14. Carbone LD, Chin AS, Burns SP et al (2014) Mortality after lower extremity fractures in men with spinal cord injury. J Bone Miner Res 29:432–439. https://doi.org/10.1002/jbmr.2050
15. Gifre L, Humbert L, Muxi A, et al (2018) Analysis of the evolution of cortical and trabecular bone compartments in the proximal femur after spinal cord injury by 3D-DXA. Osteoporos Int 29:201–209. https://doi.org/10.1007/s00198-017-4268-9
16. Garland DE, Stewart CA, Adkins RH et al (1992) Osteoporosis after spinal cord injury. J Orthop Res 10:371–378. https://doi.org/10.1002/jor.1100100309
17. Cody DD, Gross GJ, Hou FJ et al (1999) Femoral strength is better predicted by finite element models than QCT and DXA. J Biomech 32:1013–1020. https://doi.org/10.1016/S0021-9290(99)00099-8
18. Edwards WB, Schnitzer TJ, Troy KL (2013) Torsional stiffness and strength of the proximal tibia are better predicted by finite element models than DXA or QCT. J Biomech 46:1655–1662. https://doi.org/10.1016/j.jbiomech.2013.04.016
19. Falcinelli C, Schileo E, Balistreri L et al (2014) Multiple loading conditions analysis can improve the association between finite element bone strength estimates and proximal femur fractures: a preliminary study in elderly women. Bone 67:71–80. https://doi.org/10.1016/j.bone.2014.06.038
20. Keyak JH, Sigurdsson S, Karlsdottir G et al (2011) Male-female differences in the association between incident hip fracture and proximal femoral strength: a finite element analysis study. Bone 48:1239–1245. https://doi.org/10.1016/j.bone.2011.03.682
21. Edwards WB, Schnitzer TJ, Troy KL (2014) The mechanical consequence of actual bone loss and simulated bone recovery in acute spinal cord injury. Bone 60:141–147. https://doi.org/10.1016/j.bone.2013.12.012
22. Edwards WB, Schnitzer TJ, Troy KL (2013) Bone mineral loss at the proximal femur in acute spinal cord injury. Osteoporos Int 24:2461–2469. https://doi.org/10.1007/s00198-013-2323-8
23. Edwards WB, Simonian N, Haider IT et al (2018) Effects of teriparatide and vibration on bone mass and bone strength in people with bone loss and spinal cord injury: a randomized, controlled trial. J Bone Miner Res. https://doi.org/10.1002/jbmr.3525
24. Winter DA (2009) Biomechanics and motor control of human movement. John Wiley & Sons, New York
25. Cheng X, Li J, Lu Y et al (2007) Proximal femoral density and geometry measurements by quantitative computed tomography: association with hip fracture. Bone 40:169–174. https://doi.org/10.1016/j.bone.2006.06.018

26. Rho JY, Hobatho MC, Ashman RB (1995) Relations of mechanical properties to density and CT numbers in human bone. Med Eng Phys 17:347–355. https://doi.org/10.1016/1350-4533(95)97314-F
27. Dalstra M, Huiskes R, Odgaard A, van Erning L (1993) Mechanical and textural properties of pelvic trabecular bone. J Biomech 26: 523–535. https://doi.org/10.1016/0021-9290(93)90014-6
28. Rho JY (1996) An ultrasonic method for measuring the elastic properties of human tibial cortical and cancellous bone. Ultrasonics 34:777–783. https://doi.org/10.1016/S0041-624X(96)00078-9
29. Bauman WA, Spungen AM, Wang J et al (1999) Continuous loss of bone during chronic immobilization: a monozygotic twin study. Osteoporos Int 10:123–127. https://doi.org/10.1007/s001980050206
30. Allen MP (1997) Understanding regression analysis. Springer, Boston, pp 113–117
31. Ausk BJ, Huber P, Srinivasan S et al (2013) Metaphyseal and diaphyseal bone loss in the tibia following transient muscle paralysis are spatiotemporally distinct resorption events. Bone 57:413–422. https://doi.org/10.1016/j.bone.2013.09.009
32. Keaveny TM, Kopperdahl DL, Melton LJ et al (2010) Age-dependence of femoral strength in white women and men. J Bone Miner Res 25:994–1001. https://doi.org/10.1002/jbmr.091033
33. De Bruin ED, Vanwanseele B, Dambacher MA et al (2005) Long-term changes in the tibia and radius bone mineral density following spinal cord injury. Spinal Cord 43:96–101. https://doi.org/10.1038/sj.sc.3101685
34. Russo CR, Lauretani F, Seeman E et al (2006) Structural adaptations to bone loss in aging men and women. Bone 38:112–118. https://doi.org/10.1016/j.bone.2005.07.025
35. McCarthy I, Goodship A, Herzog R et al (2000) Investigation of bone changes in microgravity during long and short duration space flight: comparison of techniques. Eur J Clin Investig 30:1044–1054. https://doi.org/10.1046/j.1365-2362.2000.00719.x
36. Troy KL, Edwards WB (2018) Practical considerations for obtaining high quality quantitative computed tomography data of the skeletal system. Bone 110:58–65. https://doi.org/10.1016/j.bone.2018.01.013

Prevention of Bone Loss after Acute SCI by Zoledronic Acid: Durability, Effect on Bone Strength and Use of Biomarkers to Guide Therapy

Proposal Log Number SC130125; Award # W81XWH-14-2-0193; HRPO Log A-18350

PI: Dr. Thomas J. Schnitzer **Org:** Northwestern University Feinberg School of Medicine **Award Amount: $2,011,846**

Study/Product Aims

- Define timing and frequency of administration of zoledronic acid that will result in optimal prevention of bone loss after acute SCI.
- Evaluate the use of serum markers of bone metabolism to guide therapeutic decisions of timing and need for retreatment with zoledronic acid after acute SCI.
- Evaluate effects of zoledronic acid in mitigating loss of bone strength that occurs after acute SCI.

Approach

This was a 2 year, randomized, double-blind placebo-controlled study. Subjects were randomized at baseline and again at 12 months to receive either zoledronic acid or placebo each time. Subject were followed for 24 months with repeat DXA scans, CT scans, and serum bone markers.

IRB approval received at all sites. Enrollment and data collection is complete. Forty-nine out of 60 subjects have completed the study.

Timeline and Cost

Activities CY	14	15	16	17	18	19	20	21
Study Start-Up Activities								
Participant Enrollment								
Data Collection and Entry								
Data Analysis								
Estimated Budget ($K)	$138K	$541K	$503K	$465K	$365K	$0K	$0K	$0K

completed | original projection | covid delay | current projection

Updated: 02 June 2021

Goals/Milestones

CY14 Goals – Begin study start-up; Regulatory approval at all sites
CY15 Goals – Complete start-up, Begin recruitment and enrollment
CY16 Goals – Continue recruitment and enrollment
CY17 Goals – Complete subject enrollment (56/60 completed)
CY18 Goals – Enrollment completed (60/60); continue data collection
CY19 Goals – Continue data collection
CY20 Goals – Finalize data collection, data analysis, study report
CY21 Goals – Submit final report

Comments/Challenges/Issues/Concerns

Delayed HRPO approval, hospital move delayed projected timelines
Enrollment is 100% complete.
Closure due to the Covid-19 pandemic delayed analyses and final study report by 4 months.

Budget

Budget Expenditure to Date: (through Mar, 2021)
Projected Expenditure: $2,011,846
Actual Expenditure: $2,011,846